AN ATLAS OF ROBUST, STABLE, HIGH-DIMENSIONAL LIMIT CYCLES

ROY WILDS

Department of Mathematics and Statistics,
McGill University, 805 Sherbrooke St. West,
Montreal, Quebec, Canada H3A 2K6

LEON GLASS

Department of Physiology, McGill University,
3655 Promenade Sir William Osler,
Montreal, Quebec, Canada H3G 1Y6

We present a method for constructing dynamical systems with robust, stable limit cycles in arbitrary dimensions. Our approach is based on a correspondence between dynamics in a class of differential equations and directed graphs on the n-dimensional hypercube (n-cube). When the directed graph contains a certain type of cycle, called a cyclic attractor, then a stable limit cycle solution of the differential equations exists. A novel method for constructing regulatory systems that we call **minimal regulatory networks** from directed graphs facilitates investigation of limit cycles in arbitrarily high dimensions.

We identify two families of cyclic attractors that are present for all dimensions $n \geq 3$: *cyclic negative feedback* and *sequential disinhibition*. For each, we obtain explicit representations for the differential equations in arbitrary dimension. We also provide a complete listing of minimal regulatory networks, a representative differential equation, and a bifurcation analysis for each cyclic attractor in dimensions 3–5. This work joins discrete concepts of symmetry and classification with analysis of differential equations useful for understanding dynamics in complex biological control networks.

Keywords: Piecewise linear equations; hypercube; Hopf bifurcation; homoclinic bifurcation; inverse problem.

1. Introduction

One of the striking characteristics of the living world is the presence of diverse oscillations with periods ranging from milliseconds to a year and in spatial domains that extend from subcellular structures to whole organisms. Examples of well known oscillations include the cell cycle, heartbeat, respiration, circadian rhythm, menstrual cycle and hibernation [Glass & Mackey, 1988; Winfree, 2001]. These rhythms must be robust to a wide range of environmental perturbations. They must also be robust to mutations that occur over evolutionary time scales.

Some basic structural features lead to oscillations. Negative feedback systems, in which a product inhibits its formation, can either display a steady state or oscillation. The inhibition is not necessarily direct or immediate but can occur through several intermediary steps or with a time delay [Goodwin, 1963; Horowitz & Hill, 1989; Thomas & D'Ari, 1990; Novák & Tyson, 2008]. Less well known, but equally powerful, is the concept

of sequential disinhibition. Here the progressive removal of inhibition leads to the generation of stable oscillations, as originally proposed in models of walking in salamanders [Székely, 1965; Kling & Székely, 1968].

In the 1970s, one of us (LG) developed methods that can be used to identify logical switching networks and homologous smooth ordinary differential equations that can display stable robust oscillations [Glass & Kauffman, 1973; Glass, 1975, 1977a; Glass & Pasternack, 1978a, 1978b]. The basic idea is to first identify synchronous logical switching networks that display a certain type of stable oscillation and then to generate differential equations that capture the logical structure. Additionally, recent work by [Lu & Edwards, 2010] has generalized these earlier results by showing that stable oscillations can exist for a wide class of switching networks.

The underlying logical networks can be identified using a discrete approach. The logical networks and differential equations are determined from a directed graph on an n-dimensional hypercube (n-cube). The n-cube has 2^n vertices and $n \times 2^{n-1}$ edges. If each edge is directed in a unique orientation, there is a $1 : 1$ correspondence between logical switching networks with no self-input, and the directed n-cube graphs. Further, a special type of cycle called a cyclic attractor plays a central role. A cyclic attractor, which we define precisely in Sec. 2.1, is a structure on a directed graph that is analogous to a stable limit cycle in a differential equation. Piecewise linear differential equations that incorporate the logical structures defined by the cyclic attractors have robust stable limit cycles [Glass & Pasternack, 1978b; Mestl *et al.*, 1995]. Further, by generalizing the piecewise linear equations by substituting sigmoidal functions for step functions, we generate stable oscillations that also capture the same logical structure of the discrete switching networks [Glass & Pasternack, 1978a].

This work has relevance to several fields.

Synthetic biology: Since biological controls regulating gene expression have analogies with switching devices, it has been feasible to synthesize networks with predetermined dynamical behavior that can be predicted based on the dynamics of these networks [Elowitz & Leibler, 2000; Gardner *et al.*, 2000; Benner & Sismour, 2005].

Circuit design: Hybrid electronic networks with a programmable logic have been built to realize all five-dimensional networks by inputting the truth tables of each element as a tuple of 5×16 Boolean digits [Mason *et al.*, 2004]. Consequently, all networks described here can be implemented in hybrid electronic circuits.

Inverse problem in biology: One of the major biological problems is the determination of molecular biological control circuits based on limited information about the dynamics [Hasty *et al.*, 2001; De Jong, 2002; Perkins *et al.*, 2004]. Likewise, patterns of neural activity may be useful in determining the structure of the underlying neural network [Glass & Young, 1979]. The current paper develops methods to determine minimal networks that display robust dynamical behavior and may thus be useful for practical applications in biology.

Applied mathematics: The paper raises many problems concerning the dynamics in these systems. These include: proof of limit cycles over the range of the steepness parameter of sigmoid functions; analysis of bifurcation patterns for all networks — although most are simple with a single Hopf bifurcation, others are more complex and require more detailed analysis; extension to higher dimensions where the numbers of cyclic attractors vastly increase (we do not know the numbers of cyclic attractors in dimension six and above).

The plan of the paper is as follows. Section 2 introduces the regulatory system of differential equations and establishes the connection with a directed n-cube. In Sec. 2.1 we define cyclic attractors and describe several attributes they possess. Section 2.2 addresses the symmetry properties of the n-cube, presenting an explicit representation for the $n!2^n$ symmetry operations. We define the notion of a minimal network in Sec. 2.3 and present an algorithm for obtaining such networks. The concept of a minimal network provides a powerful tool in the task of identifying the logical structure corresponding to a directed n-cube. Section 3 investigates two families of cyclic attractors that exist for all $n \geq 3$. First, in Sec. 3.1 we consider a family for which the minimal networks have a *cyclic negative feedback* structure. Second, in Sec. 3.2 a family of cyclic attractors that have minimal networks corresponding to *sequential disinhibition* are analyzed. For both families, expressions for the minimal networks in arbitrary dimensions are derived and several properties of the differential equations are proved. A generalization of the piecewise linear regulatory networks called continuous homologues are developed in Sec. 4. We state and discuss several open

questions in Sec. 5. In the Appendix, homologous systems for all cyclic attractors in dimensions $n = 3, 4, 5$ are presented and their bifurcation structure analyzed.

2. Model and Methods

For concreteness, we consider regulatory networks based on biochemical systems in which the variables of the system are concentrations. The methods presented can, in general, be adapted to other regulatory paradigms. At the core of our approach is a logical model that captures many features of real regulatory networks [Glass & Kauffman, 1973; Glass, 1975]. They are a natural extension of the Boolean networks used by Kauffman [1969, 1993] to study properties of simple biochemical networks. For related approaches and reviews see [Thomas & D'Ari, 1990; De Jong, 2002; Edwards & Glass, 2006]. The time evolution of n species is governed by a system of piecewise differential equations:

$$\frac{dy_i}{dt} = -\gamma_i y_i + g_i(Y_{i_1}, Y_{i_2}, \ldots, Y_{i_K}), \quad i \in [1, n]. \quad (1)$$

Species i is degraded at rate γ_i and produced at rate g_i. We assume that g_i depends only on whether y_j is high or low relative to a threshold θ_j. Defining $Y_i = \alpha$ if $y_i > \theta_i$ and $Y_i = \beta$ if $y_i < \theta_i$ then α represents the high state and β the low state. We identify the regulator set $R_i \equiv \{i_1, i_2, \ldots, i_K\}$, containing the K species that regulate species i. Throughout this work, we assume that species i does not regulate itself directly ($i \notin R_i$).

Letting $x_i = y_i - \theta_i$, $X_i = (Y_i - \alpha)/(\beta - \alpha)$ and $B_i = g_i - \gamma_i \theta_i$, then Eq. (1) becomes

$$\dot{x}_i(t) = -\gamma_i x_i(t) + B_i(X_{i_1}(t),$$
$$X_{i_2}(t), \ldots, X_{i_K}(t)), \quad i \in [1, n], \quad (2)$$

where $X_i(t) = H(x_i(t)) \in \{0, 1\}$ with $H(\cdot)$ the Heaviside function. Suitable rescaling of x_i restricts B_i to the range $[-1, 1]$. To avoid technical complications that arise, we assume that $B_i \neq 0$. This condition, along with the restriction on self-input, implies that Eq. (2) possesses a unique, continuous solution. Furthermore, we shall assume that all degradation rates are the same: $\gamma_i = \gamma$.

The variables X_i are constant within any orthant of $\mathbb{R}^n$ (an orthant is the n-dimensional analog of quadrants in two dimensions). Equation (2) is a first-order linear system

within an orthant. Starting from initial condition $x(0)$ let $\{t_1, t_2, \ldots, t_k\}$ denote the times when the solution trajectory crosses an orthant boundary. Then, for $t_j < t < t_{j+1}$ the solution of Eq. (2) is

$$x_i(t) = x_i(t_j) e^{-\gamma(t-t_j)} + \frac{1}{\gamma} B_i(X_{i_1}(t_j^*),$$
$$X_{i_2}(t_j^*), \ldots, X_{i_K}(t_j^*))(1 - e^{-\gamma(t-t_j)}), \quad (3)$$

where t_j^* is any time in (t_j, t_{j+1}). Thus, the solution $x(t)$ of Eq. (2) is a sequence of solutions given by Eq. (3). Within each orthant, the trajectory is a straight line from $(x_1(t_j), x_2(t_j), \ldots, x_n(t_j))$ towards the focal point $(B_1(t_j^*), B_2(t_j^*), \ldots, B_n(t_j^*))$ (where we have abbreviated $B_i(t_j^*) = B_i(X_{i_1}(t_j^*), \ldots, X_{i_K}(t_j^*))$). If the focal point lies outside the orthant in which $(x_1(t_j^*), x_2(t_j^*), \ldots, x_n(t_j^*))$ resides, then once the orthant boundary is crossed, the trajectory evolves towards the new focal point associated with the new orthant. Because the focal point is constant for all points $(x_1, x_2, \ldots, x_n)$ within an orthant, the vector field of Eq. (2) transversally crosses the orthant's boundaries.

A directed graph can be associated with the dynamics of Eq. (2) as follows. The geometric dual of the 2^n orthants is the n-cube graph, denoted by Q_n, with each vertex corresponding to an orthant and edges connecting vertices whose orthants share an $n - 1$ dimensional boundary. Letting $V(Q_n)$ be the vertex set (we will omit the explicit dependence on Q_n unless needed), then $u \in V$ can be represented by an n-dimensional binary tuple: $u = X_1 X_2 \cdots X_n$, where $X_i = 0$ if $x_i < 0$, or $X_i = 1$ if $x_i > 0$ in the orthant u. The distance between two vertices u, v is the Hamming distance: $d_H(u, v)$, defined to be the number of components that differ between u and v. Letting $E(Q_n)$ be the edge set, it contains pairs of vertices: uv such that $d_H(u, v) = 1$. The edges are the images of the orthant boundaries in phase space. Since Eq. (2) defines a vector field that transversally crosses all the orthant boundaries, we can unambiguously associate a direction (or orientation) to each edge based on the direction of the vector field flow across the boundaries. We let $\mathbf{Q}_n$ denote a directed n-cube graph, and $\mathbf{E}(\mathbf{Q}_n)$ be the set of ordered pairs of vertices.

All edge orientations are defined via the regulation functions $B_1, B_2, \ldots, B_n$ in Eq. (2). In particular, the orientation depends only on whether $B_i > 0$ or $B_i < 0$. This motivates us to define functions f_i such that f_i depends on the same regulators (R_i) as

B_i, with $f_i = 0$ if $B_i < 0$ and $f_i = 1$ if $B_i > 0$. Additionally, it will be useful to introduce the notation that for $R_i = \{i_1, i_2, \ldots, i_K\}$ and a vertex $u \in V$, then $u_{R_i} \equiv u_{i_1} u_{i_2} \ldots u_{i_K}$, a tuple of the K components of u. Edge orientations may then be defined as follows. Let $u, v \in V$ be two adjacent vertices such that $u_i = v_i$ for $i \neq j$, for some $j \in [1, n]$, and $u_j = 0$ (implying $v_j = 1$). The edge is oriented from u to v if $f_j(u_{R_j}) = 1$ and it is oriented v to u if $f_j(u_{R_j}) = 0$. Since $j \notin R_j$, we can equivalently determine the edge direction by evaluating f_j at vertex v, with the edge oriented from u to v if $f_j(v_{R_j}) = 1$ and from v to u if $f_j(v_{R_j}) = 0$. The orientation of all edges adjacent to a vertex defines the possible flows across the boundaries of that orthant in phase space.

The quantities $(R_i, f_i)_{i=1}^n$ define the regulatory structure of Eq. (2), and we will primarily work with f_i rather than the functions B_i. This is advantageous since many of our results hold for any choice of B_i such that the sign of B_i is consistent with the definition of f_i.

The function f_i depends only on the binary states of the R_i components of $u \in V$, and as such, can be represented via a truth-table. For example, if $R_i = \{1, 2, 3\}$ then explicitly, $f_i(u_1 u_2 u_3)$ would be of the form

u_1	u_2	u_3	f_i
0	0	0	a
0	0	1	b
0	1	0	c
0	1	1	d
1	0	0	e
1	0	1	f
1	1	0	g
1	1	1	h

where $a, b, \ldots, h \in \{0, 1\}$. An equivalent representation is to define f_i to be the sequence of values: $f_i = abc \cdots h$ which along with the ordering $R_i = \{1, 2, 3\}$ uniquely determines a function of this form. Reordering the regulators $R_i = \{3, 1, 2\}$ then necessarily requires a reordering of f_i to maintain the same function.

In the particular case of each species being regulated by all $n - 1$ other species, which we term *full regulation*, and denote by $\hat{R}_i$ and $\hat{f}_i$, then one can show that there is a one-to-one map from each element of the truth-table definition of f_i and edges in $\mathbf{Q}_n$ [Glass, 1975].

2.1. *Cyclic attractors*

The correspondence between Eq. (2) and directed n-cubes goes beyond providing a geometric perspective of the differential equations. Properties of the solutions to Eq. (2) can be inferred from the topology of the directed n-cube [Glass & Pasternack, 1978b; Snoussi & Thomas, 1993; Plahte & Kjøglum, 2005].

Definition 2.1. Cycles in the n-cube.

- A cycle C in Q_n is a sequence of vertices $u^i \in V$: $C = u^1 u^2 \cdots u^L$ such that $u^i u^{i+1} \in E(Q_n)$ for $i = [1, L-1]$ and $u^L u^1 \in E(Q_n)$.
- A vertex $v \notin C$ but for which $d_H(u, v) = 1$, with $u \in C$, is called *adjacent* to the cycle C.
- A directed cycle $\mathbf{C}$ in $\mathbf{Q}_n$ is defined the same as a cycle C, but with the edges $u^i u^{i+1}$ in $\mathbf{E}(\mathbf{Q}_n)$ (with $u^{L+1} = u^1$).
- Let $\mathbf{C}$ be a directed cycle and $u \in \mathbf{C}$. There are $(n - 2)$ vertices adjacent to u that are not in $\mathbf{C}$. If each $v \notin \mathbf{C}$ that is adjacent to u is such that $vu \in \mathbf{E}$ for all $u \in \mathbf{C}$, then $\mathbf{C}$ is a **cyclic attractor**. An n-dimensional cyclic attractor $\mathbf{C}$ is only present in m-cubes with $m \geq n$ and we only consider the smallest dimension in which it is present.

The concept of cyclic attractors is related to notion of *snakes* on discrete graphs introduced by Harary *et al.* [1988]. Directed cycles $\mathbf{C} = u^1 u^2 \cdots u^L$ in n-cubes can be conveniently represented via their *coordinate sequence* (see [Glass, 1977a; Edwards & Glass, 2000]) $c = c^1 c^2 \cdots c^L$, where c^i is defined to be the coordinate that differs between u^i and u^{i+1} (with c^L the coordinate that changes between u^L and u^1). The starting vertex u^1 is arbitrary in the definition of c so that cyclical permutations of c are equivalent. The conditions for $\mathbf{C}$ to be a cyclic attractor in Definition 2.1 lead to an equivalent set of conditions for the coordinate sequence.

Definition 2.2. (From [Glass, 1977a]) Let $\mathbf{C}$ be a directed cycle and $c = c^1 c^2 \cdots c^L$ the coordinate sequence of $\mathbf{C}$. Then $\mathbf{C}$ can be an n-dimensional cyclic attractor if c satisfies the following conditions:

(1) Each coordinate in c must appear an even number of times.
(2) For any sequence of consecutive steps of length less than L, at least one coordinate must appear an odd number of times.

(3) For $L \geq 6$ then every consecutive subsequence $c^j c^{j+1} \cdots c^{j+\mu-1}$, where μ is an odd integer such that $3 \leq \mu \leq L-3$, must contain at least three coordinates which appear an odd number of times.

The first two conditions in Definition 2.2 are necessary for c to define a cycle that does not contain any shorter cycles. The third condition ensures that the edges adjacent to the cycle can be directed towards the cycle, making it attracting. This corresponds to the condition in Definition 2.1 that all nonadjacent vertices of the cycle be at least distance 2 apart.

As stated in Sec. 2, the regulatory structure defined by $(R_i, f_i)_{i=1}^n$ orients the n-cube. The following lemma establishes a connection between cyclic attractors and the orientation of the n-cube produced by $(R_i, f_i)_{i=1}^n$.

Lemma 2.1. *Letting* $\mathbf{C} = u^1 u^2 \cdots u^L$ *be a directed cycle and* $(R_i, f_i)_{i=1}^n$ *be the regulatory structure for Eq. (2) that orients* $\mathbf{Q}_n$. *Then,* $\mathbf{C}$ *is in* $\mathbf{Q}_n$ *if and only if* $f_i(u_{R_i}^j) = u_i^{j+1}$ *for all* $i \in [1, n]$ *and* $j \in [1, L]$ *(with* $u^{L+1} = u^1$*).*

Proof. Let $(R_i, f_i)_{i=1}^n$ be a regulatory structure for Eq. (2). Consider vertex u^j in $\mathbf{C}$. The conditions for a cyclic attractor are that the directed edge $u^j u^{j+1}$ be in $\mathbf{E}(\mathbf{Q}_n)$ and that the remaining $n-1$ adjacent edges in $\mathbf{E}$ be directed towards u^j. Let c^j be the component which changes between u^j and u^{j+1} (taken modulo L with $L \bmod L = L$). The directed edge $u^j u^{j+1}$ requires that $f_{c^j}(u_{R_{c^j}}^j) = u_{c^j}^{j+1}$. For the other $n-1$ edges adjacent to u^j to be directed towards u^j then $f_i(u_{R_i}^j) = u_i^j$ for $i \neq c^j$.

However, $u_i^j = u_i^{j+1}$ for $i \neq c^j$, since c^j is the only component that differs between u^j and u^{j+1}. Hence, we have $f_i(u_{R_i}^j) = u_i^{j+1}$ for $i \in [1, n]$ and $j \in [1, L]$. ∎

The connection between cyclic attractors and limit cycles was used to prove that if Eq. (2) produces an orientation of the n-cube with a cyclic attractor then a stable limit cycle exists (for $n \geq 3$) when $B_i \in \{\pm 1\}$ [Glass & Pasternack, 1978b]. In $n = 3, 4, 5$ dimensions there are 1, 3 and 18 equivalence classes of cyclic attractors, with two cyclic attractors termed equivalent if they are super imposable under a symmetry operation of the n-cube. They have all been enumerated and are reported here in Table 1 [Glass, 1977a].

Table 1. The different equivalence classes of cyclic attractors $\mathbf{C}$ in $n = 3, 4, 5$ dimensions [Glass, 1977a]. For ease in referring to the attractors later, we include an index that enumerates the attractors in each dimension. The coordinate sequence c representation of a cyclic attractor is stated in the third column. In the fourth column we report the number of unique ways that $\mathbf{C}$ can appear in $\mathbf{Q}_n$.

n	Index	c	# of Unique Orientations
3	1	123123	8
4	1	12341234	48
	2	12341243	192
	3	12314324	96
5	1	1234512345	384
	2	1234512354	1920
	3	1234513254	1920
	4	1234512534	3840
	5	1234521534	3840
	6	1234512543	1920
	7	1234513524	3840
	8	1234521543	1920
	9	1234531524	3840
	10	1231435425	768
	11	123145123145	960
	12	123145123154	1920
	13	123145132154	960
	14	123142153145	1920
	15	123142154135	960
	16	12314251231425	1920
	17	12314215321424	3840
	18	12314215231425	3840

2.2. *Symmetries of the n-cube*

The symmetry group of the n-cube graph Q_n, denoted O_n, consists of $n!2^n$ operations, each of which acts on the vertices $V(Q_n)$ (see [Coxet, 1973] for a detailed description of O_n). With the binary labeling of vertices, the elements of O_n can be defined as compositions of two simple operations: permutations and inversions. Letting $u \in V$, we define a permutation operator σ_Σ, where Σ is a permutation of $\{1, 2, \ldots, n\}$, to be $\sigma_\Sigma(u) = u_\Sigma$. The inversion operator ψ_Ψ, where $\Psi \subseteq \{1, 2, \ldots, n\}$ is such that $v = \psi_\Psi(u)$ has $v_i = u_i$ for $i \notin \Psi$ and $v_i = \bar{u}_i$ for $i \in \Psi$, where $\bar{0} = 1$ and $\bar{1} = 0$. The elements μ of O_n are the compositions of the $n!$ permutations and 2^n inversions: $\mu = \psi_\Psi \circ \sigma_\Sigma$.

O_n is defined entirely in terms of operations on the vertices. The symmetry operations of O_n partition oriented n-cubes into equivalence classes. Letting $\mathbf{Q}_n, \mathbf{H}_n$ be two directed n-cubes, then they belong to the same equivalence class if there exists $\mu \in O_n$ such that $\mu(\mathbf{Q}_n) = \mathbf{H}_n$, where equality means they have the same edge set. Within an

equivalence class, a subset of the symmetry operations are invariant. We define $I(\mathbf{Q}_n)$ to be the set of $\mu \in O_n$ such that $\mu(\mathbf{Q}_n) = \mathbf{Q}_n$.

The symmetry operations can also be applied to the coordinate sequence representation of a cyclic attractor. Because the coordinate sequence lists the changing coordinates, they are invariant under the inversion operator. For instance, the coordinate sequences $c = 1234512354$ and $\kappa = 1254321543$ define two cyclic attractors that belong to the same class (the second cyclic attractor in five-dimensions in Table 1). The permutation σ_Σ with $\Sigma = \{5, 4, 3, 2, 1\}$ is such that $\sigma_\Sigma(\kappa)$ is equivalent to c, since coordinate sequences can be cyclically shifted and still define the same cyclic attractor. Coordinate sequence κ is obtained from c via the same permutation.

The invariant symmetries $I(\mathbf{Q}_n)$ corresponding to a regulatory network of the form in Eq. (2) can provide a method for identifying discrete symmetries of the differential equations. However, in general, Eq. (2) will only share these symmetries when the values of B_i possess symmetry properties too. For instance, if $B_i \in \{\pm a\}$ (for $a \neq 0$) then $\mu \in I(\mathbf{Q}_n)$ is a symmetry of Eq. (2), with permutations operating on the indices i of x_i and inversions $X \to \overline{X}$ replaced by reflections $x \to -x$.

2.3. *Minimal networks*

Thus far we have focused on identifying the directed n-cube arising from the regulatory system Eq. (2) and deducing properties of the differential equations via analysis of the n-cube (cyclic attractors, symmetries, etc.). We now address the inverse problem: Given an orientation of an n-cube, identify the regulatory system: $(R_i, f_i)_{i=1}^n$ which produces that orientation. Once identified, any choice of B_i that is consistent with f_i yields a differential equations system [Eq. (2)]. Lemma 2.1 provides a set of constraints that the regulatory network must satisfy for a given cyclic attractor. One approach is to reformulate the constraints in terms of Boolean satisfiability. Zinovik *et al.* [2007] used an approach similar to this to obtain lower bounds on the number of equivalence classes of cyclic attractors.

Rather than working directly with Lemma 2.1, our method of solving the inverse problem is based on reducing the admissible set of regulatory equations of the form Eq. (2) which correspond to a directed n-cube. We define a **minimal regulatory network** to be a set of $(R_i, f_i)_{i=1}^n$ which yields

the desired orientation of an n-cube such that the number of regulators, $|R_i|$, is minimized for each i ($|\cdot|$ denotes cardinality). Before presenting our algorithm, we discuss two simple examples which illustrate our approach.

Consider an $n = 3$ dimensional system. The discretization of phase space arising results in a 3-cube Q_3 (see Fig. 1). From Table 1, there is only one equivalence class of cyclic attractors in the 3-cube [Glass, 1977a]. For the statement of the inverse problem, we require a specific instance of the cyclic attractor, shown in bold in Figs. 1(a) and 1(b). The cyclic attractor is the directed cycle: $\mathbf{C} = 000 \to 100 \to 110 \to 111 \to 011 \to 001 \to 000$, along with orienting the remaining six edges to make it attracting. With full regulation ($R_i = \hat{R}_i$) then each edge direction is associated with a single component of $\hat{f}_i$, as shown in Fig. 1(a). Thus, we find that the fully regulated network is given by:

$$
\begin{aligned}
\hat{R}_1 = \{2, 3\} & \quad \hat{f}_1 = 1010 \\
\hat{R}_2 = \{1, 3\} & \quad \hat{f}_2 = 0011 \\
\hat{R}_3 = \{1, 2\} & \quad \hat{f}_3 = 0101.
\end{aligned}
\tag{4}
$$

Inspection of Eq. (4) reveals that in fact each $\hat{f}_i$ only effectively depends on a single regulator. Removing this superfluous dependence, we obtain the minimal regulatory network:

$$
\begin{aligned}
R_1 = \{3\} & \quad f_1 = 10 \\
R_2 = \{1\} & \quad f_2 = 01 \\
R_3 = \{2\} & \quad f_3 = 01,
\end{aligned}
\tag{5}
$$

which is shown in Fig. 1(b).

Although the analysis and identification of the minimal network for the cyclic attractor shown in Fig. 1 was straightforward in $n = 3$, in higher dimensions several complications arise. First, not all edges in the n-cube will be oriented by specifying a cyclic attractor. Such *partially* oriented n-cubes can lead to degeneracies in the identification of regulatory functions f_i, further complicating the problem of identifying R_i such that $|R_i|$ is minimal. Second, for $n \geq 5$ cyclic attractors can have more than one possible choice for (R_i, f_i) that minimizes $|R_i|$. The following cyclic attractor in $n = 5$ dimensions demonstrates such issues and motivates our algorithm that addresses them.

$$
\begin{aligned}
C = 00101 &\to 01101 \to 11101 \to 11100 \\
&\to 11110 \to 11010 \to 01010 \to 00010 \\
&\to 00011 \to 00001 \to 00101 \to \cdots.
\end{aligned}
$$

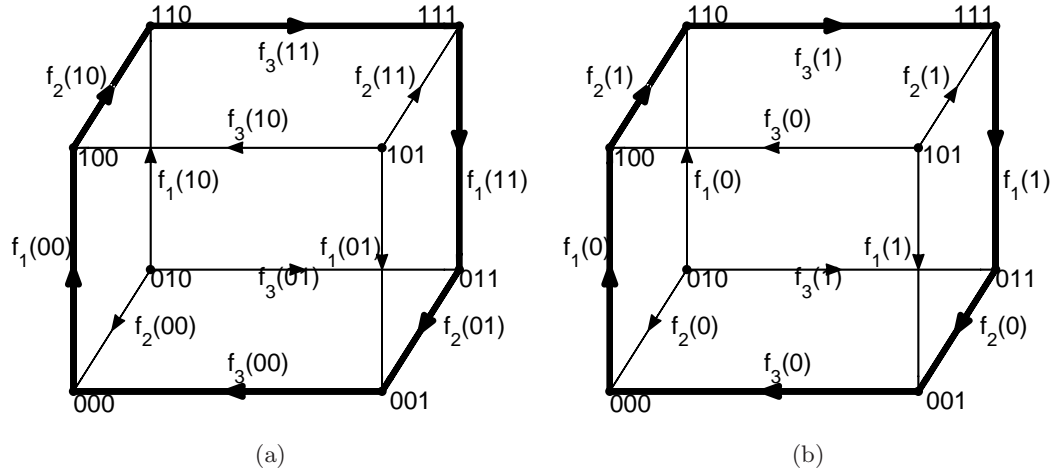(a)   (b)

Fig. 1.   A particular instance of the $n = 3$ dimensional cyclic attractor (both (a) and (b)). The regulatory functions f_i that determine the orientation of each edge are shown. In (a) we assume that each species is regulated by the other two (i.e. full regulation $R_i = \hat{R}_i$) resulting in each edge corresponding to a single component of $\hat{f}_i$. The arguments of each $\hat{f}_i$ indicate the states of the regulators: $\hat{f}_1(X_2X_3)$, $\hat{f}_2(X_1X_3)$, and $\hat{f}_3(X_1X_2)$. Plot (b) shows that a single regulator for each species is sufficient, with $f_1(X_3) = 10$, $f_2(X_1) = 01$ and $f_3(X_2) = 01$.

This is the second five-dimensional attractor in Table 1, with coordinate sequence $c = 2154312543$. In Sec. 2.2 the permutation operation that transforms c to 1234512354 (the listing in Table 1) was found to be σ_Σ with $\Sigma = \{5, 4, 3, 2, 1\}$. Orienting the 5-cube $\mathbf{Q}_5$ such that this cycle is attracting and mapping the edge directions to components of $\hat{f}_1, \ldots, \hat{f}_5$, under the assumption of full regulation we find:

u_2	u_3	u_4	u_5	$\hat{f}_1$
0	0	0	0	·
0	0	0	1	0
0	0	1	0	0
0	0	1	1	0
0	1	0	0	·
0	1	0	1	0
0	1	1	0	·
0	1	1	1	·
1	0	0	0	·
1	0	0	1	·
1	0	1	0	0
1	0	1	1	·
1	1	0	0	1
1	1	0	1	1
1	1	1	0	1
1	1	1	1	·

u_1	u_3	u_4	u_5	$\hat{f}_2$
0	0	0	0	·
0	0	0	1	0
0	0	1	0	0
0	0	1	1	0
0	1	0	0	·
0	1	0	1	1
0	1	1	0	·
0	1	1	1	·
1	0	0	0	·
1	0	0	1	·
1	0	1	0	1
1	0	1	1	·
1	1	0	0	1
1	1	0	1	1
1	1	1	0	1
1	1	1	1	·

u_1	u_2	u_4	u_5	$\hat{f}_3$
0	0	0	0	·
0	0	0	1	1
0	0	1	0	0
0	0	1	1	0
0	1	0	0	·
0	1	0	1	1
0	1	1	0	0
0	1	1	1	·
1	0	0	0	·
1	0	0	1	·
1	0	1	0	·
1	0	1	1	·
1	1	0	0	1
1	1	0	1	1
1	1	1	0	0
1	1	1	1	·

u_1	u_2	u_3	u_5	$\hat{f}_4$
0	0	0	0	1
0	0	0	1	0
0	0	1	0	·
0	0	1	1	0
0	1	0	0	1
0	1	0	1	·
0	1	1	0	·
0	1	1	1	0
1	0	0	0	·
1	0	0	1	·
1	0	1	0	·
1	0	1	1	·
1	1	0	0	1
1	1	0	1	·
1	1	1	0	1
1	1	1	1	0

u_1	u_2	u_3	u_4	$\hat{f}_5$
0	0	0	0	1
0	0	0	1	1
0	0	1	0	1
0	0	1	1	·
0	1	0	0	·
0	1	0	1	0
0	1	1	0	1
0	1	1	1	· ·
1	0	0	0	·
1	0	0	1	·
1	0	1	0	·
1	0	1	1	·
1	1	0	0	·
1	1	0	1	0
1	1	1	0	0
1	1	1	1	0

A "·" indicates that the edge was not oriented by the cyclic attractor and hence the component of $\hat{f}_i$ can be 0 or 1. If we attempt to specify a network in the form of Eq. (2) with these regulator choices, then there are eight arbitrary components of the $\hat{f}_i$ to choose for each species, amounting to a total of 40. Thus, there are $2^{40} \approx 1$ trillion networks that have this cyclic attractor. This motivates us to identify networks with the fewest arbitrary components by minimizing the number of regulators, which results in fewer networks corresponding to a given cyclic attractor.

Input: $\mathbf{Q}_n$, a (partially) directed n-cube
Output: Minimal regulatory network(s) $(R_i, f_i)_{i=1}^n$
Assign components of $\hat{f}_i$ (being $0, 1$ or $\cdot$) assuming full regulation $\hat{R}_i$;
for $i = 1$ **to** n **do**
 for $K = 0$ **to** n **do**
  foreach *combination* $R \subseteq \hat{R}_i$ *of* K *regulators* **do**
   Let f be a truth-table function of K binary variables
   foreach *binary tuple* w *of length* K **do**
    Let u be a binary tuple of length $n - 1$
    Set $u_R = w$
    Let $S = \hat{R}_i \setminus R$ be the $n - 1 - K$ regulators not in R
    Initialize $f(w) = \cdot$
    foreach *binary tuple* v *of length* $n - 1 - K$ **do**
     Set $u_S = v$
     if ($\hat{f}_i(u) = 0$ *and* $f(w) = 1$) *or* ($\hat{f}_i(u) = 1$ *and* $f(w) = 0$) **then**
      R is an invalid regulator set. Proceed to next R
     else
      Set $f(w) = \hat{f}_i(u)$
     end
    end
   end
  Have identified R, f that are valid regulators R_i, f_i
  end
 If all valid R_i, f_i are identified, continue to next i
 end
end

Algorithm 1. Algorithm for finding the regulators R_i and functions f_i that orient the edges consistent with a specified $\mathbf{Q}_n$. Note that $A \backslash B$ is the set A, minus the elements that are in B.

Proceeding as we did in the previous $n = 3$ case to identify reduced sets of regulators that yield consistent regulation functions, we find that the regulation of $\hat{f}_3$ can be simplified to $R_3 = \{4\}$ with $f_3 = 10$. For $i = 4$ we see that $R_4 = \{5\}$ with $f_4 = 10$. For species 1 and 2 we find that each requires at least two regulators, with $R_1 = \{2, 3\}$, $f_1 = 0001$ and $R_2 = \{1, 3\}$, $f_2 = 0111$ as the only choices. Thus, for $i = 1, 2, 3, 4$, by choosing the minimum number of regulators we have also removed all arbitrariness in f_i. If we now turn our attention to $i = 5$, there are no solutions with 1 or 2 regulators. There are two possible choices of regulation that depend on 3 species: $R_5 = \{1, 2, 3\}$ with $f_5 = 1101 \cdot \cdot 00$ or $R_5 = \{1, 2, 4\}$ with $f_5 = 1110 \cdot \cdot 00$. By considering only minimal networks we have reduced the approximately 1 trillion possibilities to 8 (2 choices for R_5 and 2^2 possibilities for f_5).

These two illustrative examples motivate our algorithm for finding minimal networks from (partially) oriented n-cubes, stated in Algorithm 1.

The computational cost of the algorithm is dependent on the minimal number of regulators per species. The worst case occurs when each species has full regulation, requiring us to check

$$\sum_{k=0}^{n-1} \binom{n-1}{k} 2^k$$

combinations for the regulation of species i. Making use of the binomial expansion, the sum simplifies to 2^{n-1}. Since there are n species, there are $n2^{n-1}$ possible regulatory combinations that must be considered in the worst case.

3. Families of Cyclic Attractors

The symmetries of the n-cube create equivalence classes for cyclic attractors, with two attractors being equivalent if they are related by a symmetry operation. Another notion of equivalences can be defined for attractors in different dimensions n, which we call *families*. A family of cyclic attractors

can be defined in terms of properties shared by their coordinate sequence representations. For instance, the first attractors listed in dimensions $n = 3, 4$ and 5 have the common form $c = 12\cdots n12\cdots n$. We show in Sec. 3.1 that this family gives rise to minimal networks that are *cyclic, negative feedback* systems, which have been well studied in other contexts [Hastings *et al.*, 1977; Thomas & D'Ari, 1990; Mallet-Paret & Smith, 1990; Gedeon, 1998]. The second family of attractors considered is defined by a different coordinate sequence characteristic, described in Sec. 3.2. We find that the resulting minimal networks have a form known as *sequential disinhibition* [Székely, 1965; Kling & Székely, 1968].

3.1. *Cyclic, negative feedback*

The simplest family of cyclic attractors corresponds to the coordinate sequence $c = c^1 c^2 \cdots c^{2n}$ having the form

$$c = s_1 s_2 \cdots s_n s_1 s_2 \cdots s_n, \qquad (6)$$

where $\{s_1, \ldots, s_n\}$ is a permutation of $\{1, \ldots, n\}$. From Definition 2.2 this defines a cyclic attractor for $n \geq 2$. In Theorem 3.1 we prove that minimal networks for cyclic attractors of the form in Eq. (6) have regulators R_i that form a cyclic regulatory system (that is the regulation has the form $R_i = \{i-1\}$ and $R_1 = \{n\}$, under suitable relabeling) with the f_i functions being either inhibitory ($f_i = 10$) or activating ($f_i = 01$). In Theorem 3.2 we show that there must be an odd number of inhibitory interactions implying that the network is a *cyclic, negative feedback* system [Thomas & D'Ari, 1990; Gedeon, 1998].

The number of different n-cube orientations with this cyclic attractor can be enumerated via the coordinate sequence representation in Eq. (6). There are $n!$ permutations that preserve the structure of Eq. (6). A particular orientation of the cyclic attractor can then be generated by choosing any of the 2^n vertices and constructing the cycle via the coordinate sequence, yielding $n!2^n$ attractors. However, this over counts by a factor of $2n$, since shifting the coordinate sequence and shifting the starting vertex of the cycle yields the same cycle. Therefore, there are $(n-1)!2^{n-1}$ unique orientations of the n-cube with the cyclic attractor of Eq. (6) (consistent with the results reported in the fourth column of Table 1).

Theorem 3.1. *Let* $\mathbf{C} = u^1 u^2 \ldots u^n u^{n+1} \ldots u^{2n}$ *be a cyclic attractor in n-dimensions, such that the*

coordinate sequence c for $\mathbf{C}$ is of the form in Eq. (6). Then the regulatory network with $R_{s_i} = \{s_{i-1}\}$ and

$$f_{s_i}(v_{R_{s_i}}) = \begin{cases} v_{s_{i-1}} & \text{if } u^i_{s_{i-1}} = u^i_{s_i}, \\ \overline{v}_{s_{i-1}} & \text{if } u^i_{s_{i-1}} = \overline{u}^i_{s_i}, \end{cases}$$

is the minimal network which orients the n-cube with the cyclic attractor $\mathbf{C}$.

Proof. Assume that $\mathbf{C}$ and c are as defined in the Theorem. Throughout this proof, u^j is interpreted as $u^{j \bmod 2n}$, with $0 \bmod 2n = 2n$. It is readily seen that u^j_i satisfies

$$u^j_{s_i} = \begin{cases} \overline{\alpha} & \text{for } j \in [i+1, i+n] \\ \alpha & \text{for } j \in [i+n+1, i] \end{cases}, \qquad (7)$$

with $\alpha = u^i_{s_i} \in \{0, 1\}$. The intervals $[i+1, i+n]$ and $[i+n+1, i]$ are interpreted modulo $2n$ when the right end point exceeds $2n$ (i.e. $[5, 2]$ with $n = 3$ is equivalent to $[5, 6] \cup [1, 2]$).

From Lemma 2.1 we have that f_i must be such that $f_i(u^j_{R_i}) = u^{j+1}_i$ for $j \in [1, 2n]$ and $i \in [1, n]$ with a suitable choice of R_i. Omitting the R_i subscript for the moment, then Eq. (7) implies

$$f_{s_i}(u^j) = \begin{cases} \overline{\beta} & \text{if } j \in [i, i+n-1] \\ \beta & \text{if } j \in [i+n, i-1] \end{cases}, \qquad (8)$$

for $i \in [1, n]$ and an appropriate choice of $\beta \in \{0, 1\}$. Equation (8) in light of Eq. (7) reveals that f_{s_i} depends on only the s_{i-1} component of u^j, hence $R_{s_i} = \{s_{i-1}\}$.

To determine the particular functional form that $f_{s_i}(v)$ must take, we compare the values of $u^{j+1}_{s_i}$ and $u^j_{s_{i-1}}$. These are fixed for $j \in [i+1, i+n]$ so it suffices to consider only whether $u^{i+1}_{s_i}$ and $u^i_{s_{i-1}}$ are the same or not. If they are equal, then $f_{s_i}(u^j)$ must take on the value of $u^j_{s_{i-1}}$ and hence $f_{s_i}(v) = v_{s_{i-1}}$. If they differ, then we see that $f_{s_i}(v) = \overline{v}_{s_{i-1}}$.

R_{s_i} is clearly the minimal set of regulators since it consists of only one regulator, and it is the only regulator that satisfies Eq. (8) for all $j \in [1, 2n]$. ∎

Theorem 3.2. *The regulatory network* $(R_i, f_i)^n_{i=1}$ *obtained via Theorem 3.1 contains an odd number of inhibitions.*

Proof. Assume that $\mathbf{C}, c$ and R_I, f_i are as specified via Theorem 3.1. The conditions for f_{s_i} to be

activating or inhibitory are

$$u_{s_i}^{i+1} = u_{s_{i-1}}^i \quad \text{if } f_{s_i} \text{ is activating}$$
$$u_{s_i}^{i+1} = \overline{u}_{s_{i-1}}^i \quad \text{if } f_{s_i} \text{ is inhibitory.} \tag{9}$$

We define the variable δ_i to encode the two situations for f_{s_i}. When f_{s_i} is activating then $\delta_i = 0$ and if f_{s_i} is inhibitory then $\delta_i = 1$. The two conditions in Eq. (9) can then be expressed as

$$u_{s_i}^{i+1} + u_{s_{i-1}}^i \quad \text{mod } 2 = \delta_i. \tag{10}$$

Letting i take on the values 1 to $2n$ (with $s_i = s_{i \bmod n}$) we obtain a set of $2n$ equations. However, only n of them are independent. For $i = n$ we observe that $u_{s_n}^{n+1} = \overline{u}_{s_n}^1$ from the definition of the coordinate sequence c, yielding a set of n equations with n unknowns. Letting $\alpha_i = u_{s_{i-1}}^i$, the n equations are

$$\alpha_i + \alpha_{i+1} = \delta_i \quad \text{mod } 2 \quad i = 1, \dots, n-1$$
$$\alpha_n + (1 - \alpha_1) = \delta_n \quad \text{mod } 2, \tag{11}$$

where we have made use of $\overline{\alpha} = 1 - \alpha \bmod 2$. These n equations can be reduced to the single condition

$$\sum_{i=1}^{n} \delta_i = 1 \quad \text{mod } 2. \tag{12}$$

Since $\delta_i \in \{0, 1\}$ then there must be an odd number of $\delta_i = 1$ in order for there to exist α_i (and hence $u_{s_{i-1}}^i$) satisfying Eq. (10). $\delta_i = 1$ corresponds to f_{s_i} being inhibitory, thus there must be an odd number of inhibitory regulation functions present.   ∎

We remark that Theorem 3.2 is consistent with studies of regulatory systems which fall outside of the piecewise linear model Eq. (2) (see [Thomas & D'Ari, 1990] for example).

3.2. *Sequential disinhibition*

The second family of cyclic attractors we shall consider have minimal regulatory networks known as *sequential disinhibition* systems [Székely, 1965; Kling & Székely, 1968]. These cyclic attractors have a coordinate sequence $c = c^1 c^2 \cdots c^{2n}$ of the form

$$c = s_2 s_1 s_3 s_2 \cdots s_n s_{n-1} s_1 s_n, \tag{13}$$

where $\{s_1, s_2, \dots, s_n\}$ is a permutation of $\{1, 2, \dots, n\}$. By construction, Eq. (13) satisfies the requirements of a cyclic attractor given in Definition 2.2.

The number of ways the n-cube can be oriented with this cyclic attractor can be counted via the coordinate sequence representation in Eq. (13). There are $n!$ permutations that preserve the structure of Eq. (13). A particular orientation of the cyclic attractor can then be generated by choosing any of the 2^n vertices as the initial vertex of the cycle and constructing the cycle via the coordinate sequence, yielding $n!2^n$ attractors. However, this results in an over counting by a factor of n, since shifting the coordinate sequence by an even number of positions and shifting the starting vertex of the cycle by the same number of positions yields the same cycle. Therefore, there are $(n-1)!2^n$ unique orientations of the n-cube with this cyclic attractor (consistent with the results in Table 1).

Theorem 3.3. *Let* $\mathbf{C} = u^1 u^2 \cdots u^{2n}$ *be a cyclic attractor in n-dimensions, such that the coordinate sequence for* $\mathbf{C}$ *is* $c = c^1 c^2 \cdots c^{2n} = s_2 s_1 s_3 s_2 \dots s_n s_{n-1} s_1 s_n$, *with* $\{s_1, \dots, s_n\}$ *a permutation of* $\{1, \dots, n\}$. *Then the regulatory network with* $R_{s_i} = \{1, 2, \dots, n\} \backslash \{s_i, s_{i-1}\}$ *and* f_{s_i} *is given by*

$$f_{s_i}(v_{R_{s_i}}) = \begin{cases} u_{s_i}^{\chi_i+1} & \text{if } v_{R_{s_i}} = u_{R_{s_i}}^{\chi_i} \\ \overline{u}_{s_i}^{\chi_i+1} & \text{otherwise} \end{cases},$$

is a minimal network which orients the n-cube such that $\mathbf{C}$ *is a cyclic attractor.*

Proof. Assume that $c = c^1 c^2 \cdots c^{2n}$ has the form $c = s_2 s_1 s_3 s_2 \cdots s_n s_{n-1} s_1 s_n$ where $\{s_1, s_2, \dots, s_n\}$ is a permutation of $\{1, 2, \dots, n\}$. Furthermore, let $\mathbf{C} = u^1 u^2 \cdots u^{2n}$ be the vertices of the cyclic attractor. Define χ_i such that $c^{\chi_i} = s_i$ and $c^{\chi_i+3 \bmod 2n} = s_i$, where $2n \bmod 2n = 2n$. χ_i is uniquely defined provided $n \geq 4$, while for $n = 3$ we specify $\chi_1 = 2$, $\chi_2 = 1, \chi_3 = 3$. χ_i indexes the element in c where component s_i changes such that it again changes three steps later in the cycle.

We now proceed analogous to the proof of Theorem 3.1. Lemma 2.1 implies that f_{s_i} must satisfy $f_{s_i}(u_{R_{s_i}}^j) = u_{s_i}^{j+1}$. From the definition of c we find that $u_{s_i}^j$ is described by

$$u_{s_i}^j = \begin{cases} \alpha & \text{if } j \in [\chi_i + 1, \chi_i + 3] \\ \overline{\alpha} & \text{if } j \in [\chi_i + 4, \chi_i] \end{cases}, \tag{14}$$

where $\alpha \in \{0, 1\}$ and the intervals are taken modulo $2n$ (i.e. $[5, 2]$ with $n = 3$ is equivalent to $[5, 6] \cup [1, 2]$). Insertion of Eq. (14) into Lemma 2.1 yields

$$f_{s_i}(u_{R_{s_i}}^j) = \begin{cases} \alpha & \text{if } j \in [\chi_i, \chi_i + 2] \\ \overline{\alpha} & \text{if } j \in [\chi_i + 3, \chi_i - 1] \end{cases}. \tag{15}$$

We proceed by identifying the minimal set of regulators R_{s_i} such that Eq. (15) holds.

Inspection of c reveals that for $j \in [\chi_i, \chi_i + 2]$ (one of the ranges in Eq. (15)) two components of u^j change: s_i and s_{i-1}. Thus, since f_{s_i} is constant over that range then $s_i, s_{i-1} \notin R_{s_i}$. Defining $\Lambda_i = \{s_1, s_2, \ldots, s_n\} \backslash \{s_i, s_{i-1}\}$, then $R_{s_i} \subseteq \Lambda_i$.

Claim. $R_{s_i} = \Lambda_i$.

To prove this, we must show that $\Lambda_i \subseteq R_{s_i}$ (the other inclusion has already been shown). Suppose that $\Lambda_i \supset R_{s_i}$. Then, there must be $\Omega \subset \Lambda_i$ for which $R_{s_i} = \Omega$, since Lemma 2.1 guarantees the existence of an R_{s_i}.

Assume that $\Omega = \Lambda_i \backslash \{s_m\}$, for some $m \notin \{i, i-1\}$. To show that $R_{s_i} \neq \Omega$ we find $j \in [\chi_i, \chi_i + 2]$ and $k \in [\chi_i + 3, \chi_i - 1]$ such that $u_\Omega^j = u_\Omega^k$ implying that $\alpha = \overline{\alpha}$ from Eq. (15), a contradiction.

We claim that $j = \chi_i$ and $k = \chi_m + 3$ are such that $u_\Omega^j = u_\Omega^k$. This is easily seen if we inspect $c^{\chi_i} \cdots c^{\chi_m+3} = s_i s_{i-1} s_{i+1} s_i \cdots s_{m-1} s_{m-2} s_m s_{m-1}$. The only components that appear an odd number of times are s_{i-1} and s_m. Therefore, u^{χ_i} and u^{χ_m+3} differ only in those two coordinates, but agree in all others. Hence, $u_\Omega^{\chi_i} = u_\Omega^{\chi_m+3}$ and it follows that Ω cannot be a regulator set for f_{s_i}. Although we only considered Ω which had a single element removed from Λ_i, we see that this argument holds for the removal of an arbitrary number of elements from Λ_i. Hence, we have shown $R_{s_i} \subseteq \Lambda_i$.

Therefore, $R_{s_i} = \{s_1, s_2, \ldots, s_n\} \backslash \{s_i, s_{i-1}\}$.

Returning to Eq. (15) we thus find that f_{s_i} is such that

$$f_{s_i}(v_{R_{s_i}}) = \begin{cases} \alpha & \text{if } v_{R_{s_i}} = u_{R_{s_i}}^{\chi_i}, \\ \overline{\alpha} & \text{otherwise} \end{cases}$$

where $\alpha = u_{s_i}^{\chi_i+1}$. ∎

The specification of f_{s_i} in Theorem 3.3 is not the most generic one. For $n \geq 5$ there are arbitrary components of f_{s_i}; however, the choice in Theorem 3.3 is a consistent choice. Additionally, with c as defined in Eq. (13) there are two particular choices for the initial vertex of the cyclic attractor u^1 which yield particularly simple forms for f_i. First, if u^1 is such that $u_{s_1}^1 = 0$ and $u_{s_i}^1 = 1$ for $i > 1$ then $f_i = 11 \cdots 10$. That is, f_i is a *not or* function of its regulators R_i. Second, if u^1 is such that $u_{s_1}^1 = 1$ and $u_{s_i}^1 = 0$ for $i > 1$ (the inverse of the previous u^1) then $f_i = 100 \ldots 0$, which is a *not and* function of its regulators. These two results follow directly from application of Theorem 3.3 to the particular cycles $\mathbf{C}$ that are produced from c and the two choices of u^1.

4. Continuous Homologues with Stable Limit Cycles

The results of Secs. 3.1 and 3.2 yield regulatory networks that have limit cycle oscillations in arbitrary dimensions. Equation (2) is an approximation to the chemical kinetics that are typically used to describe such systems. In particular, the Heaviside function $H(x)$ may be replaced by a sigmoidal function $h(x)$ that smoothly changes from low to high levels. We make use of a general method (see for example [Glass, 1977b; Glass & Pasternack, 1978a; Plahte *et al.*, 1998; Plahte & Kjøglum, 2005]) of transforming the piecewise linear equations of Eq. (2) into smooth versions with a piecewise linear limit. Such systems have been termed continuous homologues of Eq. (2) by [Glass & Pasternack, 1978b].

Assume that B_i in Eq. (2) takes on only values ± 1. It then follows that $B_i = 2f_i - 1$, from the definition of f_i. This transforms Eq. (2) into

$$\dot{x}_i(t) = -\gamma x_i(t) + 2f_i(X_{R_i}) - 1, \quad i \in [1, n]. \quad (16)$$

The first step in constructing the continuous homologue of Eq. (16) is to obtain the min-term expansion of f_i [Harrison, 1965]. Letting $R_i = \{i_1, \ldots, i_K\}$, then for each combination of inputs $X_{i_1} X_{i_2} \cdots X_{i_K}$ that has $f_i(X_{i_1} \cdots X_{i_K}) = 1$, we define a product of the K regulator variables, with X_{i_m} appearing if $X_{i_m} = 1$ in the input value and $(1 - X_{i_m})$ appearing if $X_{i_m} = 0$ in the input value. Adding together all such terms we obtain an algebraic expression for f_i.

For instance, if $R_i = \{1, 2\}$ and $f_i = 1011$, then in truth-table format we have

X_1	X_2	f_i
0	0	1
0	1	0
1	0	1
1	1	1

Observing that $f_i = 1$ if $X_1 X_2 = 00$, $X_1 X_2 = 10$ or $X_1 X_2 = 11$ then from the first combination $X_1 X_2 = 00$, we obtain the term $(1 - X_1) \times (1 - X_2)$. $X_1 X_2 = 10$ contributes $X_1 \times (1 - X_2)$ and $X_1 X_2 = 11$ contributes $X_1 \times X_2$. f_i is then represented by adding all contributions, yielding $f_i = (1 - X_1)(1 - X_2) + X_1(1 - X_2) + X_1 X_2$ (omitting the explicit multiplication symbol $\times$). This simplifies to $f_i = 1 - X_2 + X_1 X_2$.

The continuous homologue of Eq. (16) is then obtained by replacing $X_i = H(x_i)$ in the algebraic expression for f_i by $X_i = h(x_i, \eta)$. We require $h(x, \eta)$ to be a smooth sigmoidal function that monotonically increases from 0 to 1 and which approaches the Heaviside function as $\eta \to \infty$. Defining $\mathcal{F}_i$ as the function obtained by replacing X_i with h_i in the min-term expansion of f_i, then the continuous homologue of Eq. (2) is

$$\dot{x}_i = -\gamma_i x_i + 2\mathcal{F}_i(x_{R_i}, \eta) - 1. \qquad (17)$$

There are several natural choices for $h(x, \eta)$ (see for example [Glass & Pasternack, 1978a; Hertz *et al.*, 1991]), such as

Hill $\qquad \dfrac{x^\eta}{q^\eta + x^\eta}$

tanh $\qquad \dfrac{1}{2}(1 + \tanh(\eta x))$.

arctan $\qquad \dfrac{1}{\pi}\left(\dfrac{\pi}{2} + \arctan(\eta x)\right)$

In the Appendix the tanh function is used to construct continuous homologues of all the cyclic attractors in $n = 3, 4$ and 5.

4.1. *Stable limit cycles in continuous homologues of cyclic negative feedback systems*

With mild assumptions on the function $h(x, \eta)$ used in the derivation of the homologous versions for the cyclic negative feedback networks that were derived in Sec. 3.1 we present a proof that for η sufficiently large then an asymptotically stable limit cycle exists provided it is hyperbolic.

Assume that $h(x, \eta) = (1 + Z(x, \eta))/2$ where $Z(x, \eta)$ is a monotonically increasing function of x from -1 to $+1$. Additionally, assume $Z(x, \eta)$ is an odd function of x and that the partial derivative of Z, with respect to x, evaluated at $x = 0$, is an increasing function of η. This final condition implies that $Z(x = 0, \eta)$ gets steeper as η increases.

Recall from Theorem 3.1 that f_i is either an activating or inhibitory function. Define κ_i to be 1 if f_i is activating and $\kappa_i = -1$ if f_i is inhibitory. Without loss of generality, assume that $R_i = \{i-1\}$ with $R_1 = \{n\}$. Finally, we rescale time by a factor of γ. Then, the cyclic, negative feedback continuous homologue of Eq. (16) is

$$\dot{x}_i = -x_i + \kappa_i Z(x_{i-1}, \eta). \qquad (18)$$

From Theorem 3.2 we know that there are an odd number of f_i which are inhibitory implying an odd

number of $\kappa_i = -1$. Since Eq. (18) is a cyclic system with monotonic interaction functions, then the Poincaré–Bendixson theory developed by Mallet-Paret and Smith [1990] can be applied. Theorem 4.2 in [Mallet-Paret & Smith, 1990] applied to Eq. (18) implies that if there is a unique fixed point x^* and the linearized system about x^* has at least two eigenvalues with positive real part then a hyperbolic limit cycle is asymptotically stable. We do not pursue the feature of hyperbolicity here, but will prove that Eq. (18) satisfies the assumptions of Theorem 4.2.

From Eq. (18), $x^* = (0, 0, \ldots, 0)$ is always a fixed point solution since Z is an odd function of x_i. Further, we claim that it is the unique fixed point solution of Eq. (18). To prove this, observe that Eq. (18) is invariant under the transformation:

$$\begin{aligned} x_i &\to x_{i+1} && \text{if } \kappa_{i+1} = 1 \\ x_i &\to -x_{i+1} && \text{if } \kappa_{i+1} = -1 \end{aligned}, \quad \text{for } i = 1, \ldots, n$$

where $x_{n+1} = x_1$. This transformation cyclically shifts all indices by 1, and since $Z(x, \eta)$ is an odd function, then the reflection when $\kappa_i = -1$ retains the correct sign. Since Eq. (18) is invariant under this operation, so too are fixed point solutions x^*. Let M be the transformation described above. Then M has the matrix representation

$$M = \begin{pmatrix} 0 & \kappa_2 & 0 & 0 & \ldots & 0 \\ 0 & 0 & \kappa_3 & 0 & \ldots & 0 \\ \vdots & & \ddots & & & \vdots \\ \kappa_1 & 0 & 0 & \ldots & 0 & 0 \end{pmatrix}.$$

Thus, x^* must satisfy $x^* = Mx^*$ or equivalently, $(I - M)x^* = 0$ where I is the n by n identity matrix. The determinant of $I - M$ is

$$\det(I - M) = 1 - (-1)^n \prod_{i=1}^{n}(-\kappa_i). \qquad (19)$$

The sign of the product is determined by how many κ_i are 1. Since there are always an odd number of $\kappa_i = -1$ then if n is even, there are an odd number of $\kappa_i = 1$ while if n is odd, there are an even number. Because the product is multiplied by $(-1)^n$ it follows that $\det(I - M) = 2$ for all n. Therefore, $x^* = (0, 0, \ldots, 0)$ is the unique solution of $x^* = Mx^*$.

We now characterize the eigenvalue structure of Eq. (18), linearized about x^*. Letting $\zeta_i = x_i - x_i^*$ the first order expansion of Eq. (18) is

$$\dot{\zeta}_i = -\zeta_i + \rho \kappa_i \zeta_{i-1}, \qquad (20)$$

where

$$\rho = \frac{\partial Z}{\partial x}(0, \eta) \tag{21}$$

is the derivative with respect to x of Z, evaluated at the fixed point $x^* = 0$. In matrix form, Eq. (20) is $\dot{\zeta} = A\zeta$, where the matrix A has eigenvalues λ_k given by

$$\lambda_k = -1 + \rho \exp\left(i\frac{(2k+1)\pi}{n}\right),$$
$$k = 0, \ldots, n-1, \tag{22}$$

where i in Eq. (22) is the unit imaginary number. We see that λ_0 and λ_{n-1} are the complex conjugates with largest real part. At $\rho^* = (\cos(\pi/n))^{-1}$ they transversally cross the imaginary axis (away from the origin) and thus a Hopf bifurcation occurs. This is closely related to the *secant* condition that has been studied previously for cyclic feedback systems [Tyson & Othmer, 1978; Thron, 1991; Arcak & Sontag, 2006]. Since ρ is an increasing function of η, it follows that for η sufficiently large, then there are eigenvalues with positive real part. Thus, hyperbolic periodic orbits of Eq. (18) are asymptotically stable.

5. Discussion

In this paper and the Appendix, we present stable, robust limit cycle oscillations for regulatory systems described by Eq. (2). In the course of this work, we have identified a number of open questions and conjectures, which we briefly discuss.

5.1. *Symmetries of the n-cube and structure of the regulatory functions*

There is an interesting interplay between the symmetries of the n-cube and the minimal regulatory structure (R_i, f_i) derived from it. Although two different embeddings of a cyclic attractor may be symmetrically equivalent, the functional form of the regulatory functions can differ. For instance, the cyclic attractor in $n = 3$ dimensions has eight symmetrically equivalent embeddings in the 3-cube (see Table 1). Six of these embeddings correspond to permutations of the minimal network

$$\begin{aligned} R_1 &= \{3\} & f_1 &= 10 \\ R_2 &= \{1\} & f_2 &= 01 \\ R_3 &= \{2\} & f_3 &= 01, \end{aligned} \tag{23}$$

while the other two embeddings are permutations of

$$\begin{aligned} R_1 &= \{3\} & f_1 &= 10 \\ R_2 &= \{1\} & f_2 &= 10 \\ R_3 &= \{2\} & f_3 &= 10. \end{aligned} \tag{24}$$

From a regulatory systems perspective, these two networks differ substantially in that the first contains activating ($f_i = 01$) interactions while the second consists of only inhibiting ($f_i = 10$) interactions. In biophysical systems, these differences in the type of regulation can play an important role (see for instance [Mangan & Alon, 2003]) even though from a mathematical perspective the networks are in the same equivalence class. The classical feedback inhibition networks of biochemical systems correspond to Eq. (23) [Thomas & D'Ari, 1990; Gedeon, 1998], whereas Eq. (24) with three inhibitory elements corresponds to sequential disinhibition [Kling & Székely, 1968; Glass & Young, 1979]. Thus, the underlying logical structure of the repressilator circuit developed by Elowitz and Leibler [2000] which consists of a loop with three elements, each of which inhibits the next in turn, was known to provide a basis for oscillations well before the circuit was synthesized in bacteria.

5.2. *Equivalence classes of cyclic attractors in high dimensions*

For $n \geq 6$ the equivalence classes of cyclic attractors have not been found, although some lower bounds have been computed [Zinovik *et al.*, 2007]. A possible approach would be to use the coordinate sequence representation: c, of a cyclic attractor. It is simple to determine if c is a cyclic attractor via Definition 2.2. However, determining if two different coordinate sequences define cyclic attractors that are in the same equivalence class is difficult. Exhaustively searching all $n!$ permutation operations (recall the coordinate sequence representation is invariant to inversions) to see if there exists an operation that maps one to the other, is not computationally feasible for large n.

An alternative method is to integrate Eq. (2) assuming it is a cyclic attractor. If the periods of the limit cycles differ, then they do not belong to the same equivalence class. Since the equations are piecewise linear, exact integration can be performed to find the period accurately, subject only to machine precision. However, since two nonequivalent networks might have the same period, further

analysis would have to be carried out to check the symmetries of all networks having the same period.

5.3. *Impact of dimension n on robustness of limit cycles*

Analysis of the bifurcation diagrams in the Appendix reveals the following trend: as n increases, the value of η for which a stable limit cycle emerges decreases. This was also identified in Sec. 4.1 for the cyclic negative feedback system (ρ^* decreased as n increased). We believe that this suggests that as the dimension n increases the constraints on the flows in phase space needed for stable limit cycles is such that the attracting properties of the cyclic attractors become less important. If this holds, then in high dimensions one could construct robust regulatory networks from cycles that are *almost* cyclic attractors; having a few adjacent edges that are not directed towards the cycle. This would dramatically increase the number of different regulatory systems exhibiting limit cycle oscillations.

5.4. *Impact of the properties of Boolean functions on symmetries of the n-cube*

There are many different classifications of Boolean functions such as monotone functions [Harrison, 1965], canalizing functions [Kauffman, 1993; Aldana *et al.*, 2003], and Post classes [Post, 1921; Shmulevich *et al.*, 2003]. Although there has been some research on the properties of Boolean switching networks when the logical functions are restricted to certain classes [Kauffman, 1993; Aldana *et al.*, 2003], we are not aware of similar investigation into the properties of Eq. (2). In particular, it would be worthwhile to investigate connections between the properties of the Boolean functions and the symmetries of the oriented n-cube. For instance, many of the five-dimensional cyclic attractors considered in the Appendix have minimal networks with f_i that contain arbitrary components. Depending on how these arbitrary components are chosen the resulting regulatory structure may or may not preserve the invariant symmetries of the cyclic attractor.

5.5. *Minimal covering formulation of the minimal network problem*

In Sec. 2.3 an algorithm for finding the minimal network, given a (partially) oriented n-cube $\mathbf{Q}_n$,

was described. An alternative formulation of the problem is in terms of disjoint coverings of the n-cube. Recall that the task is to find $(R_i, f_i)_{i=1}^n$ with $|R_i|$ minimized, such that for all binary tuples u of length $n-1$ with $\hat{f}_i(u) \neq \cdot$, then $f_i(u_{R_i}) = \hat{f}_i(u)$, where $\hat{f}_i$ is directly obtained from $\mathbf{Q}_n$ under the assumption of full regulation.

Rather than viewing $\hat{f}_i$ as a Boolean function of $n-1$ variables, instead consider an $n-1$ dimensional cube. Color each vertex of this cube as follows:

(i) Black if $\hat{f}_i = 0$, when evaluated at the binary labeling of the vertex.
(ii) White if $\hat{f}_i = 1$, when evaluated at the binary labeling of the vertex.
(iii) Uncolored if $\hat{f}_i = \cdot$, when evaluated at the binary labeling of the vertex.

Next, define a k-cube of an m-cube (with $0 \leq k \leq m$) to be a subgraph of the m-cube graph, such that the subgraph has the topology of a k-cube. A convenient representation of a k-cube is to use a generalization of a binary tuple as follows. Let w be an m-dimensional tuple such that the components w_i satisfy $w_i \in \{0, 1, *\}$ for $i \in [1, m]$. By setting $m - k$ of the components of w to be 0 or 1, and the remaining k components set to $*$, then a k-cube is defined by letting $*$ take on all 2^k possible combinations of 0 and 1. For instance, letting $m = 3$ and considering a $k = 1$-cube defined to be $w = 0 * 1$, the vertices of the 3-cube that are in the subgraph w are 001 and 011, along with the edge between them.

We introduce the notion of a *k-cube parallel covering* of the m-cube (denoted W_π) as follows. Let π be a subset of $m - k$ distinct elements chosen from $\{1, 2, \ldots, m\}$. Define W_π to be the set of all 2^{m-k} possible ways of defining w such that $w_i \in \{0, 1\}$ for $i \in \pi$ and $w_i = *$ for $i \notin \pi$. For instance, returning to the $m = 3$ example considered with $w = 0 * 1$, then this 1-cube is one member of W_π defined by $\pi = \{1, 3\}$. The remaining three 1-cubes that are in W_π would be: $0 * 0$, $1 * 0$ and $1 * 1$. By construction, the k-cube parallel covering W_π is a disjoint set of subgraphs that cover the m-cube.

It then follows that for a coloring of the $n-1$ cube determined by $\hat{f}_i$, suppose W_π defines a parallel covering of k-cubes, with each k-cube not containing both black and white vertices, and k is the largest such possible value. Then $R_i = \{i_{\pi_1}, i_{\pi_2}, \ldots, i_{\pi_{n-1-k}}\}$ is a minimal regulator set and the minimal regulatory function f_i is defined by the

color (if any vertices are colored) of each of the 2^{n-1-k} k-cubes in W_π.

The problem of finding a *k-cube parallel covering* of a colored n-cube appears closely related to classic problems in discrete Mathematics on coverings. We are not aware of a precise correspondence between this problem and any that have been previously studied, but would not be surprised if there are connections.

5.6. *Impact of symmetries on bifurcation structure*

In the Appendix we present a listing of the cyclic attractor equivalence classes in dimensions $n = 3, 4$ and 5. For each cyclic attractor, a particular choice of the oriented n-cube is chosen (from the many symmetrically equivalent ones) and a bifurcation analysis of the corresponding minimal regulatory network is presented.

If we transform the regulatory networks via the symmetry operations of the n-cube, is the bifurcation structure preserved? Numerical results (not shown) indicate that the precise properties of the bifurcation structure can change (such as the value of η where a Hopf bifurcation occurs). However, we have observed that the bifurcation diagrams of the different networks obtained via symmetry operations are qualitatively similar. Is there a global result implying that they must be homeomorphic under symmetry transformations of the n-cube?

6. Conclusions

We have presented a method of constructing and analyzing regulatory systems in arbitrary dimensions that possess stable limit cycles. Existence of robust, stable limit cycles is guaranteed in the case of piecewise linear regulatory systems. However, numerical bifurcation analysis of the continuous homologues derived for each cyclic attractor in dimensions 3–5 also found stable periodic dynamics. These observations support the conjecture that continuous homologue systems obtained from minimal networks for cyclic attractors have robust, stable limit cycles for suitable choices of the sigmoidal functions. The robustness of the dynamics to parameter perturbations highlights the role of the regulatory structure in determining the dynamics.

The analytic tractability of the piecewise linear paradigm allowed construction and insight into the properties of two families of cyclic attractors: cyclical negative feedback in Sec. 3.1 and

sequential disinhibition in Sec. 3.2. This approach can be applied to other families of cyclic attractors not considered here. Alternatively, analysis of the continuous homologues can be undertaken either numerically or using the symmetry properties (such as in Sec. 4.1) of the directed n-cube corresponding to the minimal network.

Rich bifurcation structures are identified in several of the attractors in five dimensions (see the Appendix). Typically supercritical Hopf bifurcations lead to stable limit cycles as η is increased. The 12th, 15th, 16th and 18th contain saddle-node limit cycle bifurcations. In these systems, there exists an interval of η with bistable behavior: both a stable fixed point and stable limit cycle exist, along with an unstable limit cycle. For the 12th, 16th and 18th attractors the unstable limit cycle collides with the fixed point in a subcritical Hopf bifurcation (as η is increased) resulting in a unique stable limit cycle. A homoclinic bifurcation occurs in the 14th and 15th attractors, with a stable limit cycle persisting as η increases.

In conclusion, we have developed a method for constructing differential equations that have a transparent logical structure and support robust limit cycles. Our method for constructing these equations is based solely on discrete mathematics and involves the analysis of symmetry properties of directed n-cubes and minimal coverings. Although, the resulting atlas of representative equations for minimal networks contains network architectures such as negative feedback and sequential disinhibition, to the best of our knowledge most of the network architectures that we identify here have never been identified in natural or man-made systems. Thus, the listing of the oscillatory networks in this work provides a basis for identification of such networks in natural systems, as well as providing information that can be used to synthesize these networks using biological or electronic components. Finally, the analysis and numerical studies suggest a large number of questions for future investigations.

References

Aldana, M., Coppersmith, S. & Kadanoff, L. P. [2003] "Boolean dynamics with random couplings,"

in *Perspectives and Problems in Nonlinear Science*, eds. Kaplan, E., Marsden, J. E. & Sreenivasan, K. R. (Springer, NY), pp. 23–89.

Arcak, M. & Sontag, E. D. [2006] "Diagonal stability of a class of cyclic systems and its connection with the secant criterion," *Automatica* **42**, 1531–1537.

Benner, S. A. & Sismour, A. M. [2005] "Synthetic biology," *Nature Rev. Genet.* **6**, 533–543.

Bogacki, L. & Shampine, L. F. [1989] "A 3(2) pair of Runge–Kutta formulas," *Appl. Math. Lett.* **2**, 1–9.

Coxet, H. S. M. [1973] *Regular Polytopes* (Dover, NY).

De Jong, H. [2002] "Modeling and simulation of genetic regulatory systems: A literature review," *J. Comput. Biol.* **9**, 67–103.

Doedel, E. J., Champneys, A., Fairgrieve, T., Kuznetsov, Y., Oldeman, B., Paffenroth, R., Sandstede, B., Wang, X. & Zhang, C. [2006] *AUTO-07P: Continuation and Bifurcation Software for Ordinary Differential Equations* (Concordia University, Montreal).

Edwards, R. & Glass, L. [2000] "Combinatorial explosion in model gene networks," *Chaos* **10**, 691–704.

Edwards, R. & Glass, L. [2006] "A calculus for relating the dynamics and structure of complex biological networks," in *Adventures in Chemical Physics*, A Special Volume of Advances in Chemical Physics, Vol. 132, eds. Berry, R. S. & Jortner, J. (John Wiley, NJ), pp. 151–178.

Elowitz, M. B. & Leibler, S. [2000] "A synthetic oscillatory network of transcriptional regulators," *Nature* **403**, 335–338.

Gardner, T. S., Cantor, C. R. & Collins, J. J. [2000] "Construction of a genetic toggle switch in Escherichia coli," *Nature* **403**, 339–342.

Gedeon, T. [1998] "Cyclic feedback systems," *Mem. Amer. Math. Soc.* **134**, 1–73.

Glass, L. & Kauffman, S. A. [1973] "The logical analysis of continuous, non-linear biochemical control networks," *J. Theor. Biol.* **39**, 103–129.

Glass, L. [1975] "Combinatorial and topological methods in nonlinear chemical kinetics," *J. Chem. Phys.* **63**, 1325–1335.

Glass, L. [1977a] "Combinatorial aspects of dynamics in biological systems," in *Statistical Mechanics and Statistical Methods in Theory and Applications*, ed. Landman, U. (Plenum, NY), pp. 585–611.

Glass, L. [1977b] "Global analysis of nonlinear chemical kinetics," in *Statistical Mechanics, Part B: Time Dependent Processes*, ed. Berne, B. (Plenum, NY), pp. 311–349.

Glass, L. & Pasternack, J. S. [1978a] "Prediction of limit cycles in mathematical models of biological oscillations," *Bull. Math. Biol.* **40**, 27–44.

Glass, L. & Pasternack, J. S. [1978b] "Stable oscillations in mathematical models of biological control systems," *J. Math. Biol.* **6**, 207–223.

Glass, L. & Young, R. E. [1979] "Structure and dynamics of neural network oscillators," *Brain Res.* **179**, 207–218.

Glass, L. & Mackey, M. C. [1988] *From Clocks to Chaos: The Rhythms of Life* (Princeton University Press, NJ).

Goodwin, B. C. [1963] *Temporal Organization in Cells* (Academic Press, NY).

Harary, F., Hayes, J. P. & Wu, H. J. [1988] "A survey of the theory of hypercube graphs," *Comput. Math. Appl.* **15**, 277–289.

Harrison, M. A. [1965] *Introduction to Switching and Automata Theory* (McGraw-Hill, NY).

Hastings, S., Tyson, J. J. & Webster, D. [1977] "Existence of periodic solutions for negative feedback equations," *J. Diff. Eqs.* **25**, 39–64.

Hasty, J., McMillen, D., Isaacs, F. & Collins, J. J. [2001] "Computational studies of gene regulatory networks: In numero molecular biology," *Nat. Rev. Genet.* **2**, 268–279.

Hertz, J., Krogh, A. & Palmer, R. G. [1991] *Introduction to the Theory of Neural Computation* (Addison Wesley, Reading, MA).

Horowitz, P. & Hill, W. [1989] *The Art of Electronics* (Cambridge University Press, NY).

Kauffman, S. A. [1969] "Metabolic stability and epigenesis in randomly constructed genetic nets," *J. Theor. Biol.* **22**, 437–467.

Kauffman, S. A. [1993] *The Origins of Order: Self-Organization and Selection in Evolution* (Oxford University Press, NY).

Kling, U. & Székely, G. [1968] "Simulation of rhythmic nervous activities," *Biol. Cybern.* **5**, 89–103.

Lu, L. & Edwards, R. [2010] "Structural principles for periodic orbits in glass networks," *J. Math. Biol.*, to appear.

Mallet-Paret, J. & Smith, H. L. [1990] "The Poincaré–Bendixson theorem for monotone cyclic feedback systems," *J. Dyn. Diff. Eqs.* **2**, 367–421.

Mangan, S. & Alon, U. [2003] "Structure and function of the feed-forward loop network motif," *Proc. Nat. Acad. Sci. U.S.A.* **100**, 11980–11985.

Mason, J., Linsay, P. S., Collins, J. J. & Glass, L. [2004] "Evolving complex dynamics in electronic models of genetic networks," *Chaos* **14**, 707–715.

Mestl, T., Plahte, E. & Omholt, S. W. [1995] "Periodic solutions in systems of piecewise-linear differential equations," *Dyn. Stab. Syst.* **10**, 179–193.

Novák, B. & Tyson, J. J. [2008] "Design principles of biochemical oscillators," *Nat. Rev. Mol. Cell Biol.* **9**, 981–991.

Perkins, T. J., Hallett, M. & Glass, L. [2004] "Inferring models of gene expression dynamics," *J. Theor. Biol.* **230**, 289–300.

Plahte, E., Mestl, T. & Omholt, S. W. [1998] "A methodological basis for description and analysis of systems

with complex switch-like interactions," *J. Math. Biol.* **36**, 321–348.

Plahte, E. & Kjøglum, S. [2005] "Analysis and generic properties of gene regulatory networks with graded response functions," *Physica D* **201**, 150–176.

Post, E. L. [1921] "Introduction to a general theory of elementary propositions," *Am. J. Math.* **43**, 163–185.

Shmulevich, I., Lahdesmaki, H., Dougherty, E. R., Astola, J. & Zhang, W. [2003] "The role of certain Post classes in Boolean network models of genetic networks," *Proc. Nat. Acad. Sci. U.S.A.* **100**, 10734–10739.

Snoussi, E. H. & Thomas, R. [1993] "Logical identification of all steady states: The concept of feedback loop characteristic states," *Bull. Math. Biol.* **55**, 973–991.

Székely, G. [1965] "Logical network for controlling limb movements in *Urodela*," *Acta Physiologica Acad. Sci. Hung.* **27**, 285–289.

Thomas, R. & D'Ari, R. [1990] *Biological Feedback* (CRC Press, Boca Raton, FL).

Thron, C. D. [1991] "The secant condition for instability in biochemical feedback control I. The role of cooperativity and saturability," *Bull. Math. Biol.* **53**, 383–401.

Tyson, J. J. & Othmer, H. G. [1978] "The dynamics of feedback control circuits in biochemical pathways," *Progress in Theoretical Biology*, pp. 1–62.

Winfree, A. T. [2001] *The Geometry of Biological Time* (Springer, NY).

Zinovik, I., Kroening, D. & Chebiryak, Y. [2007] "An algebraic algorithm for the identification of glass networks with periodic orbits along cyclic attractors," *Lecture Notes in Computer Science* **4545**, 140–154.

Appendix

Analysis of All Cyclic Attractors in Dimensions 3–5

For the numerical analysis of the cyclic attractors we choose the tanh based sigmoid function given by

$$h(x, \eta) = \frac{1}{2} \left(1 + \tanh(\eta x) \right), \qquad (A.1)$$

with the convention that $h_i = h(x_i, \eta)$. Upon choosing specific embeddings of the cyclic attractors (recall that there are many choices for the embedding, listed in Table 1), the minimal networks for each of the cyclic attractors in Table 1 are explicitly derived and the continuous homologues presented in Secs. A.1 through A.22. The second cyclic attractor in four dimensions and all attractors but the first one considered in five dimensions have either multiple possible regulator sets to choose from or arbitrary components in the regulatory functions. A particular set of regulators and assignment of the arbitrary components are chosen, and the resulting

minimal regulatory network definition is presented for each attractor. The attractors corresponding to the cyclical negative feedback and sequential disinhibition classes have several embeddings considered, highlighting the theoretical results that were obtained in Secs. 3.1 and 3.2. We summarize the solution structure for each minimal network with a figure containing four panels (a)–(d).

(a) The directed n-cube with the cyclic attractor in bold is shown. The minimal network $(R_i, f_i)_{i=1}^n$ is obtained from the (partially) oriented n-cube arising from orienting the cycle and adjacent edges. The completely oriented n-cube corresponds to the obtained $(R_i, f_i)_{i=1}^n$.

(b) Integrated dynamics (using an adaptive second order Runge–Kutta method [Bogacki & Shampine, 1989]) of the continuous homologue system with η fixed at a value such that stable periodic dynamics are present, based on the results in panel (c).

(c) Results of numerical bifurcation analysis of the continuous homologue system obtained using the AUTO-07p software tool [Doedel *et al.*, 2006]. Bifurcations (Hopf, Pitchfork and Homoclinic) are indicated via symbols that are identified in the figure legend. The extremum values of the solution x_1 are plotted as η varies. Fixed point solutions are shown in blue with solid lines stable and dashed unstable. Limit cycle solutions are in black with the maximum and minimum value of the limit cycle trajectory plotted at each η, with solid lines stable and dashed unstable.

(d) The period of the limit cycle solution for the continuous homologue system (also obtained via AUTO-07p). Exact integration of Eq. (16) yields the period of the piecewise limit ($\eta \to \infty$) which is shown by the dashed horizontal line.

In order to present the 4-cubes clearly, we only identify the outer vertex labels. The labels of the inner vertices have the first component being 0 with the last three components the same as the adjacent outer vertex which is labeled.

To present the directed 5-cubes that the cyclic attractors are embedded in, we use two 4-cubes. The latter four components of the vertex label are the same as used in the 4-cubes, described above. The left 4-cube has a 0 prefixed to the vertex labels and the right one has a 1. The edge connecting the left and right four-cubes is represented by the vertex being either solid or open. A solid vertex has

4072   *R. Wilds & L. Glass*

the edge corresponding to changing the first component of the vertex label directed towards that cube and vice versa for the open vertex symbols. For instance, an open vertex at label 1000 in the left 4-cube implies that the edge connecting 01000 (left 4-cube) to 11000 (right 4-cube) is directed from 01000 to 11000.

A.1. *Attractor 1 in three dimensions*

The single cyclic attractor in three-dimensions contains either one or three inhibitory interactions (proved in Sec. 3.1). For three inhibitions the regulatory system is

$$
\begin{aligned}
R_1 &= \{3\} & f_1 &= 10 \\
R_2 &= \{1\} & f_2 &= 10 \\
R_3 &= \{2\} & f_3 &= 10,
\end{aligned}
\tag{A.2}
$$

with continuous homologue

$$
\begin{aligned}
\dot{x}_1 &= -x_1 + 1 - 2h_3 \\
\dot{x}_2 &= -x_2 + 1 - 2h_1 \\
\dot{x}_3 &= -x_3 + 1 - 2h_2.
\end{aligned}
\tag{A.3}
$$

Bifurcation analysis confirms the theoretical results presented in Sec. 4.1 with the Hopf bifurcation occurring at $\eta = 2$. The solution structure of Eqs. (A.2) and (A.3) is shown in Fig. 2.

With a single inhibitory interaction, the regulatory system is

$$
\begin{aligned}
R_1 &= \{3\} & f_1 &= 10 \\
R_2 &= \{1\} & f_2 &= 01 \\
R_3 &= \{2\} & f_3 &= 01,
\end{aligned}
\tag{A.4}
$$
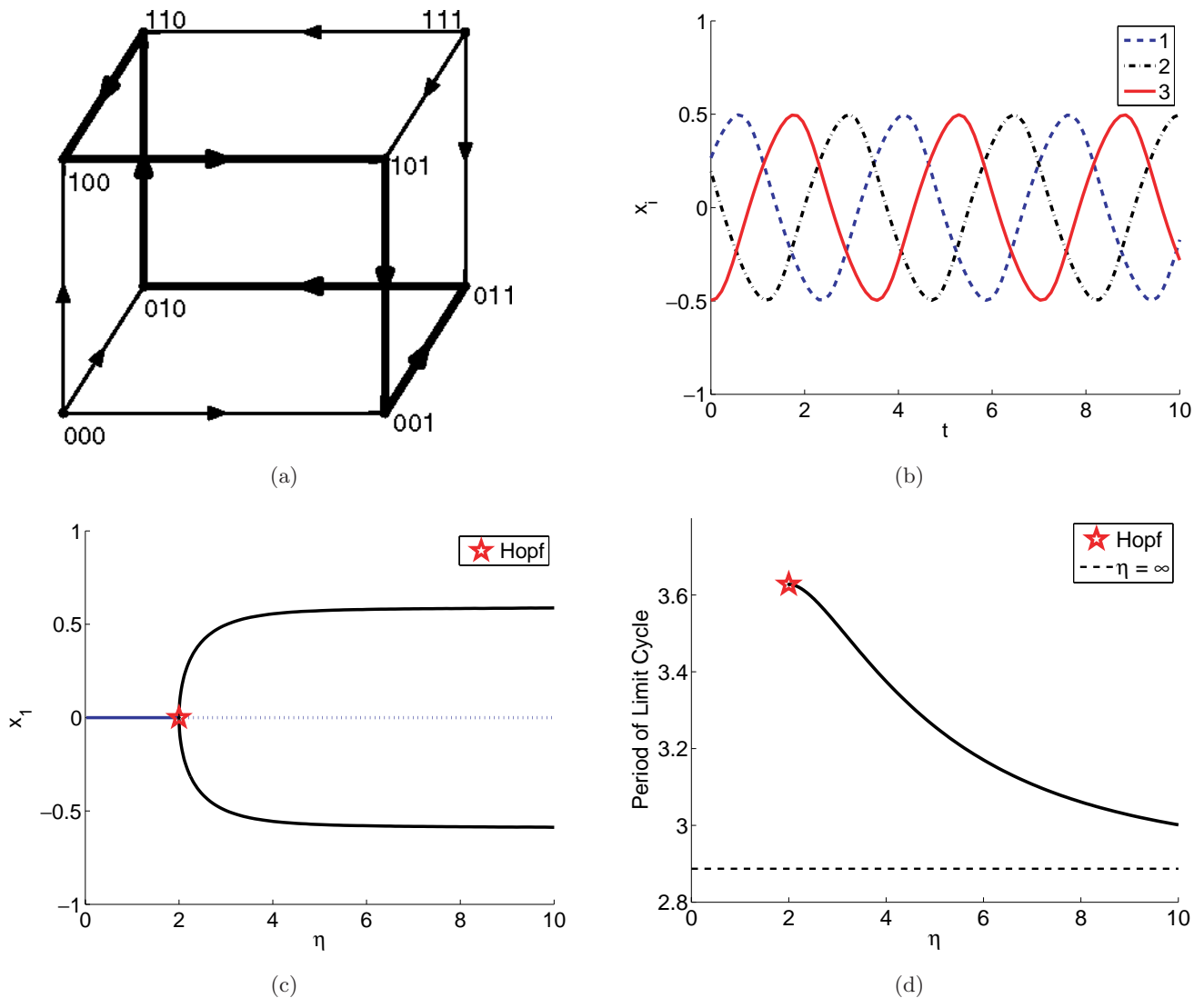
Fig. 2.   Solution structure of the first embedding considered for the single cyclic attractor in three dimensions [see Eq. (A.3)]. Trajectory in (b) has $\eta = 3$. Refer to the Appendix for an explanation of panels.

(a)

(b)

(c)

(d)
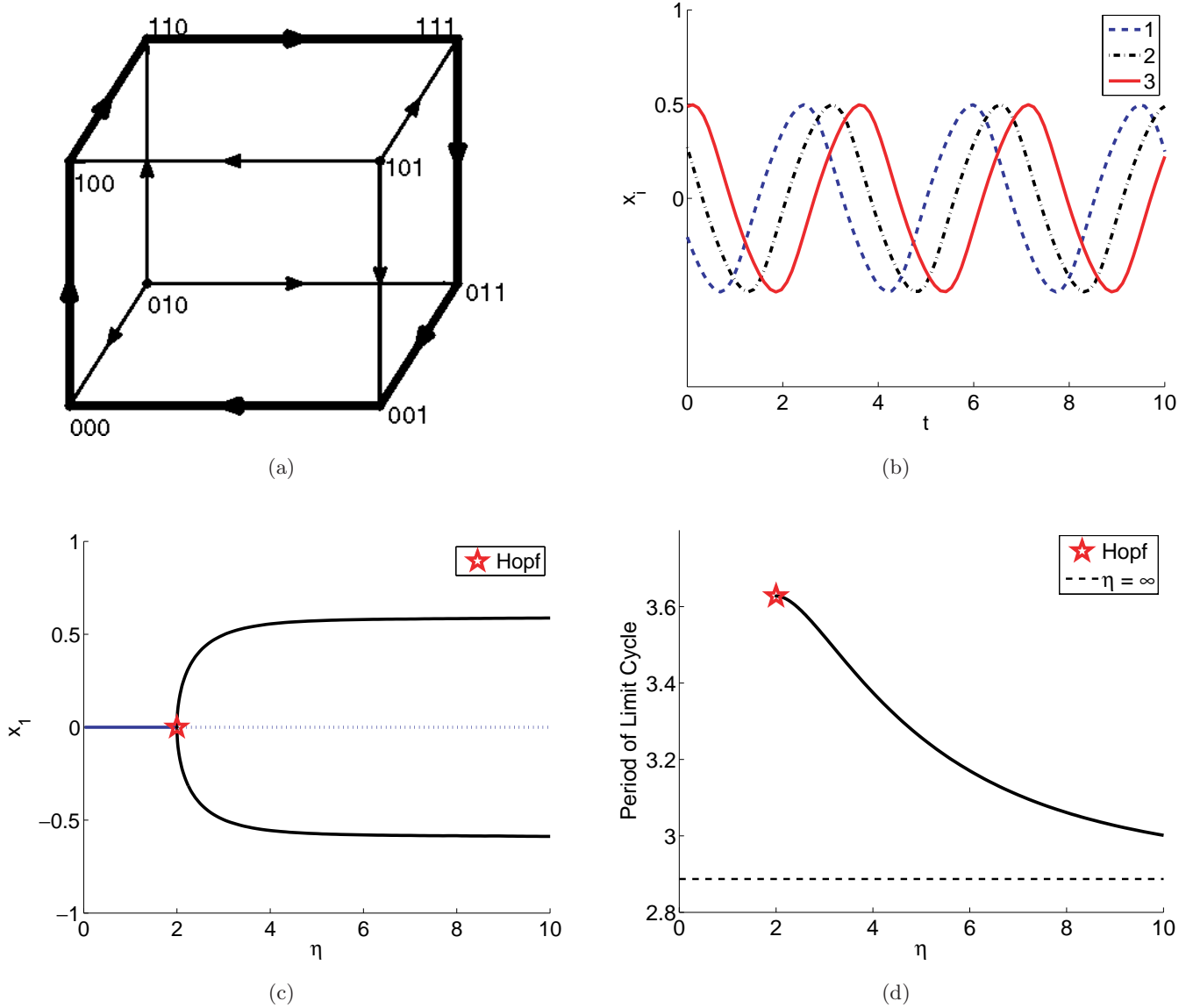
Fig. 3.   Solution structure of the second embedding considered for the single cyclic attractor in three dimensions [see Eq. (A.5)]. Trajectory in (b) has $\eta = 3$. Refer to the Appendix for an explanation of panels.

$$\begin{aligned}
\dot{x}_1 &= -x_1 + 1 - 2h_3 \\
\dot{x}_2 &= -x_2 + 2h_1 - 1 \\
\dot{x}_3 &= -x_3 + 2h_2 - 1.
\end{aligned} \qquad (A.5)$$

The solution structure of Eqs. (A.4) and (A.5) is shown in Fig. 3.

A.2. *Attractor 1 in four dimensions*

As for three dimensions, there are two choices for the cyclical negative feedback consisting of either three or one inhibitory interaction. We choose the case of three inhibitions, yielding

$$\begin{aligned}
R_1 &= \{4\} \quad f_1 = 01 \\
R_2 &= \{1\} \quad f_2 = 10 \\
R_3 &= \{2\} \quad f_3 = 10 \\
R_4 &= \{3\} \quad f_4 = 10,
\end{aligned} \qquad (A.6)$$

$$\begin{aligned}
\dot{x}_1 &= -x_1 + 2h_4 - 1 \\
\dot{x}_2 &= -x_2 + 1 - 2h_1 \\
\dot{x}_3 &= -x_3 + 1 - 2h_2 \\
\dot{x}_4 &= -x_4 + 1 - 2h_3.
\end{aligned} \qquad (A.7)$$

Numerical bifurcation analysis of Eq. (A.7) confirms the results of Sec. 4.1 with a supercritical bifurcation taking place. The solution structure of Eqs. (A.6) and (A.7) is shown in Fig. 4.

(a)

(b)

(c)

(d)
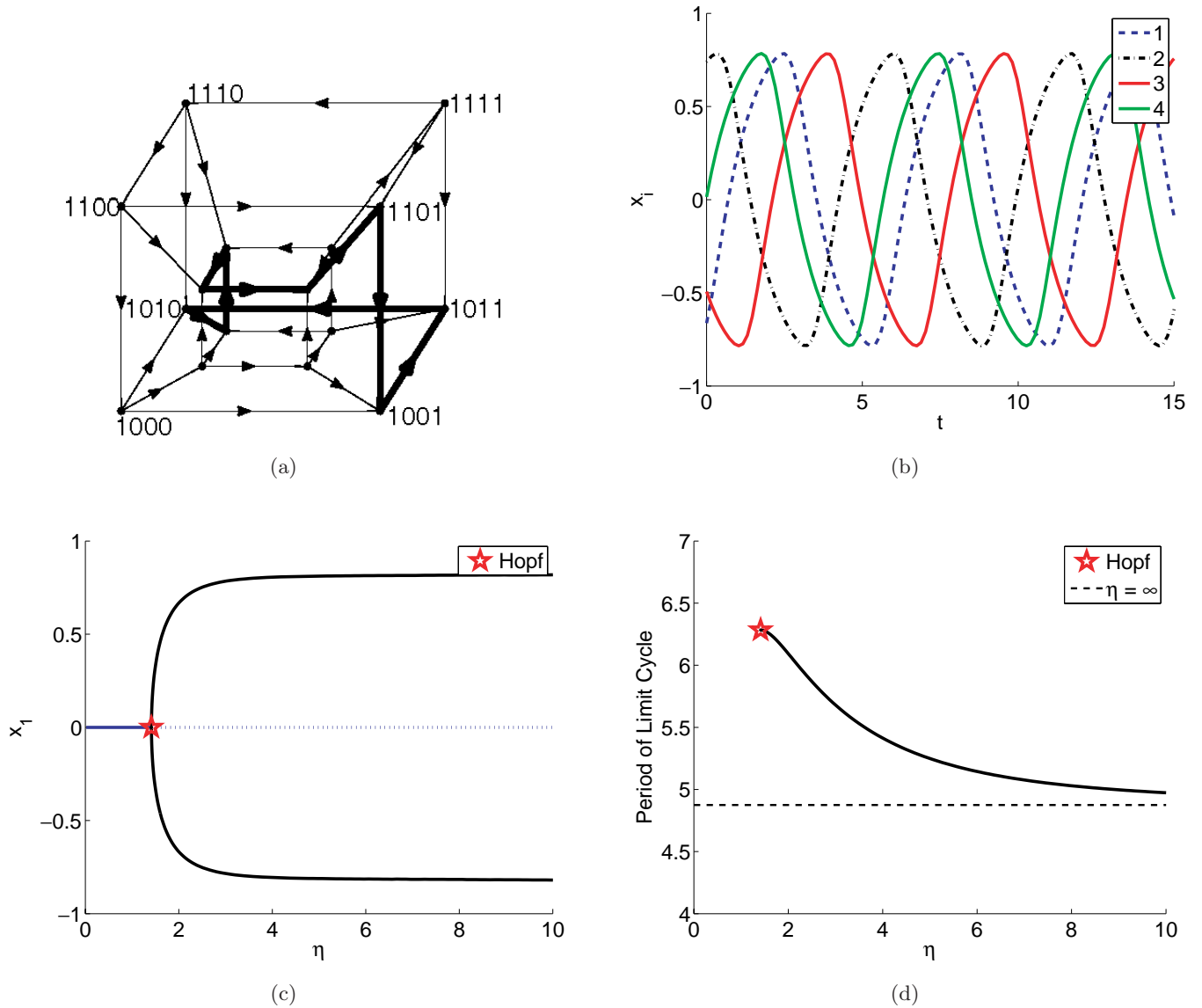
Fig. 4.   Solution structure of the first cyclic attractor in four dimensions [Eq. (A.7)]. Trajectory in (b) has $\eta = 3$. Refer to the Appendix for an explanation of panels.
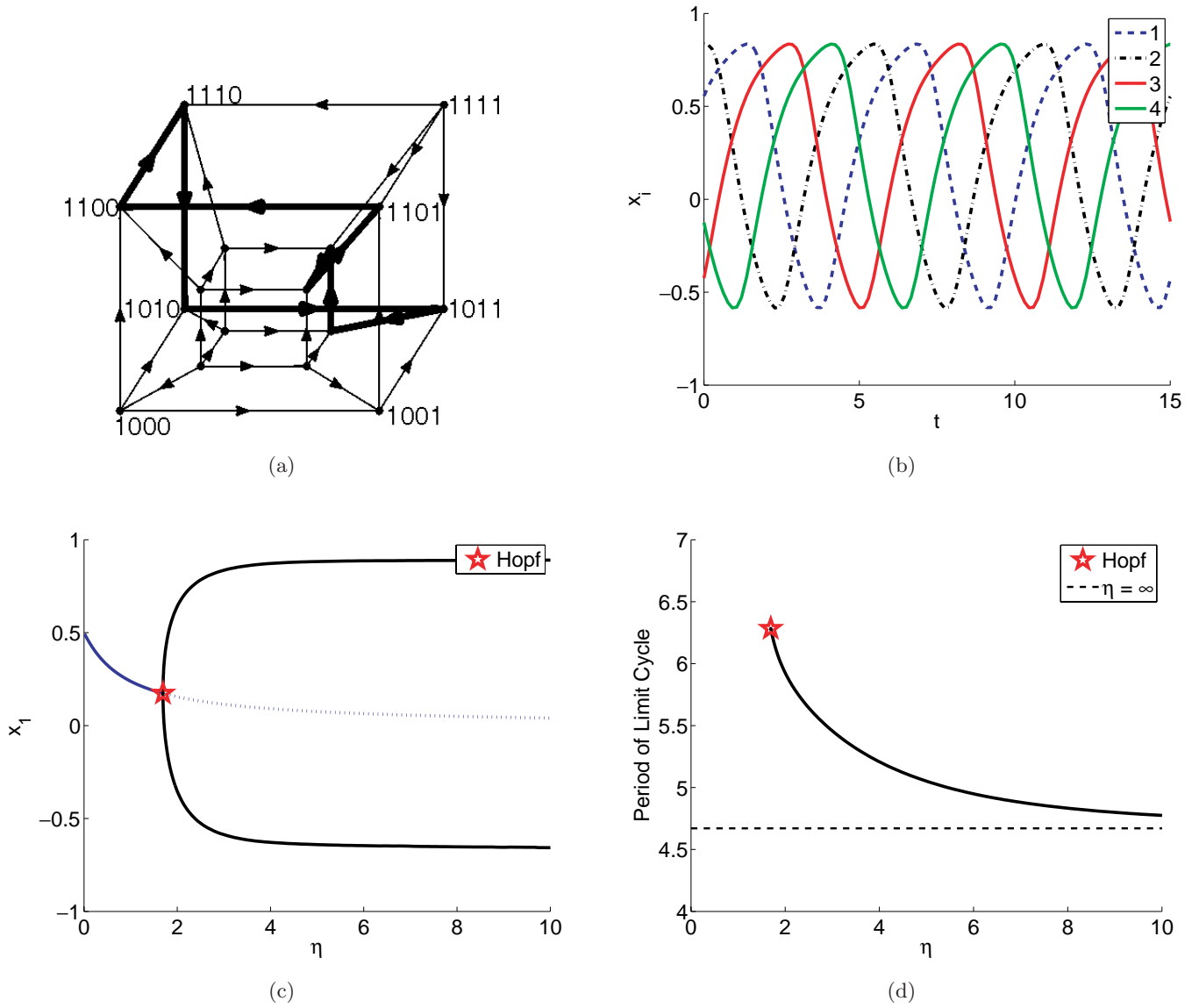
A.3.   *Attractor 2 in four dimensions*

Choosing an embedding of the second cyclic attractor in four dimensions from Table 1 yields

$$
\begin{aligned}
R_1 &= \{2,3\} & f_1 &= 0001 \\
R_2 &= \{1,3\} & f_2 &= 0111 \\
R_3 &= \{4\} & f_3 &= 10 \\
R_4 &= \{1,2,3\} & f_4 &= 11011000,
\end{aligned}
\tag{A.8}
$$

$$
\begin{aligned}
\dot{x}_1 &= -x_1 + 2h_2 h_3 - 1 \\
\dot{x}_2 &= -x_2 + 2h_3 - 2h_1 h_3 + 2h_1 - 1 \\
\dot{x}_3 &= -x_3 + 2h_4 - 1 \\
\dot{x}_4 &= -x_4 + 1 - 2h_2 + 2h_2 h_3 - 2h_1 h_3.
\end{aligned}
\tag{A.9}
$$

The fixed point solution is not constant as was the case for the cyclical negative feedback attractor. However, the bifurcation diagram is similar with a super-critical Hopf bifurcation destabilizing the fixed point yielding a limit cycle. The solution structure of Eqs. (A.8) and (A.9) is shown in Fig. 5.

A.4.   *Attractor 3 in four dimensions*

The third, four-dimensional cyclic attractor in Table 1 belongs to the class of sequential disinhibitions discussed in Sec. 3.2. We analyze two embeddings of the cyclic attractor, one which yields the *not or* regulation form discussed in Sec. 3.2 and a second embedding that yields the *not and* form.
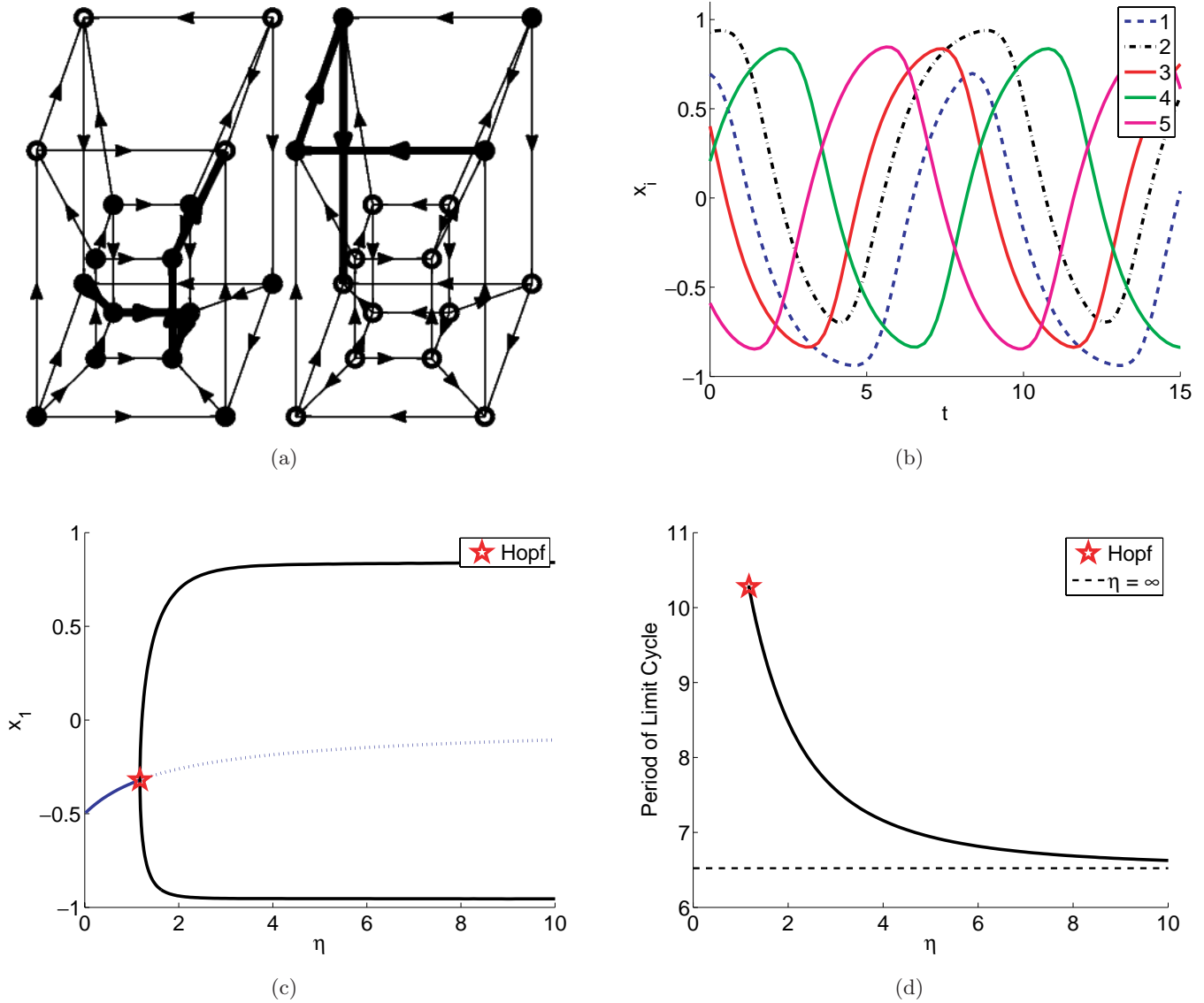
(a)

(b)

(c)

(d)
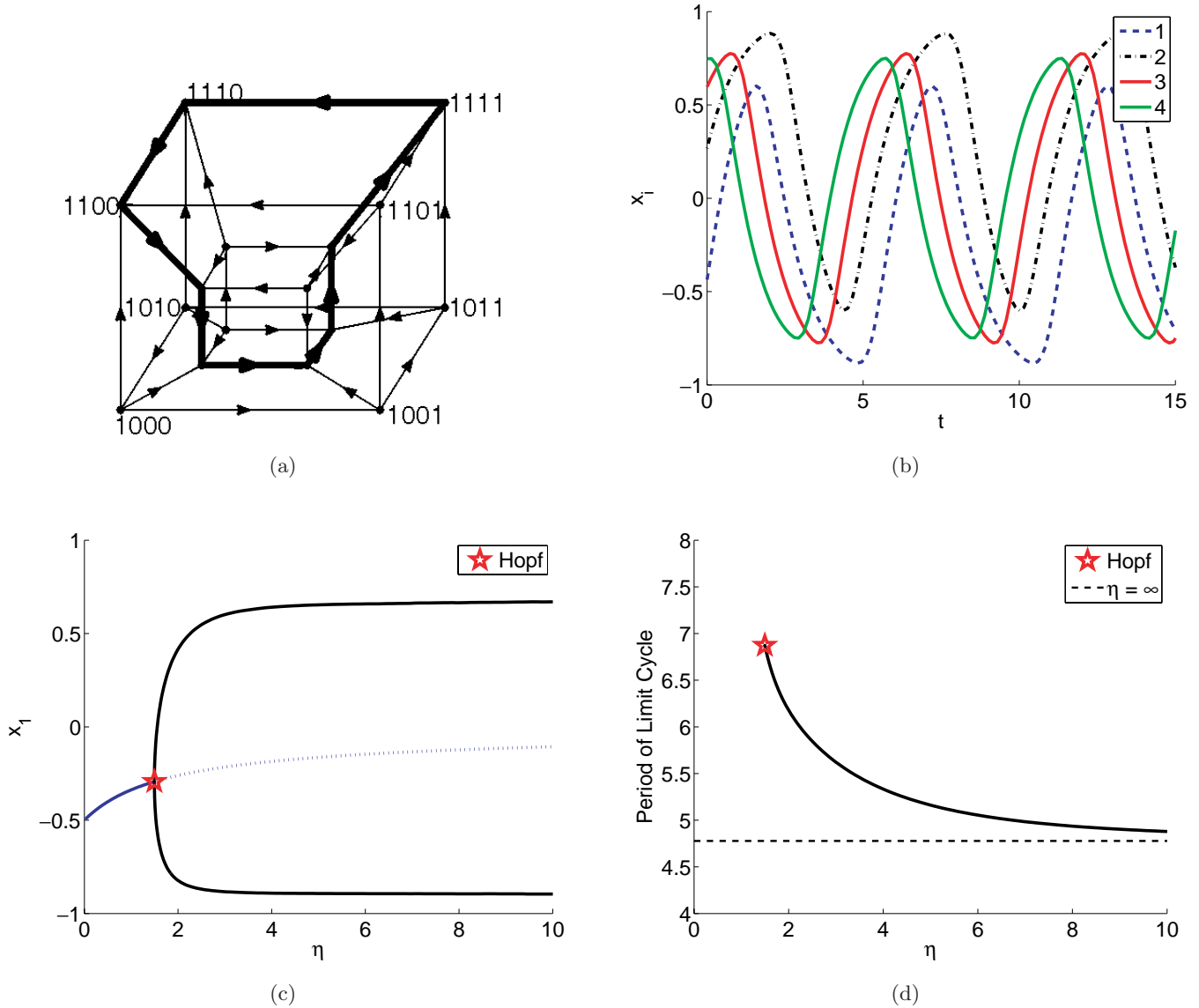
Fig. 5.   Solution structure of the second cyclic attractor in four dimensions [Eq. (A.9)]. Trajectory in (b) has $\eta = 3$. Refer to the Appendix for an explanation of panels.

The embedding shown in Fig. 6(a), yields the minimal network

$$
\begin{aligned}
R_1 &= \{3, 4\} & f_1 &= 1000 \\
R_2 &= \{1, 3\} & f_2 &= 1000 \\
R_3 &= \{2, 4\} & f_3 &= 1000 \\
R_4 &= \{1, 2\} & f_4 &= 1000,
\end{aligned}
\tag{A.10}
$$

consisting of *not or* functions of two inputs.

$$
\begin{aligned}
\dot{x}_1 &= -x_1 + 1 - 2h_4 - 2h_3 + 2h_3 h_4 \\
\dot{x}_2 &= -x_2 + 1 - 2h_3 - 2h_1 + 2h_1 h_3 \\
\dot{x}_3 &= -x_3 + 1 - 2h_4 - 2h_2 + 2h_2 h_4 \\
\dot{x}_4 &= -x_4 + 1 - 2h_2 - 2h_1 + 2h_1 h_2.
\end{aligned}
\tag{A.11}
$$

The solution structure of Eqs. (A.10) and (A.11) is shown in Fig. 6.

The second embedding considered is shown in Fig. 7(a), yielding the minimal network:

$$
\begin{aligned}
R_1 &= \{3, 4\} & f_1 &= 1110 \\
R_2 &= \{1, 3\} & f_2 &= 1110 \\
R_3 &= \{2, 4\} & f_3 &= 1110 \\
R_4 &= \{1, 2\} & f_4 &= 1110,
\end{aligned}
\tag{A.12}
$$

$$
\begin{aligned}
\dot{x}_1 &= -x_1 + 1 - 2h_3 h_4 \\
\dot{x}_2 &= -x_2 + 1 - 2h_1 h_3 \\
\dot{x}_3 &= -x_3 + 1 - 2h_2 h_4 \\
\dot{x}_4 &= -x_4 + 1 - 2h_1 h_2.
\end{aligned}
\tag{A.13}
$$

The solution structure of Eqs. (A.12) and (A.13) is shown in Fig. 7.

(a)

(b)

(c)

(d)
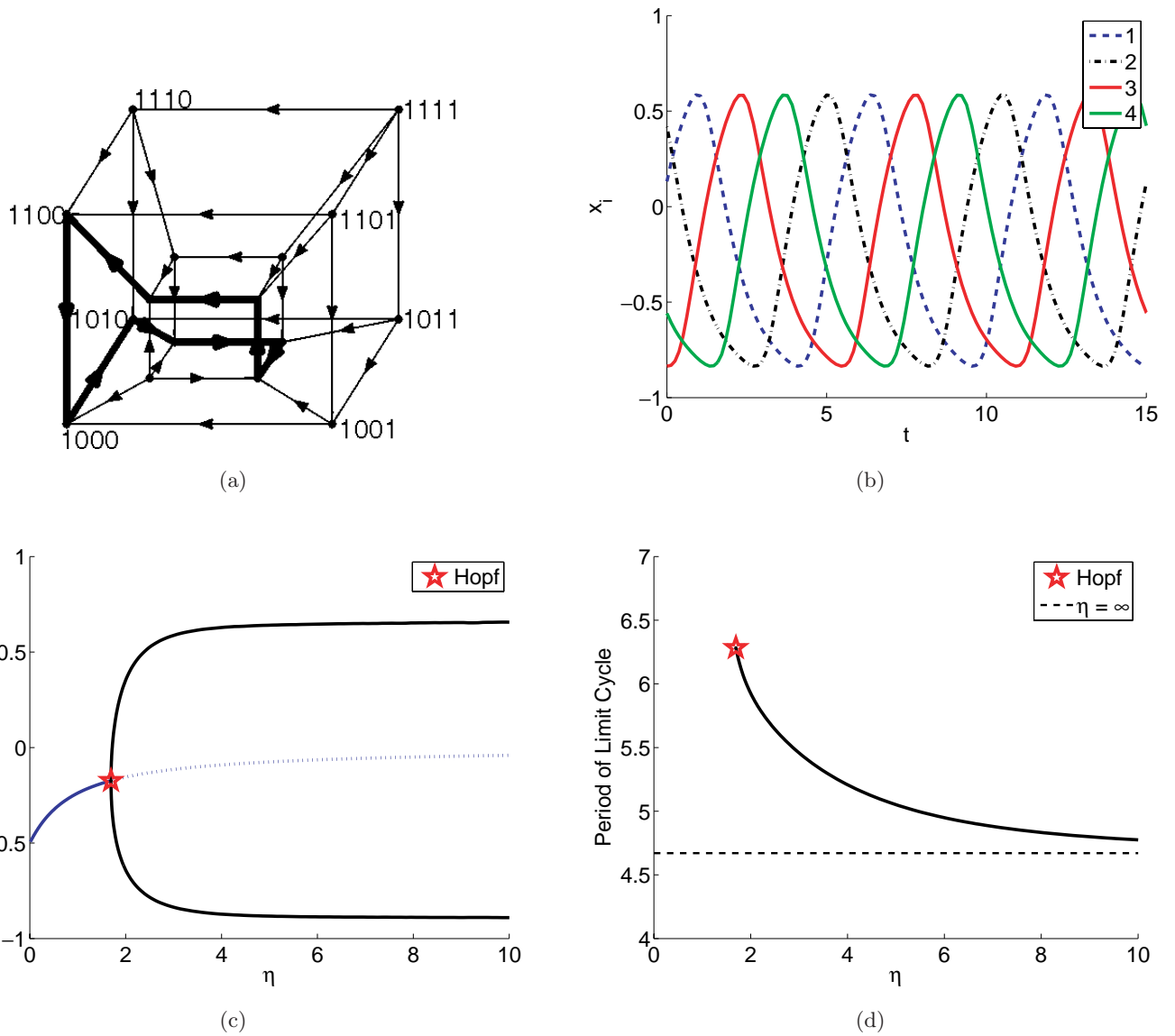
Fig. 6.   Solution structure of the first embedding of the third cyclic attractor in four dimensions considered here [see Eq. (A.11)]. Trajectory in (b) has $\eta = 3$. Refer to the Appendix for an explanation of panels.

(a)

(b)

(c)

(d)

Fig. 7. Solution structure of the second embedding of the third cyclic attractor in four dimensions considered here [see Eq. (A.13)]. Trajectory in (b) has $\eta = 3$. Refer to the Appendix for an explanation of panels.
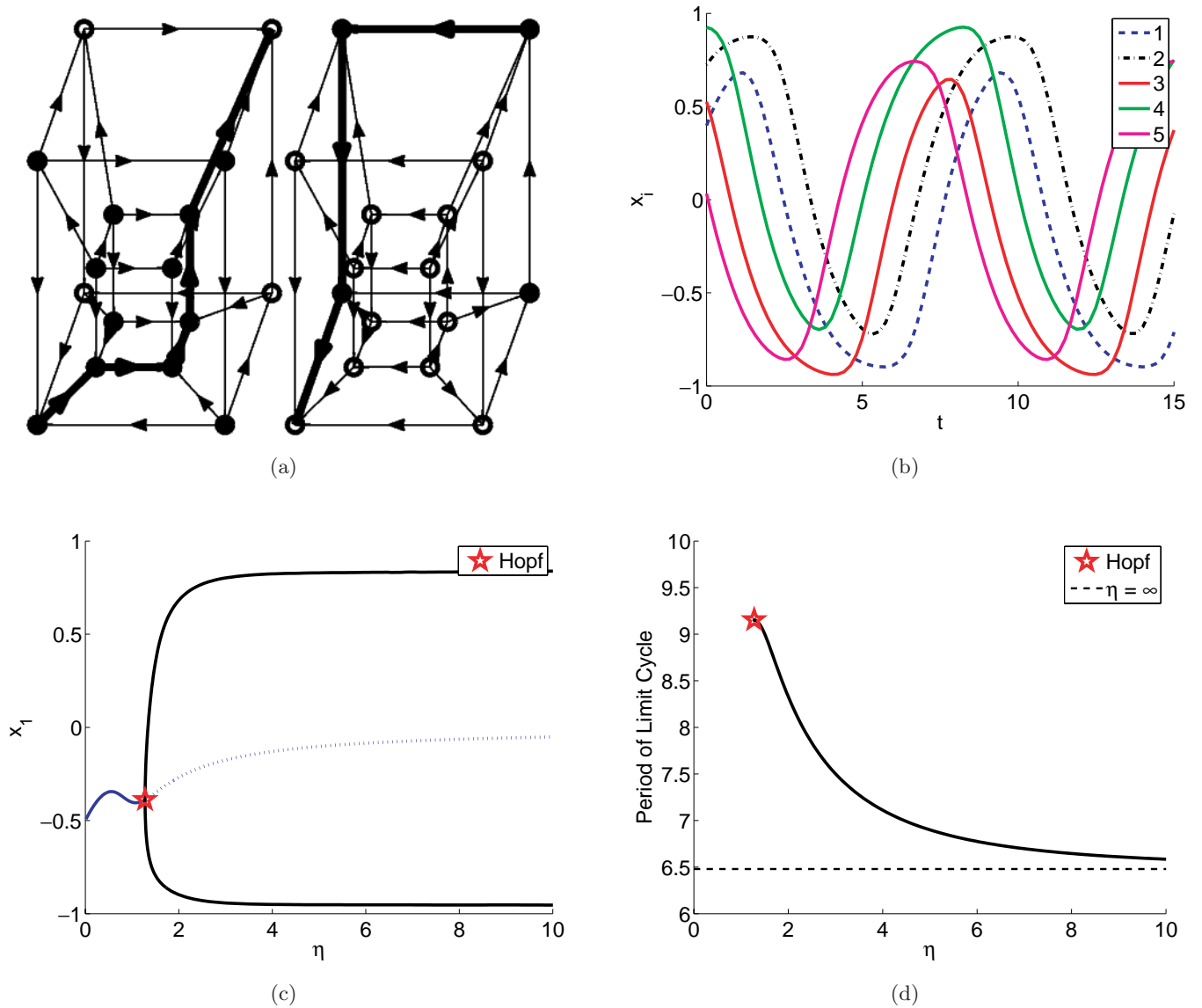
(a)

(b)

(c)

(d)
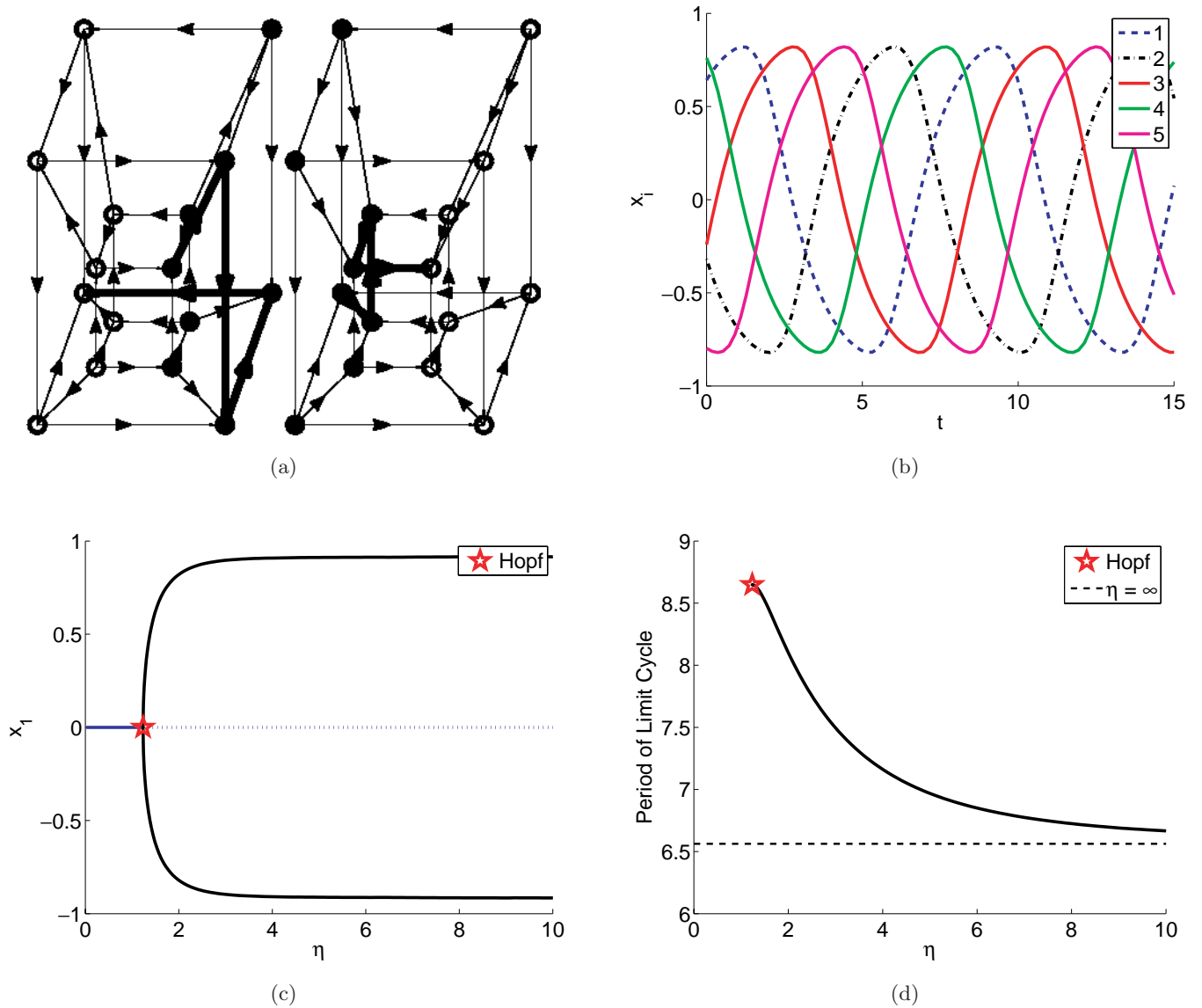
Fig. 8.   Solution structure of the first cyclic attractor in five dimensions [Eq. (A.15)]. Trajectory in (b) has $\eta = 2$. Refer to the Appendix for an explanation of panels.

A.5.   *Attractor 1 in five dimensions*

We consider only one embedding of the cyclical negative feedback attractor in five dimensions, as the analysis does not differ from that in three and four dimensions.

$$
\begin{aligned}
R_1 &= \{5\} & f_1 &= 10 \\
R_2 &= \{1\} & f_2 &= 10 \\
R_3 &= \{2\} & f_3 &= 10 \\
R_4 &= \{3\} & f_4 &= 10 \\
R_5 &= \{4\} & f_5 &= 10,
\end{aligned}
\tag{A.14}
$$

$$
\begin{aligned}
\dot{x}_1 &= -x_1 + 1 - 2h_5 \\
\dot{x}_2 &= -x_2 + 1 - 2h_1
\end{aligned}
$$

$$
\begin{aligned}
\dot{x}_3 &= -x_3 + 1 - 2h_2 \\
\dot{x}_4 &= -x_4 + 1 - 2h_3 \\
\dot{x}_5 &= -x_5 + 1 - 2h_4.
\end{aligned}
\tag{A.15}
$$

The solution structure of Eqs. (A.14) and (A.15) is shown in Fig. 8.

A.6.   *Attractor 2 in five dimensions*

$$
\begin{aligned}
R_1 &= \{2,3\} & f_1 &= 0001 \\
R_2 &= \{1,3\} & f_2 &= 0111 \\
R_3 &= \{4\} & f_3 &= 10 \\
R_4 &= \{5\} & f_4 &= 10 \\
R_5 &= \{1,2,4\} & f_5 &= 11101000,
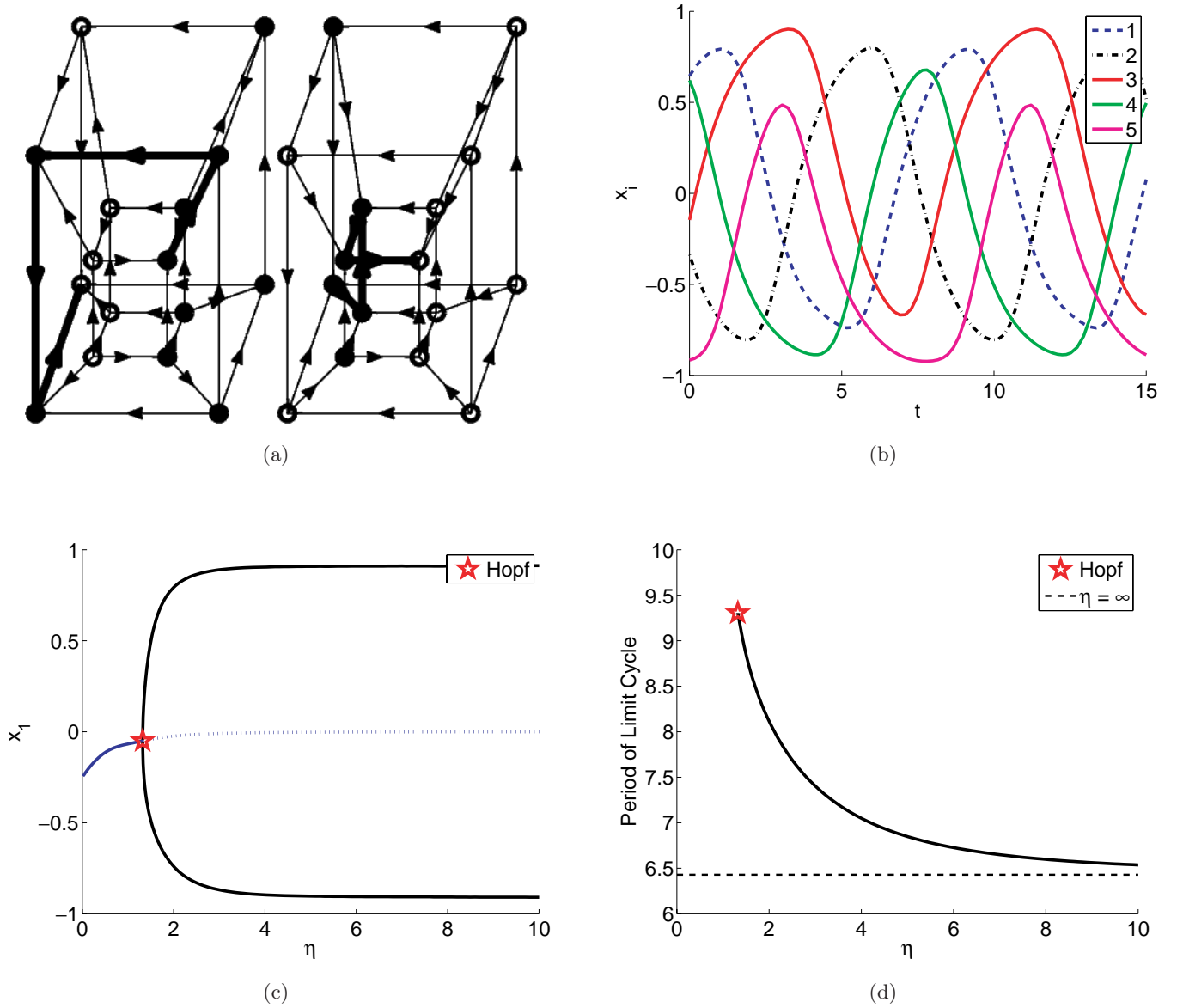\end{aligned}
\tag{A.16}
$$

(a)

(b)

(c)

(d)

Fig. 9. Solution structure of the second cyclic attractor in five dimensions [Eq. (A.17)]. Trajectory in (b) has $\eta = 2$. Refer to the Appendix for an explanation of panels.

$$
\begin{aligned}
\dot{x}_1 &= -x_1 + 2h_2h_3 - 1 \\
\dot{x}_2 &= -x_2 + 2h_3 - 2h_1h_3 + 2h_1 - 1 \\
\dot{x}_3 &= -x_3 + 1 - 2h_4 \\
\dot{x}_4 &= -x_4 + 1 - 2h_5 \\
\dot{x}_5 &= -x_5 + 1 - 2h_2h_4 - 2h_1h_4 \\
&\quad - 2h_1h_2 + 4h_1h_2h_4.
\end{aligned}
\tag{A.17}
$$

The solution structure of Eqs. (A.16) and (A.17) is shown in Fig. 9.

A.7. Attractor 3 in five dimensions

$$
\begin{aligned}
R_1 &= \{2,4\} & f_1 &= 0001 \\
R_2 &= \{1,3\} & f_2 &= 0111
\end{aligned}
$$

$$
\begin{aligned}
R_3 &= \{4,5\} & f_3 &= 0001 \\
R_4 &= \{3,5\} & f_4 &= 0111 \\
R_5 &= \{1,2,4\} & f_5 &= 11010000,
\end{aligned}
\tag{A.18}
$$

$$
\begin{aligned}
\dot{x}_1 &= -x_1 + 2h_2h_4 - 1 \\
\dot{x}_2 &= -x_2 + 2h_3 - 2h_1h_3 + 2h_1 - 1 \\
\dot{x}_3 &= -x_3 + 2h_4h_5 - 1 \\
\dot{x}_4 &= -x_4 + 2h_5 - 2h_3h_5 + 2h_3 - 1 \\
\dot{x}_5 &= -x_5 + 1 - 2h_2 + 2h_2h_3 - 2h_1 \\
&\quad + 2h_1h_2 - 2h_1h_2h_3.
\end{aligned}
\tag{A.19}
$$

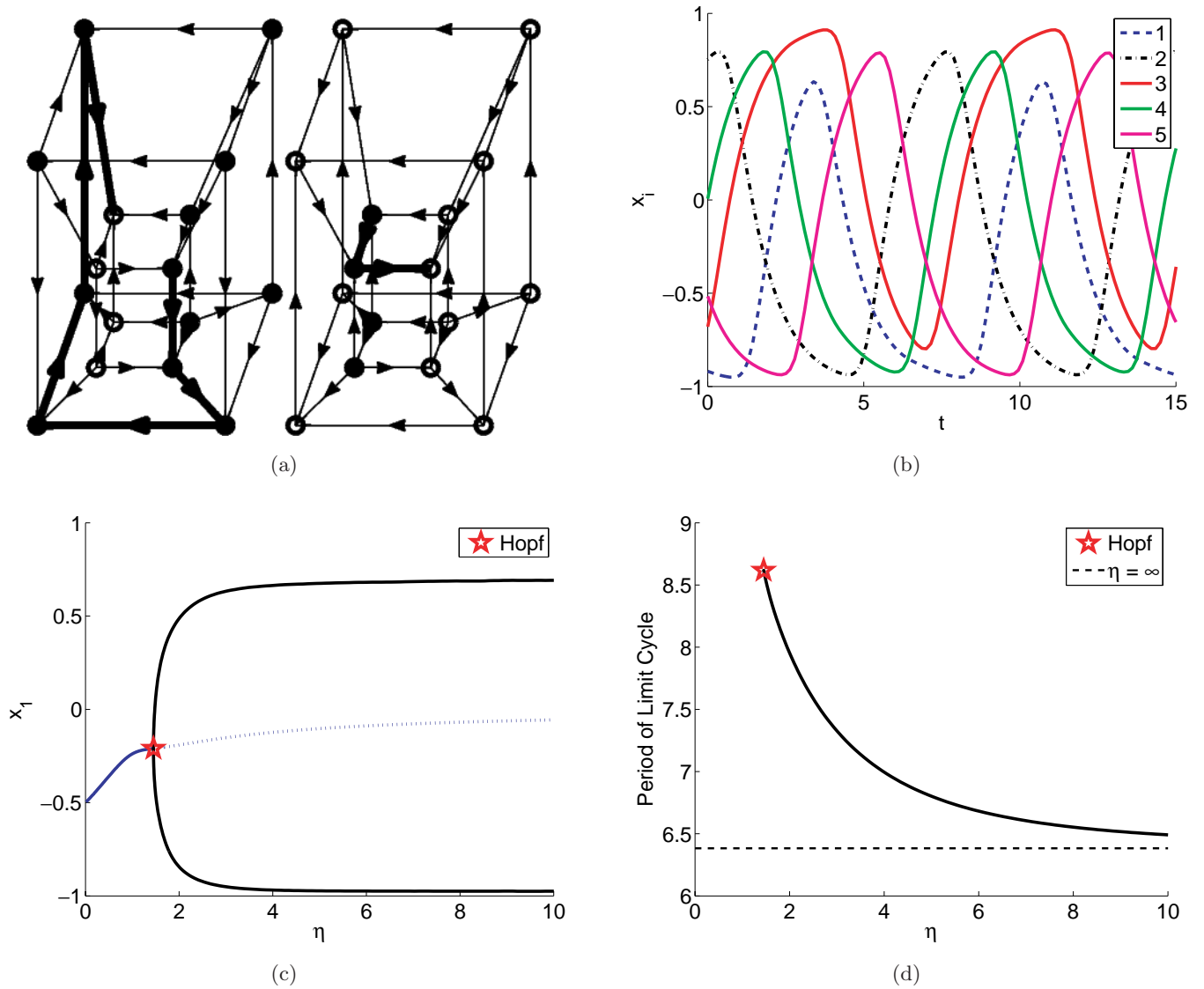The solution structure of Eqs. (A.18) and (A.19) is shown in Fig. 10.

Fig. 10.   Solution structure of the third cyclic attractor in five dimensions [Eq. (A.19)]. Trajectory in (b) has $\eta = 2$. Refer to the Appendix for an explanation of panels.

A.8. *Attractor 4 in five dimensions*

$$
\begin{aligned}
&R_1 = \{2, 4, 5\} \quad f_1 = 10100010 \\
&R_2 = \{1\} \qquad\quad f_2 = 10 \\
&R_3 = \{2, 5\} \qquad f_3 = 1101 \\
&R_4 = \{3\} \qquad\quad f_4 = 10 \\
&R_5 = \{2, 4\} \qquad f_5 = 1000,
\end{aligned}
\tag{A.20}
$$

$$
\begin{aligned}
\dot{x}_1 &= -x_1 + 1 - 2h_5 - 2h_2 + 2h_2 h_5 \\
&\quad + 2h_2 h_4 - 2h_2 h_4 h_5 \\
\dot{x}_2 &= -x_2 + 1 - 2h_1 \\
\dot{x}_3 &= -x_3 + 1 - 2h_2 + 2h_2 h_5 \\
\dot{x}_4 &= -x_4 + 1 - 2h_3 \\
\dot{x}_5 &= -x_5 + 1 - 2h_4 - 2h_2 + 2h_2 h_4.
\end{aligned}
\tag{A.21}
$$

The solution structure of Eqs. (A.20) and (A.21) is shown in Fig. 11.

A.9. *Attractor 5 in five dimensions*

$$
\begin{aligned}
&R_1 = \{2, 5\} \quad f_1 = 1000 \\
&R_2 = \{3\} \qquad f_2 = 10 \\
&R_3 = \{1, 4\} \quad f_3 = 0111 \\
&R_4 = \{1, 5\} \quad f_4 = 1000 \\
&R_5 = \{2, 4\} \quad f_5 = 1000,
\end{aligned}
\tag{A.22}
$$

$$
\begin{aligned}
\dot{x}_1 &= -x_1 + 1 - 2h_5 - 2h_2 + 2h_2 h_5 \\
\dot{x}_2 &= -x_2 + 1 - 2h_3 \\
\dot{x}_3 &= -x_3 + 2h_4 - 2h_1 h_4 + 2h_1 - 1
\end{aligned}
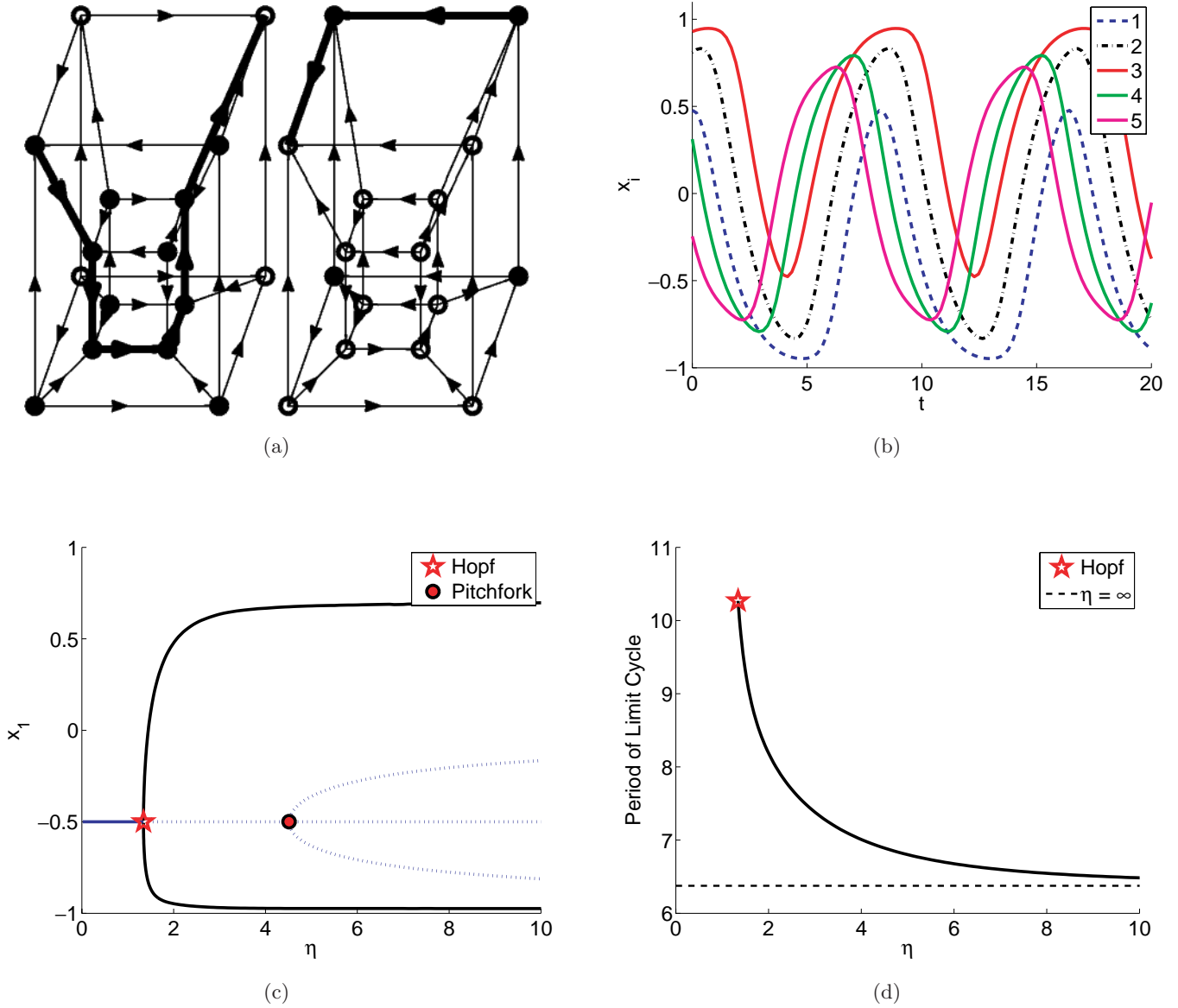$$

(a)

(b)

(c)

(d)

Fig. 11.   Solution structure of the fourth cyclic attractor in five dimensions [Eq. (A.21)]. Trajectory in (b) has $\eta = 2$. Refer to the Appendix for an explanation of panels.

$$\dot{x}_4 = -x_4 + 1 - 2h_5 - 2h_1 + 2h_1 h_5$$
$$\dot{x}_5 = -x_5 + 1 - 2h_4 - 2h_2 + 2h_2 h_4.$$
$$(\text{A.23})$$

The solution structure of Eqs. (A.22) and (A.23) is shown in Fig. 12.

A.10.   *Attractor 6 in five dimensions*

$$
\begin{aligned}
R_1 &= \{2, 4\} & f_1 &= 0001 \\
R_2 &= \{1, 3, 4\} & f_2 &= 00010111 \\
R_3 &= \{2, 4\} & f_3 &= 0111 \\
R_4 &= \{5\} & f_4 &= 01 \\
R_5 &= \{1, 3, 4\} & f_5 &= 11011000,
\end{aligned}
\qquad (\text{A.24})
$$

$$
\begin{aligned}
\dot{x}_1 &= -x_1 + 2h_2 h_4 - 1 \\
\dot{x}_2 &= -x_2 + 2h_3 h_4 - 4h_1 h_3 h_4 \\
&\quad + 2h_1 h_4 + 2h_1 h_3 - 1 \\
\dot{x}_3 &= -x_3 + 2h_4 - 2h_2 h_4 + 2h_2 - 1 \\
\dot{x}_4 &= -x_4 + 2h_5 - 1 \\
\dot{x}_5 &= -x_5 + 1 - 2h_3 + 2h_3 h_4 - 2h_1 h_4.
\end{aligned}
\qquad (\text{A.25})
$$

The solution structure of Eqs. (A.24) and (A.25) is shown in Fig. 13.

A.11.   *Attractor 7 in five dimensions*

$$
\begin{aligned}
R_1 &= \{2, 3\} & f_1 &= 0001 \\
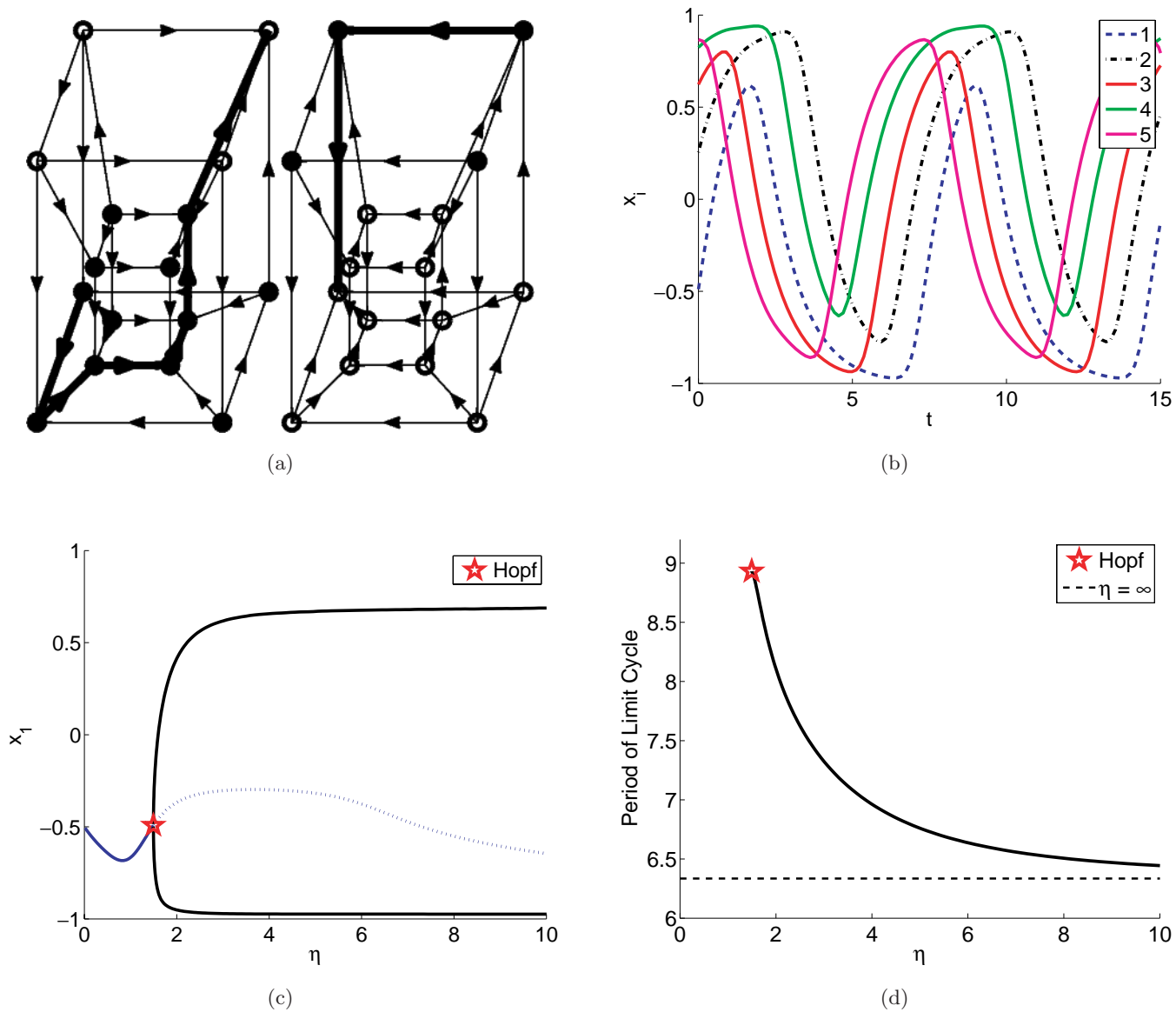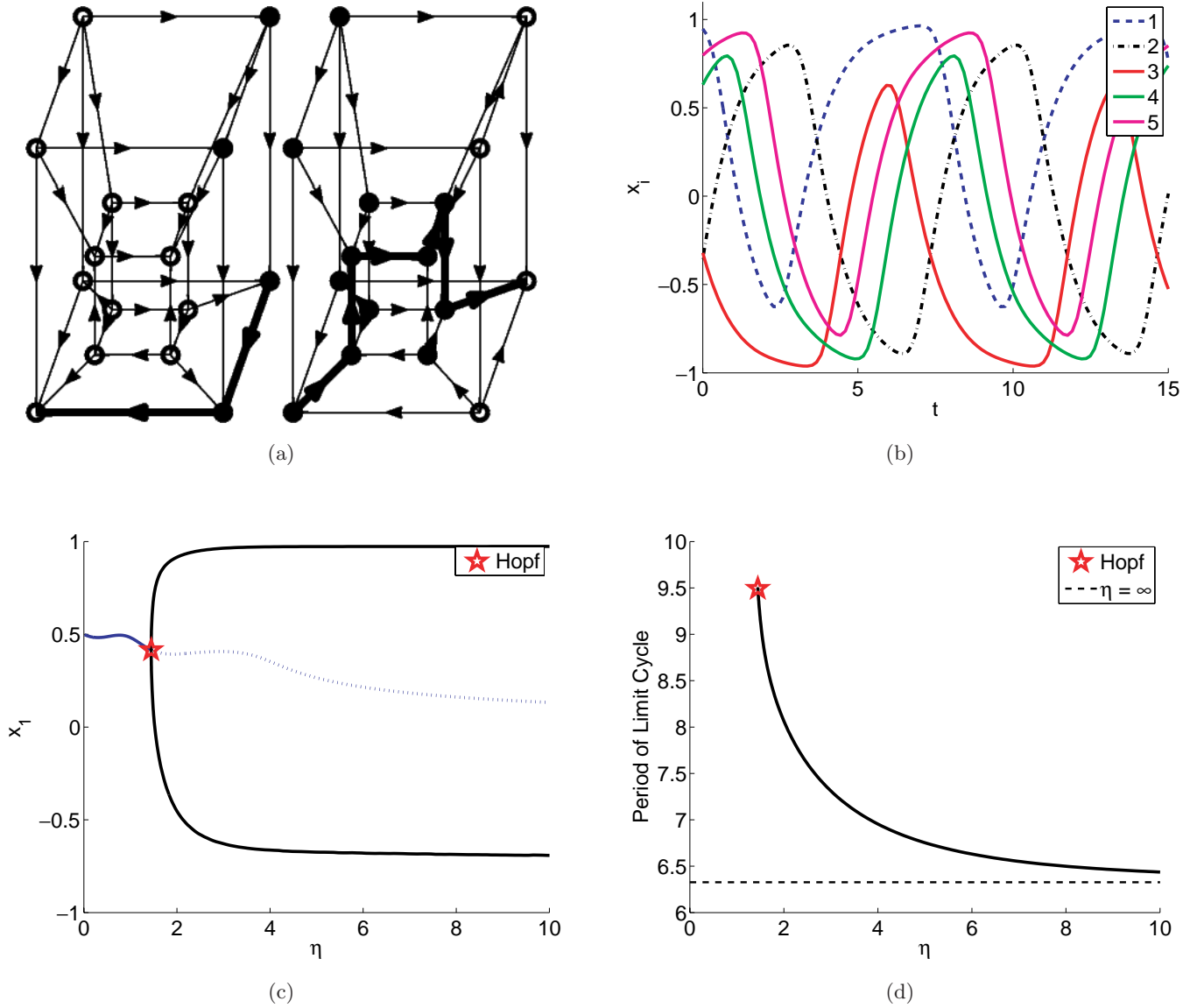R_2 &= \{3, 4, 5\} & f_2 &= 00100011
\end{aligned}
$$

Fig. 12.   Solution structure of the fifth cyclic attractor in five dimensions [Eq. (A.23)]. Trajectory in (b) has $\eta = 3$. Refer to the Appendix for an explanation of panels.

$$R_3 = \{4, 5\} \qquad f_3 = 0001$$
$$R_4 = \{1, 5\} \qquad f_4 = 0111$$
$$R_5 = \{1, 2, 3\} \quad f_5 = 11010000,$$

$$(A.26)$$

$$\dot{x}_1 = -x_1 + 2h_2 h_3 - 1$$
$$\dot{x}_2 = -x_2 + 2h_4 - 2h_4 h_5 + 2h_3 h_4 h_5 - 1$$
$$\dot{x}_3 = -x_3 + 2h_4 h_5 - 1$$
$$\dot{x}_4 = -x_4 + 2h_5 - 2h_1 h_5 + 2h_1 - 1$$
$$\dot{x}_5 = -x_5 + 1 - 2h_2 + 2h_2 h_3$$
$$\qquad - 2h_1 + 2h_1 h_2 - 2h_1 h_2 h_3.$$

$$(A.27)$$

The solution structure of Eqs. (A.26) and (A.27) is shown in Fig. 14.

A.12.   *Attractor 8 in five dimensions*

$$R_1 = \{2, 5\} \qquad f_1 = 1110$$
$$R_2 = \{1, 3, 4\} \quad f_2 = 11000100$$
$$R_3 = \{2, 4\} \qquad f_3 = 1000$$
$$R_4 = \{1, 5\} \qquad f_4 = 0001$$
$$R_5 = \{3, 4\} \qquad f_5 = 0111,$$

$$(A.28)$$

$$\dot{x}_1 = -x_1 + 1 - 2h_2 h_5$$
$$\dot{x}_2 = -x_2 + 1 - 2h_3 - 2h_1 + 2h_1 h_4$$
$$\qquad + 2h_1 h_3 - 2h_1 h_3 h_4$$
$$\dot{x}_3 = -x_3 + 1 - 2h_4 - 2h_2 + 2h_2 h_4$$
$$\dot{x}_4 = -x_4 + 2h_1 h_5 - 1$$
$$\dot{x}_5 = -x_5 + 2h_4 - 2h_3 h_4 + 2h_3 - 1.$$

$$(A.29)$$

(a)

(b)

(c)

(d)

Fig. 13. Solution structure of the sixth cyclic attractor in five dimensions [Eq. (A.25)]. Trajectory in (b) has $\eta = 2$. Refer to the Appendix for an explanation of panels.

The solution structure of Eqs. (A.28) and (A.29) is shown in Fig. 15.

A.13. *Attractor 9 in five dimensions*

$$R_1 = \{3, 4\} \qquad f_1 = 0111$$
$$R_2 = \{1, 5\} \qquad f_2 = 1000$$
$$R_3 = \{1, 2, 5\} \qquad f_3 = 00001000$$
$$R_4 = \{1, 2, 3, 5\} \quad f_4 = 0000100010001000$$
$$R_5 = \{1, 4\} \qquad f_5 = 0010,$$

$$\text{(A.30)}$$

$$\dot{x}_1 = -x_1 + 2h_4 - 2h_3 h_4 + 2h_3 - 1$$
$$\dot{x}_2 = -x_2 + 1 - 2h_5 - 2h_1 + 2h_1 h_5$$
$$\dot{x}_3 = -x_3 + 2h_1 - 2h_1 h_5 - 2h_1 h_2 + 2h_1 h_2 h_5 - 1$$
$$\dot{x}_4 = -x_4 + 2h_2 - 2h_2 h_5 - 2h_2 h_3 + 2h_2 h_3 h_5$$
$$\qquad - 2h_1 h_2 + 2h_1 h_2 h_5 + 2h_2 h_1 h_3$$
$$\qquad - 2h_2 h_1 h_3 h_5 + 2h_1 - 2h_1 h_5 - 2h_1 h_3$$
$$\qquad + 2h_1 h_3 h_5 - 1$$
$$\dot{x}_5 = -x_5 + 2h_1 - 2h_1 h_4 - 1.$$

$$\text{(A.31)}$$

The solution structure of Eqs. (A.30) and (A.31) is shown in Fig. 16.

Fig. 14.   Solution structure of the seventh cyclic attractor in five dimensions [Eq. (A.27)]. Trajectory in (b) has $\eta = 3$. Refer to the Appendix for an explanation of panels.

(a)

(b)

(c)

(d)

Fig. 15. Solution structure of the eighth cyclic attractor in five dimensions [Eq. (A.29)]. Trajectory in (b) has $\eta = 3$. Refer to the Appendix for an explanation of panels.
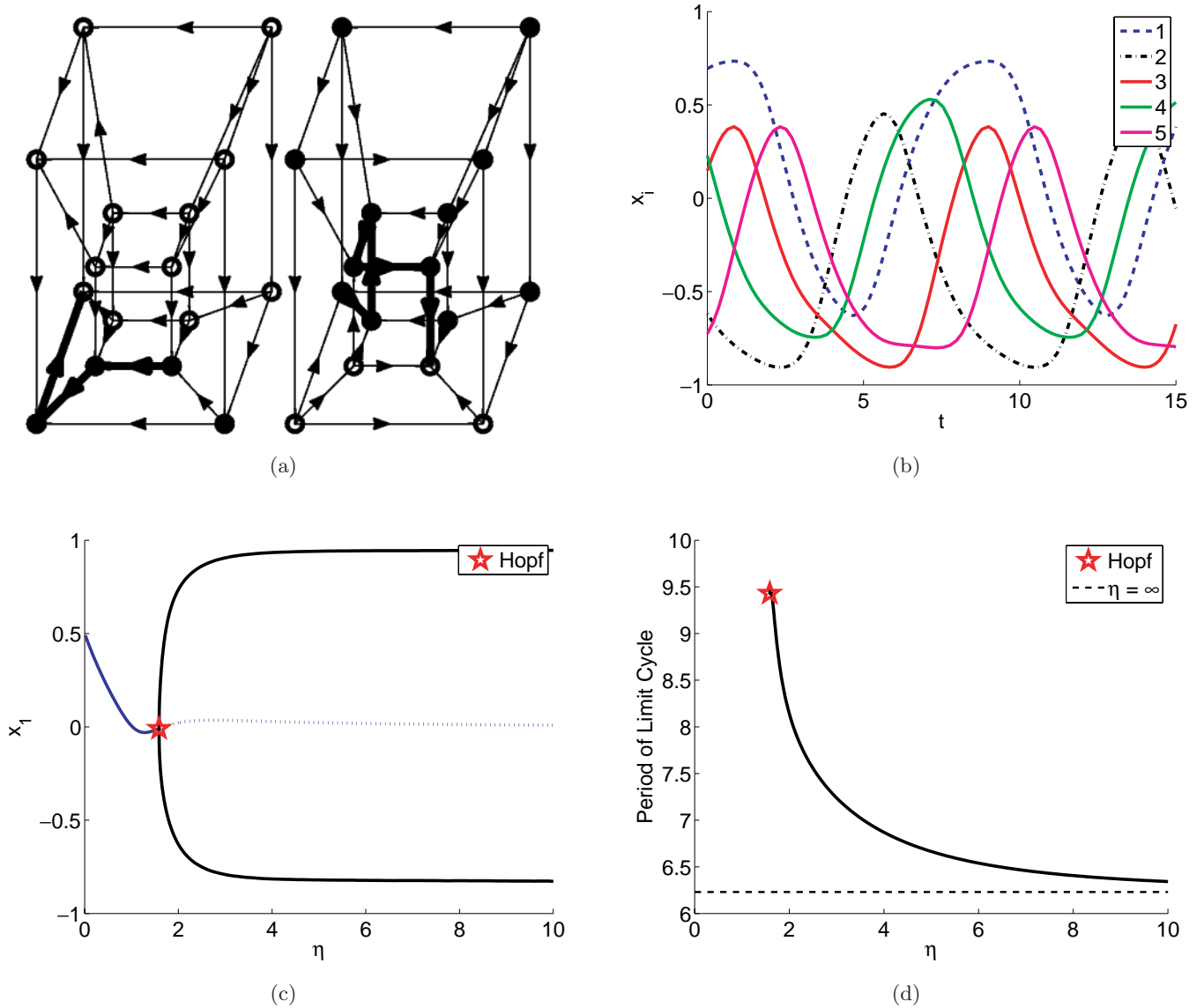
Fig. 16.   Solution structure of the ninth cyclic attractor in five dimensions [Eq. (A.31)]. Trajectory in (b) has $\eta = 2$. Refer to the Appendix for an explanation of panels.

A.14.   *Attractor 10 in five dimensions*

This cyclic attractor belongs to the sequential disinhibition class. As we did in four dimensions, we consider two embeddings: one yielding the *not or* functions for f_i and the second the *not and* functions.

$$
\begin{aligned}
R_1 &= \{3, 4, 5\} & f_1 &= 10000000 \\
R_2 &= \{1, 4, 5\} & f_2 &= 10000000 \\
R_3 &= \{1, 2, 5\} & f_3 &= 10000000 \\
R_4 &= \{1, 2, 3\} & f_4 &= 10000000 \\
R_5 &= \{2, 3, 4\} & f_5 &= 10000000,
\end{aligned}
\tag{A.32}
$$

$$
\begin{aligned}
\dot{x}_1 &= -x_1 + 1 - 2h_5 - 2h_4 + 2h_4h_5 \\
&\quad - 2h_3 + 2h_3h_5 + 2h_3h_4 - 2h_3h_4h_5 \\
\dot{x}_2 &= -x_2 + 1 - 2h_5 - 2h_4 + 2h_4h_5 \\
&\quad - 2h_1 + 2h_1h_5 + 2h_1h_4 - 2h_1h_4h_5 \\
\dot{x}_3 &= -x_3 + 1 - 2h_5 - 2h_2 + 2h_2h_5 \\
&\quad - 2h_1 + 2h_1h_5 + 2h_1h_2 - 2h_1h_2h_5 \\
\dot{x}_4 &= -x_4 + 1 - 2h_3 - 2h_2 + 2h_2h_3 \\
&\quad - 2h_1 + 2h_1h_3 + 2h_1h_2 - 2h_1h_2h_3 \\
\dot{x}_5 &= -x_5 + 1 - 2h_4 - 2h_3 + 2h_3h_4 \\
&\quad - 2h_2 + 2h_2h_4 + 2h_2h_3 - 2h_2h_3h_4.
\end{aligned}
\tag{A.33}
$$

The solution structure of Eqs. (A.32) and (A.33) is shown in Fig. 17.
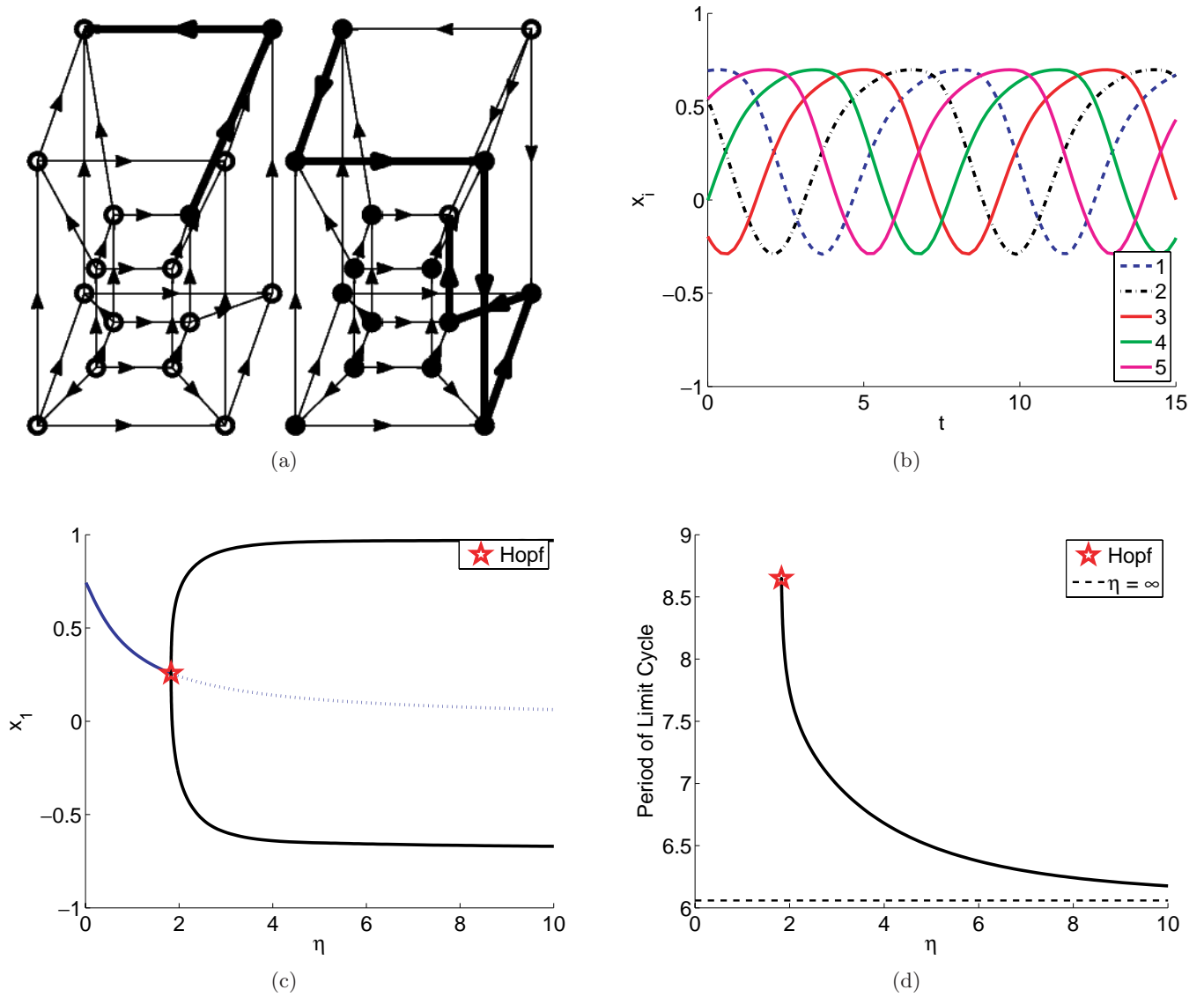
(a)

(b)

(c)

(d)
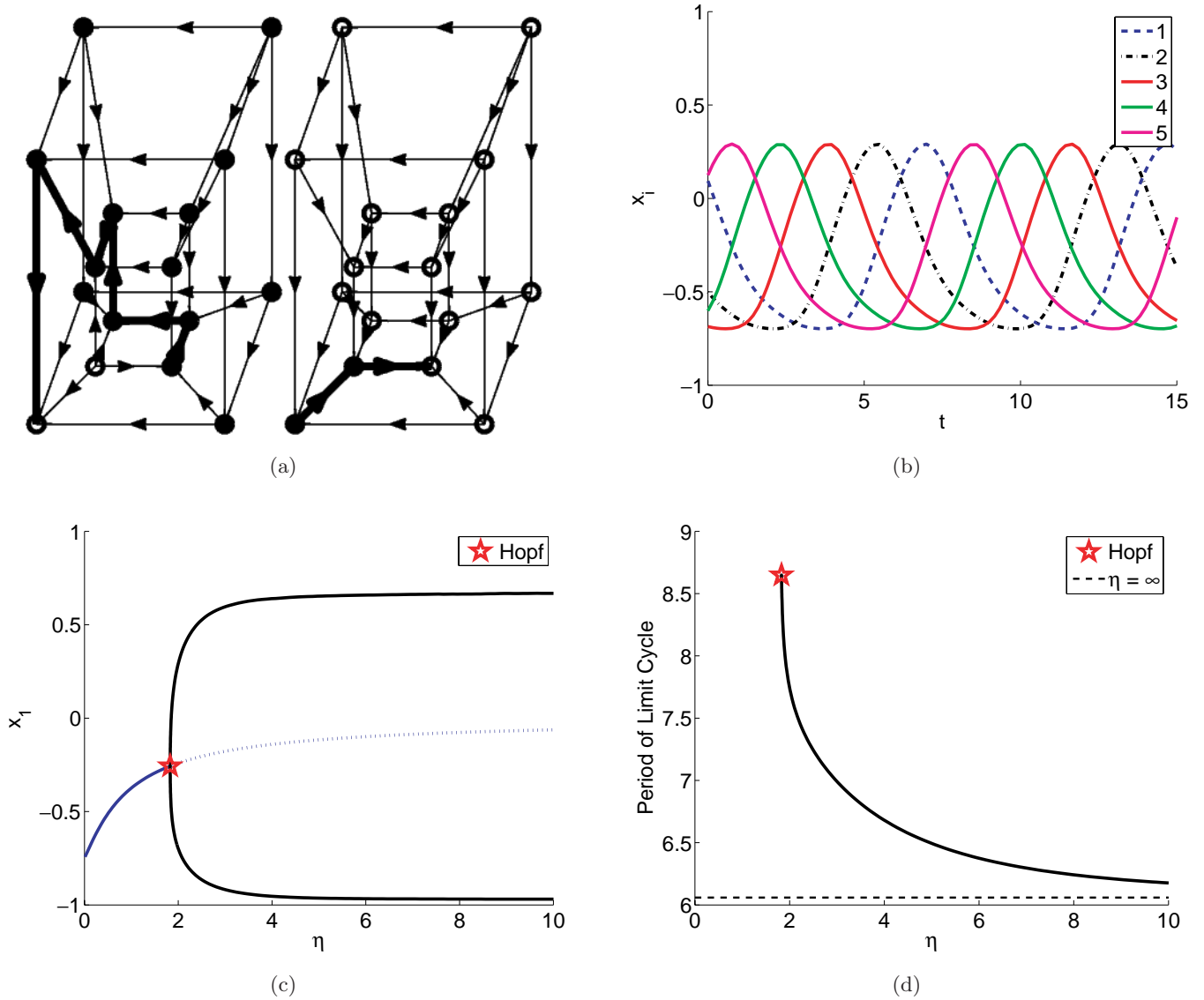
Fig. 17.   Solution structure of the first embedding of the tenth cyclic attractor in five dimensions considered here [see Eq. (A.33)]. Trajectory in (b) has $\eta = 2$. Refer to the Appendix for an explanation of panels.

$$
\begin{aligned}
R_1 &= \{3,4,5\} \quad f_1 = 11111110 \\
R_2 &= \{1,4,5\} \quad f_2 = 11111110 \\
R_3 &= \{1,2,5\} \quad f_3 = 11111110 \\
R_4 &= \{1,2,3\} \quad f_4 = 11111110 \\
R_5 &= \{2,3,4\} \quad f_5 = 11111110,
\end{aligned}
\tag{A.34}
$$

$$
\begin{aligned}
\dot{x}_1 &= -x_1 + 1 - 2h_3 h_4 h_5 \\
\dot{x}_2 &= -x_2 + 1 - 2h_1 h_4 h_5 \\
\dot{x}_3 &= -x_3 + 1 - 2h_1 h_2 h_5 \\
\dot{x}_4 &= -x_4 + 1 - 2h_1 h_2 h_3 \\
\dot{x}_5 &= -x_5 + 1 - 2h_2 h_3 h_4 .
\end{aligned}
\tag{A.35}
$$

The solution structure of Eqs. (A.34) and (A.35) is shown in Fig. 18.

A.15.   *Attractor 11 in five dimensions*

$$
\begin{aligned}
R_1 &= \{2\} \qquad\;\; f_1 = 01 \\
R_2 &= \{1,3,5\} \quad f_2 = 00100111 \\
R_3 &= \{4\} \qquad\;\; f_3 = 10 \\
R_4 &= \{1,3,5\} \quad f_4 = 01110010 \\
R_5 &= \{1,3\} \qquad f_5 = 1001,
\end{aligned}
\tag{A.36}
$$

$$
\begin{aligned}
\dot{x}_1 &= -x_1 + 2h_2 - 1 \\
\dot{x}_2 &= -x_2 + 2h_3 - 2h_3 h_5 + 2h_1 h_5 - 1 \\
\dot{x}_3 &= -x_3 + 2h_4 - 1 \\
\dot{x}_4 &= -x_4 + 2h_5 - 2h_3 h_5 \\
&\quad - 2h_1 h_5 + 2h_3 - 1 \\
\dot{x}_5 &= -x_5 + 1 - 2h_3 - 2h_1 + 4h_1 h_3 .
\end{aligned}
\tag{A.37}
$$

Fig. 18.   Solution structure of the second embedding of the tenth cyclic attractor in five dimensions considered here [see Eq. (A.35)]. Trajectory in (b) has $\eta = 2$. Refer to the Appendix for an explanation of panels.

The solution structure of Eqs. (A.36) and (A.37) is shown in Fig. 19.

A.16.   *Attractor 12 in five dimensions*

$$
\begin{aligned}
R_1 &= \{2,3,5\} \quad f_1 = 01110000 \\
R_2 &= \{1,4,5\} \quad f_2 = 01110000 \\
R_3 &= \{4\} \qquad\; f_3 = 10 \\
R_4 &= \{2,3,5\} \quad f_4 = 11011000 \\
R_5 &= \{1,2,3\} \quad f_5 = 00100100,
\end{aligned}
$$

$$ \text{(A.38)} $$

$$
\begin{aligned}
\dot{x}_1 = -x_1 &+ 2h_5 - 2h_5h_3 - 2h_5h_2 \\
&+ 2h_5h_2h_3 + 2h_3 - 2h_2h_3 - 1
\end{aligned}
$$

$$
\begin{aligned}
\dot{x}_2 = -x_2 &+ 2h_5 - 2h_5h_4 - 2h_5h_1 \\
&+ 2h_5h_1h_4 + 2h_4 - 2h_1h_4 - 1 \\
\dot{x}_3 = -x_3 &+ 1 - 2h_4 \\
\dot{x}_4 = -x_4 &+ 1 - 2h_3 + 2h_5h_3 - 2h_5h_2 \\
\dot{x}_5 = -x_5 &+ 2h_2 - 2h_2h_3 \\
&- 2h_2h_1 + 2h_1h_3 - 1.
\end{aligned}
$$

$$ \text{(A.39)} $$

The solution structure of Eqs. (A.38) and (A.39) is shown in Fig. 20.

A.17.   *Attractor 13 in five dimensions*

$$
\begin{aligned}
R_1 &= \{2,4,5\} \qquad f_1 = 01110000 \\
R_2 &= \{1,3,5\} \qquad f_2 = 01110000
\end{aligned}
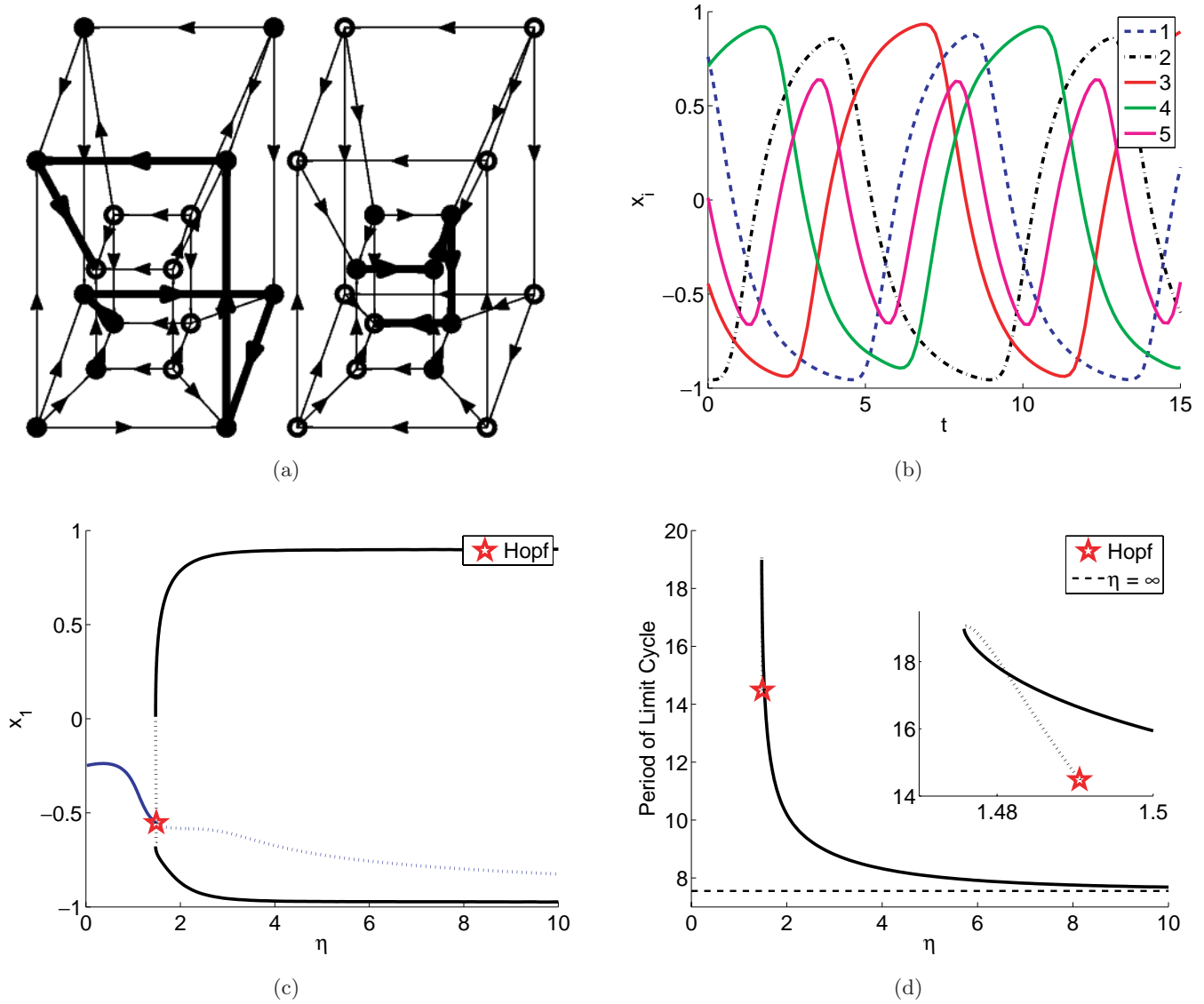$$

(a)

(b)

(c)

(d)
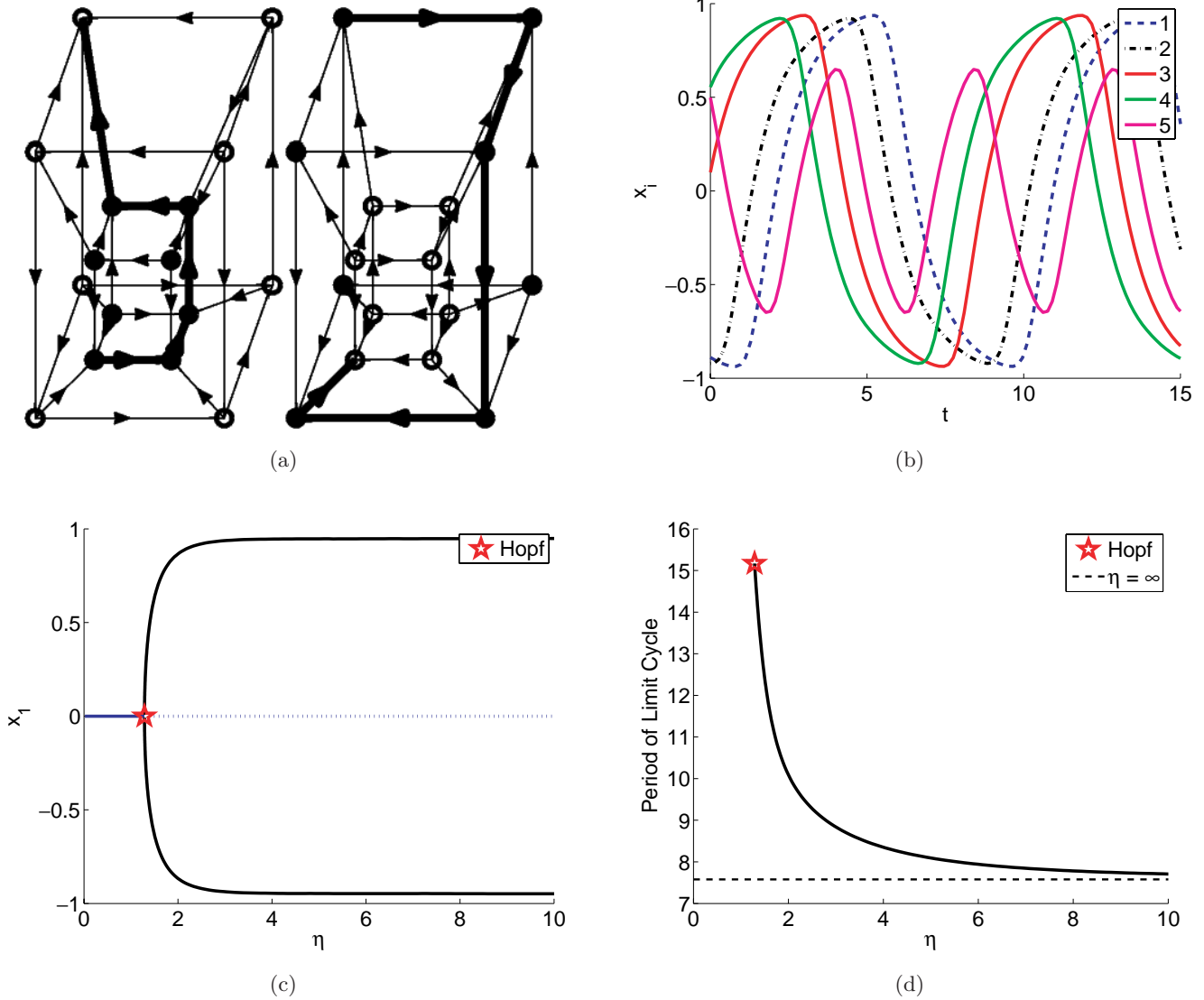
Fig. 19. Solution structure of the 11th cyclic attractor in five dimensions [Eq. (A.37)]. Trajectory in (b) has $\eta = 3$. Refer to the Appendix for an explanation of panels.

$$R_3 = \{1, 4, 5\} \qquad f_3 = 11001101$$
$$R_4 = \{2, 3, 5\} \qquad f_4 = 11001101$$
$$R_5 = \{1, 2, 3, 4\} \quad f_5 = 0000001101010000,$$

$$\text{(A.40)}$$

$$\dot{x}_1 = -x_1 + 2h_5 - 2h_5 h_4 - 2h_5 h_2$$
$$\qquad + 2h_5 h_2 h_4 + 2h_4 - 2h_2 h_4 - 1$$
$$\dot{x}_2 = -x_2 + 2h_5 - 2h_5 h_3 - 2h_5 h_1$$
$$\qquad + 2h_5 h_1 h_3 + 2h_3 - 2h_1 h_3 - 1$$
$$\dot{x}_3 = -x_3 + 1 - 2h_4 + 2h_1 h_4 h_5$$
$$\dot{x}_4 = -x_4 + 1 - 2h_3 + 2h_2 h_3 h_5$$
$$\dot{x}_5 = -x_5 + 2h_2 h_3 - 2h_2 h_3 h_1$$
$$\qquad + 2h_1 h_4 - 2h_1 h_4 h_2 - 1.$$

$$\text{(A.41)}$$

The solution structure of Eqs. (A.40) and (A.41) is shown in Fig. 21.

A.18. *Attractor 14 in five dimensions*

$$R_1 = \{2, 3, 5\} \qquad f_1 = 00001101$$
$$R_2 = \{1, 3, 4, 5\} \quad f_2 = 0000111001011110$$
$$R_3 = \{1, 2, 4\} \qquad f_3 = 01110001 \qquad \text{(A.42)}$$
$$R_4 = \{2, 3, 5\} \qquad f_4 = 01110000$$
$$R_5 = \{1, 3, 4\} \qquad f_5 = 11100111,$$

$$\dot{x}_1 = -x_1 + 2h_2 - 2h_2 h_3 + 2h_2 h_3 h_5 - 1$$
$$\dot{x}_2 = -x_2 - 2h_3 h_4 h_5 + 2h_3$$
$$\qquad + 2h_1 h_5 - 2h_3 h_1 h_5 - 1$$
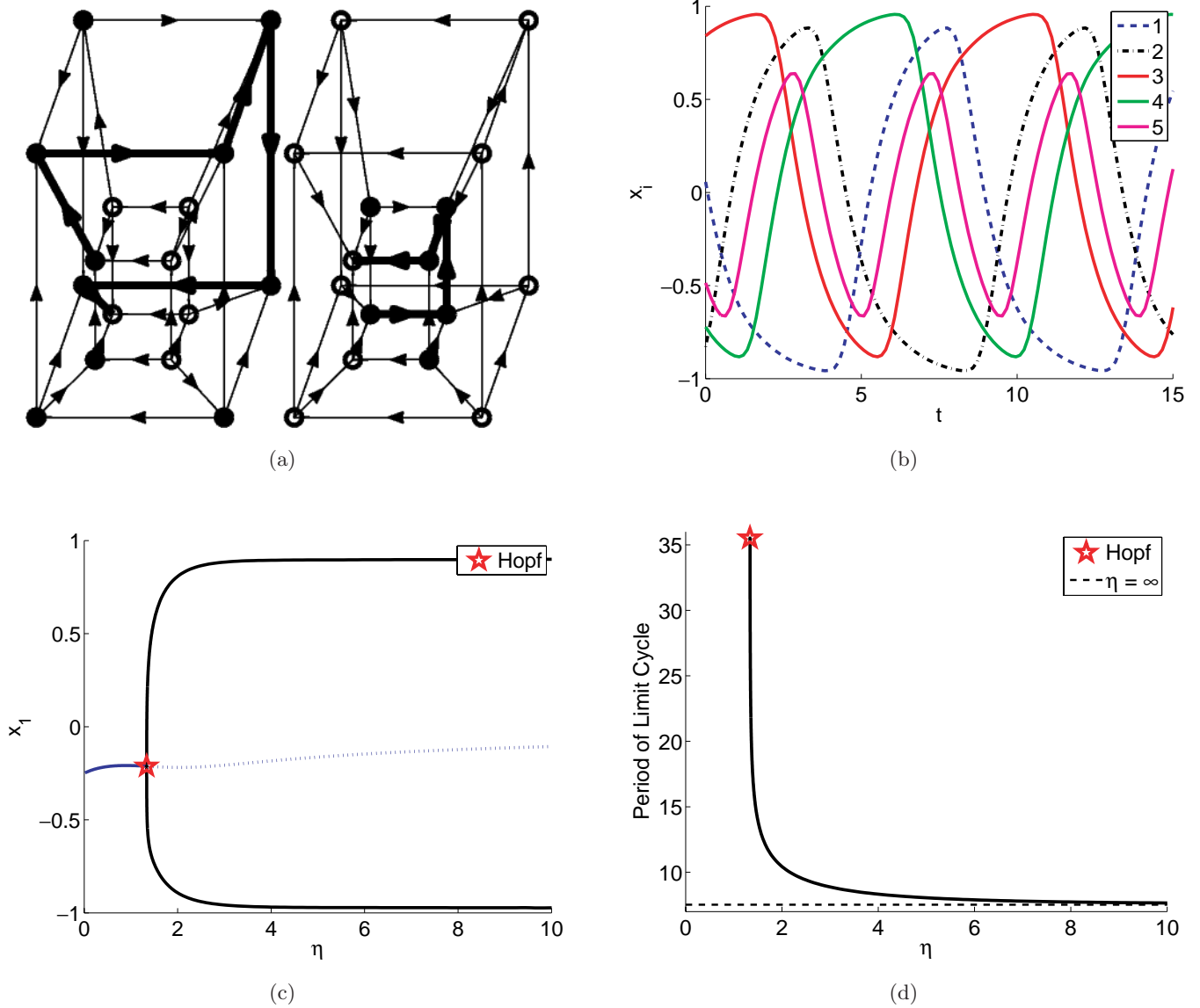
(a)

(b)

(c)

(d)

Fig. 20.   Solution structure of the 12th cyclic attractor in five dimensions [Eq. (A.39)]. Trajectory in (b) has $\eta = 3$. Refer to the Appendix for an explanation of panels. The inset in (d) is a magnification near the Hopf bifurcation.

$$\dot{x}_3 = -x_3 + 2h_4 - 2h_4 h_2 - 2h_1 h_4$$
$$+ 4h_1 h_2 h_4 + 2h_2 - 2h_1 h_2 - 1$$
$$\dot{x}_4 = -x_4 + 2h_5 - 2h_3 h_5 - 2h_2 h_5$$
$$+ 2h_2 h_3 h_5 + 2h_3 - 2h_2 h_3 - 1$$
$$\dot{x}_5 = -x_5 + 1 - 2h_3 h_4$$
$$- 2h_1 + 2h_1 h_4 + 2h_1 h_3.$$
$$(A.43)$$

The solution structure of Eqs. (A.42) and (A.43) is shown in Fig. 22.

A.19.   *Attractor 15 in five dimensions*

$$R_1 = \{2, 3, 4, 5\} \quad f_1 = 0000010000001100$$
$$R_2 = \{1, 3, 4, 5\} \quad f_2 = 1101000110001100$$

$$R_3 = \{1, 2, 4, 5\} \quad f_3 = 1110001101000100$$
$$R_4 = \{1, 2, 3, 5\} \quad f_4 = 0000011100000000$$
$$R_5 = \{1, 2, 3, 4\} \quad f_5 = 0010110000100000,$$
$$(A.44)$$

$$\dot{x}_1 = -x_1 + 2h_3 h_5 - 2h_3 h_5 h_4 - 2h_3 h_5 h_2$$
$$+ 2h_3 h_5 h_2 h_4 + 2h_2 h_3 - 2h_2 h_3 h_4 - 1$$
$$\dot{x}_2 = -x_2 + 1 - 2h_3 - 2h_4 + 2h_4 h_5 - 2h_1 h_3 h_4$$
$$+ 2h_1 h_3 h_5 - 2h_1 h_3 h_4 h_5$$
$$+ 2h_1 h_3 + 2h_3 h_4 - 2h_1 h_5$$
$$\dot{x}_3 = -x_3 + 1 + 2h_2 h_4 h_5 - 2h_2 - 2h_1$$
$$+ 2h_2 h_4 - 2h_4 h_5 + 2h_1 h_5 + 2h_1 h_2$$
$$- 2h_1 h_2 h_4 h_5 - 2h_1 h_2 h_4$$
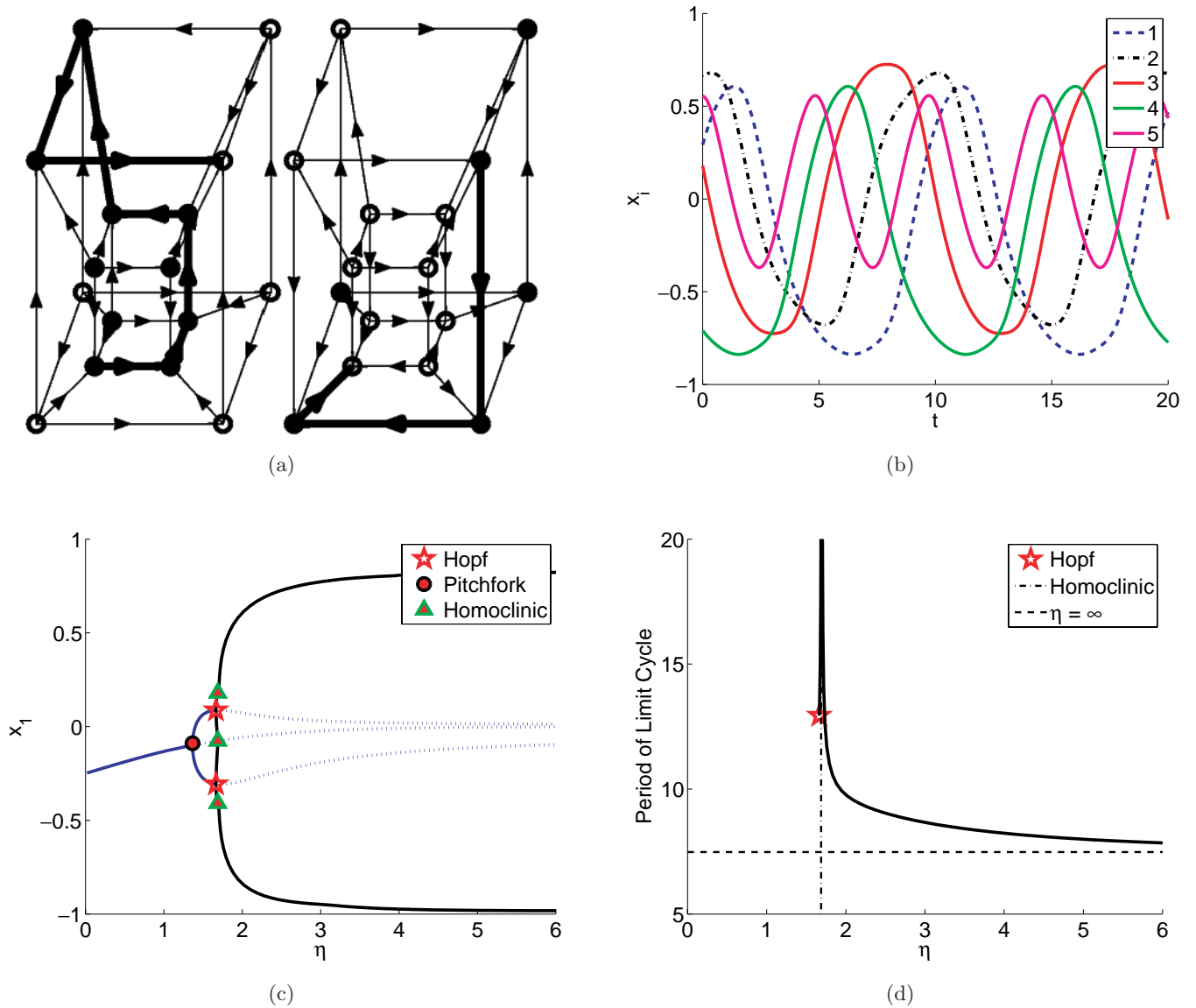
(a)

(b)

(c)

(d)

Fig. 21. Solution structure of the 13th cyclic attractor in five dimensions [Eq. (A.41)]. Trajectory in (b) has $\eta = 3$. Refer to the Appendix for an explanation of panels.

$$\dot{x}_4 = -x_4 + 2h_2h_5 - 2h_3h_5h_2 - 2h_1h_2h_5$$
$$\quad + 2h_2h_5h_1h_3 + 2h_2h_3 - 2h_2h_3h_1 - 1$$
$$\dot{x}_5 = -x_5 + 2h_2 + 2h_3 - 4h_2h_3$$
$$\quad + 2h_2h_3h_4 - 2h_3h_4 - 2h_1h_2 + 2h_2h_3h_1 - 1.$$
$$(A.45)$$

The solution structure of Eqs. (A.44) and (A.45) is shown in Fig. 23.

A.20. *Attractor 16 in five dimensions*

$$R_1 = \{3, 5\} \qquad f_1 = 1001$$
$$R_2 = \{1, 3, 4\} \quad f_2 = 01100000$$
$$R_3 = \{2, 4, 5\} \quad f_3 = 10101100$$

$$R_4 = \{1, 3, 5\} \qquad f_4 = 11001010$$
$$R_5 = \{1, 2, 3, 4\} \quad f_5 = 1100001010100010,$$
$$(A.46)$$

$$\dot{x}_1 = -x_1 + 1 - 2h_5 - 2h_3 + 4h_3h_5$$
$$\dot{x}_2 = -x_2 + 2h_4 - 4h_4h_3 - 2h_4h_1$$
$$\quad + 4h_4h_1h_3 + 2h_3 - 2h_1h_3 - 1$$
$$\dot{x}_3 = -x_3 + 1 - 2h_5 + 2h_2h_5 - 2h_2h_4$$
$$\dot{x}_4 = -x_4 + 1 - 2h_3 - 2h_1h_5 + 2h_1h_3$$
$$\dot{x}_5 = -x_5 + 1 - 2h_2h_3h_4 - 2h_3 - 2h_2$$
$$\quad + 2h_1h_3 - 2h_4h_1 - 2h_1h_2h_3$$
$$\quad + 2h_1h_2h_4 + 4h_2h_3.$$
$$(A.47)$$

(a)

(b)

(c)

(d)

Fig. 22.   Solution structure of the 14th cyclic attractor in five dimensions [Eq. (A.43)]. Trajectory in (b) has $\eta = 2$. Refer to the Appendix for an explanation of panels.
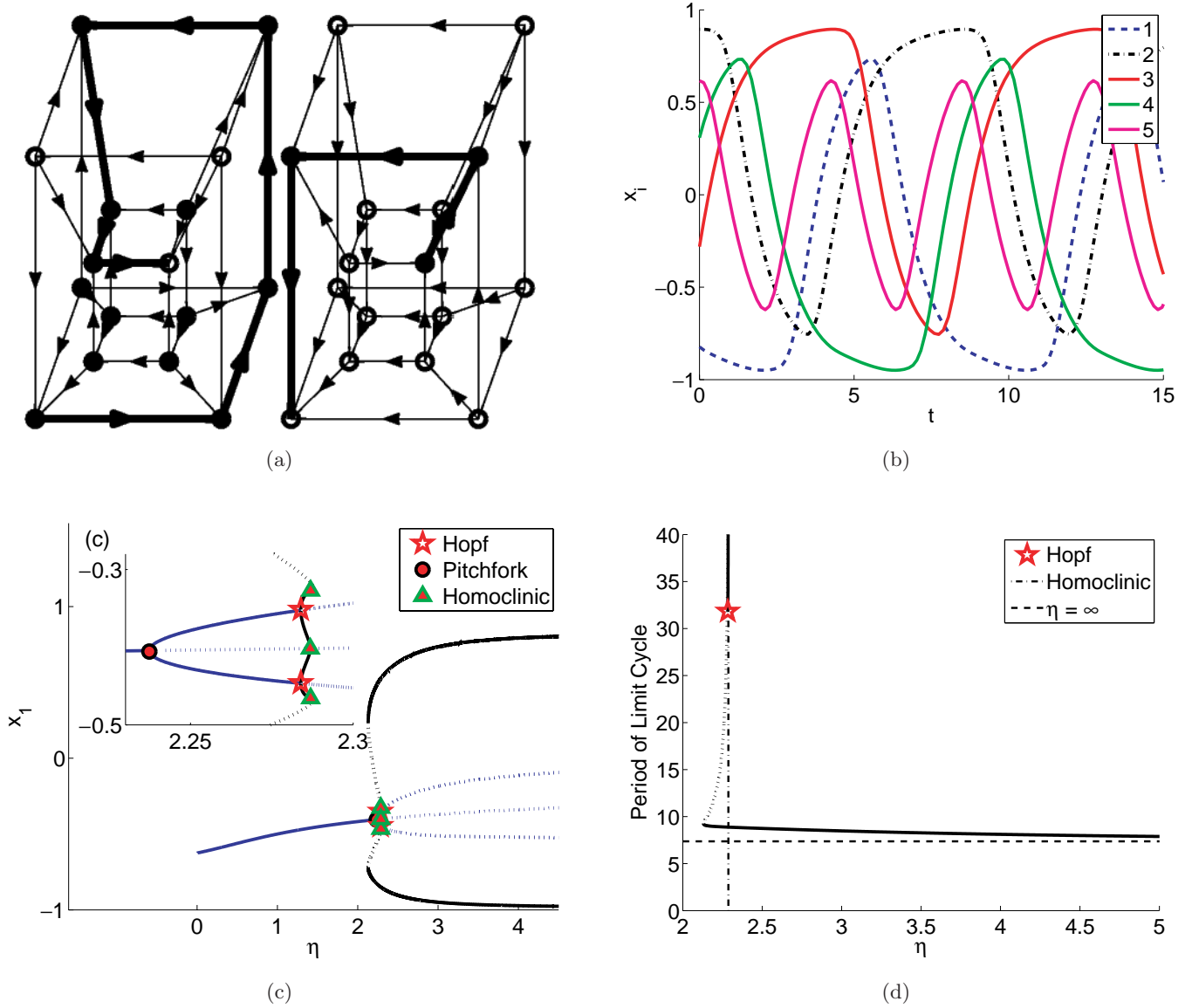
(a)

(b)

(c)

(d)

Fig. 23.   Solution structure of the 15th cyclic attractor in five dimensions [Eq. (A.45)]. Trajectory in (b) has $\eta = 3$. Refer to the Appendix for an explanation of panels. The inset in (c) is a magnification showing the details of the various bifurcations.
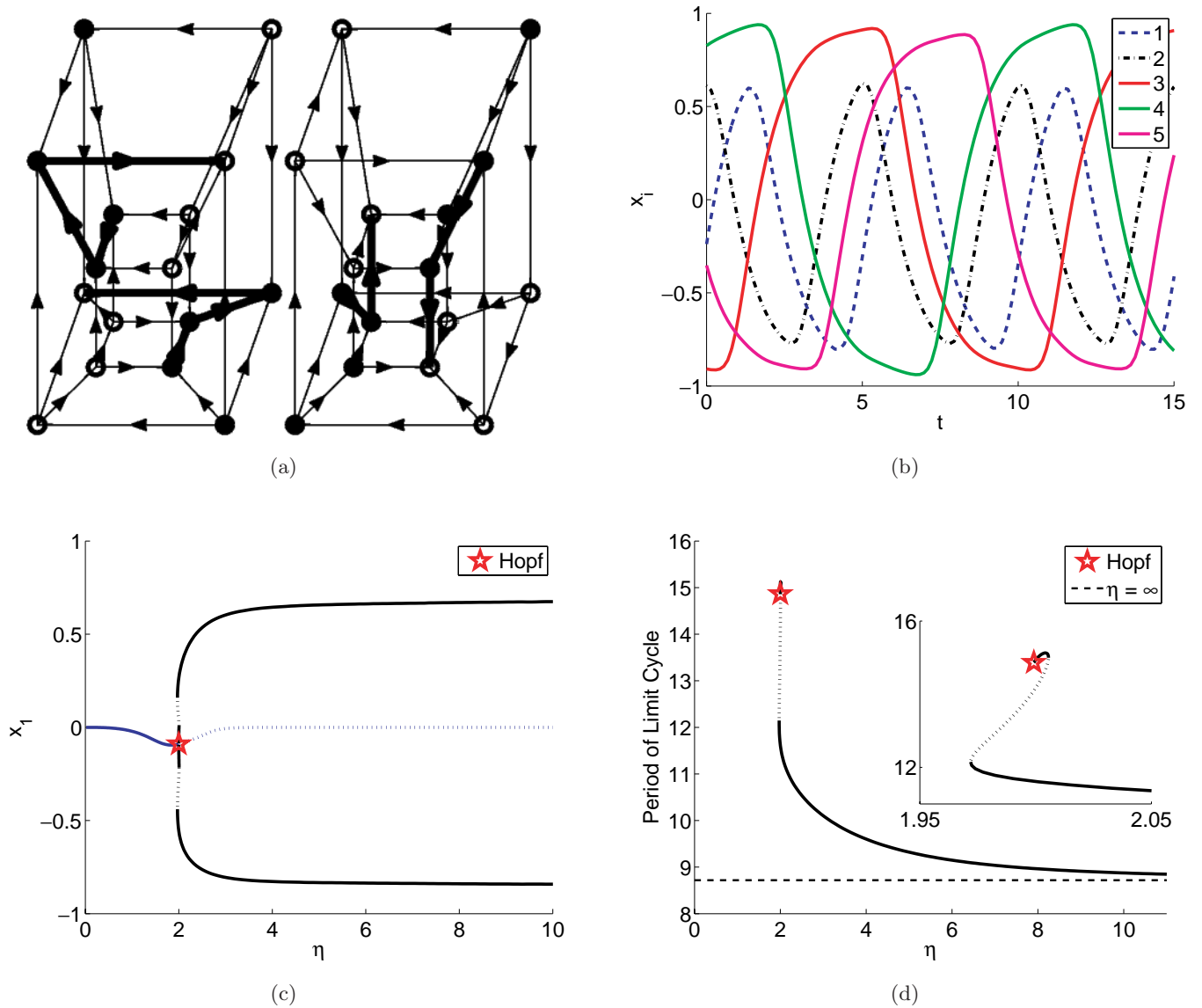
(a)

(b)

(c)

(d)

Fig. 24.   Solution structure of the 16th cyclic attractor in five dimensions [Eq. (A.47)]. Trajectory in (b) has $\eta = 3$. Refer to the Appendix for an explanation of panels. The inset in (d) is a magnification near the Hopf bifurcation.

The solution structure of Eqs. (A.46) and (A.47) is shown in Fig. 24.

A.21.   *Attractor 17 in five dimensions*

$$
\begin{aligned}
R_1 &= \{2, 3, 4, 5\} & f_1 &= 1010000011101100 \\
R_2 &= \{1, 3, 4\} & f_2 &= 01100010 \\
R_3 &= \{2, 4, 5\} & f_3 &= 10101000 \\
R_4 &= \{1, 2, 3, 5\} & f_4 &= 1100110010101000 \\
R_5 &= \{1, 2, 3, 4\} & f_5 &= 1100000010101010,
\end{aligned}
$$

(A.48)

$$
\begin{aligned}
\dot{x}_1 &= -x_1 + 2h_4 - 2h_4h_5 - 2h_4h_3 + 2h_4h_3h_5 \\
&\quad - 2h_4h_2h_5 - 2h_4h_2h_3 + 2h_4h_2h_3h_5 + 2h_2h_5 \\
&\quad - 2h_2h_3h_5 + 2h_2h_3 - 1 \\
\dot{x}_2 &= -x_2 + 2h_4 - 4h_4h_3 - 2h_4h_1 \\
&\quad + 2h_4h_1h_3 + 2h_3 - 1 \\
\dot{x}_3 &= -x_3 + 1 - 2h_5 - 2h_4h_2 + 2h_4h_2h_5 \\
\dot{x}_4 &= -x_4 + 2h_5h_1h_3 + 2h_5h_1h_2 \\
&\quad + 2h_2 + 2h_5 + 2h_1 - 2h_2h_3 + 2h_2h_3h_5 \\
&\quad - 2h_3h_5 - 2h_2h_5 - 2h_1h_2 - 4h_5h_1 - 1 \\
\dot{x}_5 &= -x_5 + 1 - 2h_2 - 2h_3 + 2h_2h_3 \\
&\quad + 2h_4h_1h_3 - 2h_4h_1 + 2h_1h_2 - 2h_1h_2h_3h_4.
\end{aligned}
$$

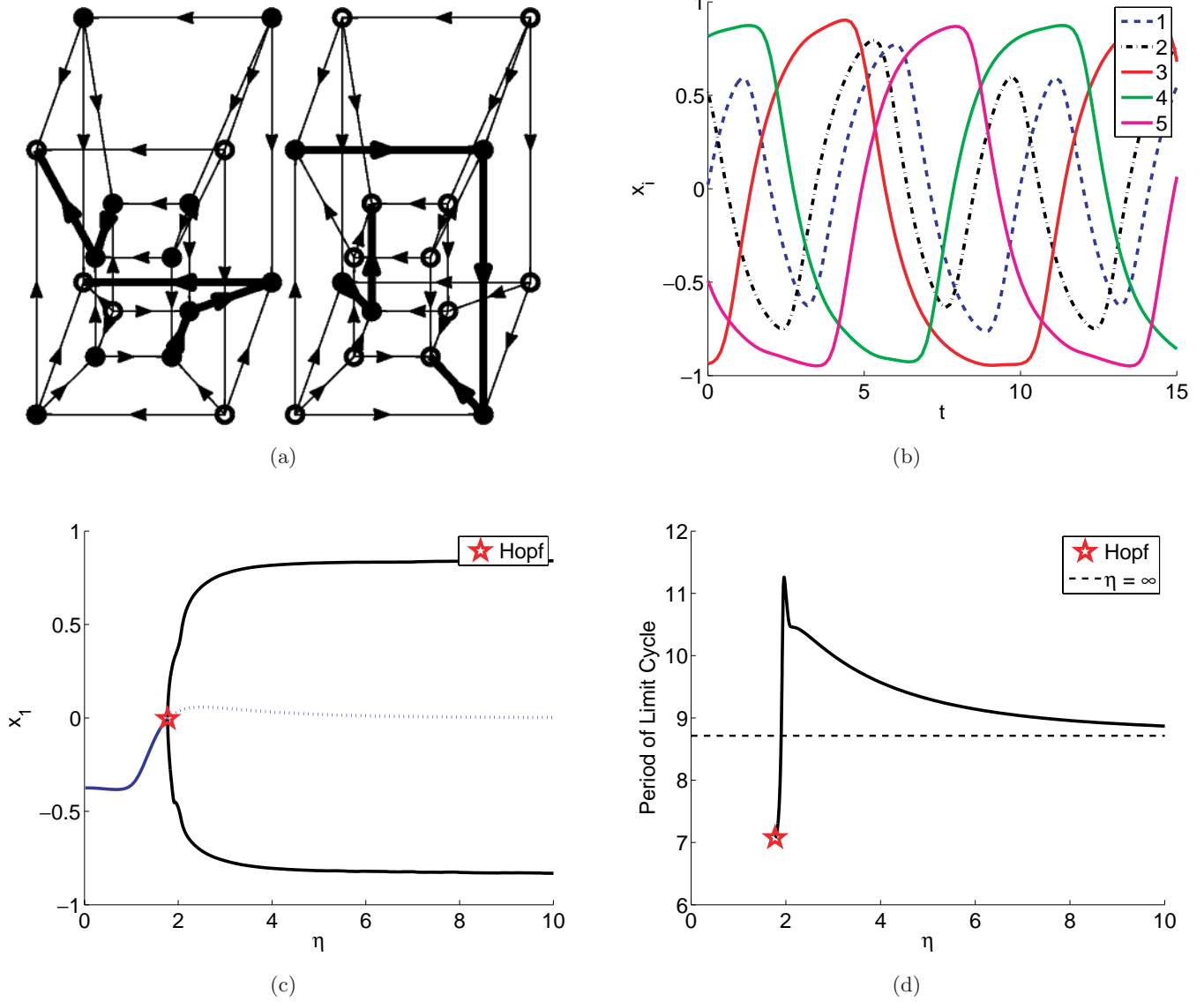(A.49)

(a)

(b)

(c)

(d)

Fig. 25.   Solution structure of the 17th cyclic attractor in five dimensions [Eq. (A.49)]. Trajectory in (b) has $\eta = 3$. Refer to the Appendix for an explanation of panels.

The solution structure of Eqs. (A.48) and (A.49) is shown in Fig. 25.

A.22. *Attractor 18 in five dimensions*

$$
\begin{aligned}
R_1 &= \{2, 3, 5\} & f_1 &= 10011011 \\
R_2 &= \{1, 3, 4, 5\} & f_2 &= 1011100010001000 \\
R_3 &= \{2, 4, 5\} & f_3 &= 10101100 \\
R_4 &= \{1, 2, 3, 5\} & f_4 &= 1100110010101000 \\
R_5 &= \{1, 2, 3, 4\} & f_5 &= 1100000010101010,
\end{aligned}
\tag{A.50}
$$

$$
\begin{aligned}
\dot{x}_1 = -x_1 + 1 - 2h_5 - 2h_3 + 4h_3h_5 \\
+ 2h_2h_3 - 2h_2h_3h_5
\end{aligned}
$$

$$
\begin{aligned}
\dot{x}_2 &= -x_2 + 2h_3 + 2h_4 - 2h_3h_5 + 2h_4h_3h_5 \\
&\quad + 2h_4h_1h_3 - 4h_4h_3 - 2h_4h_1 - 1 \\
\dot{x}_3 &= -x_3 + 1 - 2h_5 + 2h_2h_5 - 2h_2h_4 \\
\dot{x}_4 &= -x_4 + 2h_2 + 2h_5 + 2h_1 + 2h_2h_3h_5 \\
&\quad - 2h_2h_3 - 2h_3h_5 - 2h_2h_5 + 2h_1h_3h_5 \\
&\quad - 4h_1h_5 + 2h_5h_1h_2 - 2h_1h_2 - 1 \\
\dot{x}_5 &= -x_5 + 1 - 2h_2 - 2h_3 + 2h_2h_3 \\
&\quad + 2h_1h_3 - 2h_4h_1 + 2h_1h_2h_4 - 2h_1h_2h_3h_4.
\end{aligned}
\tag{A.51}
$$

The solution structure of Eqs. (A.50) and (A.51) is shown in Fig. 26.
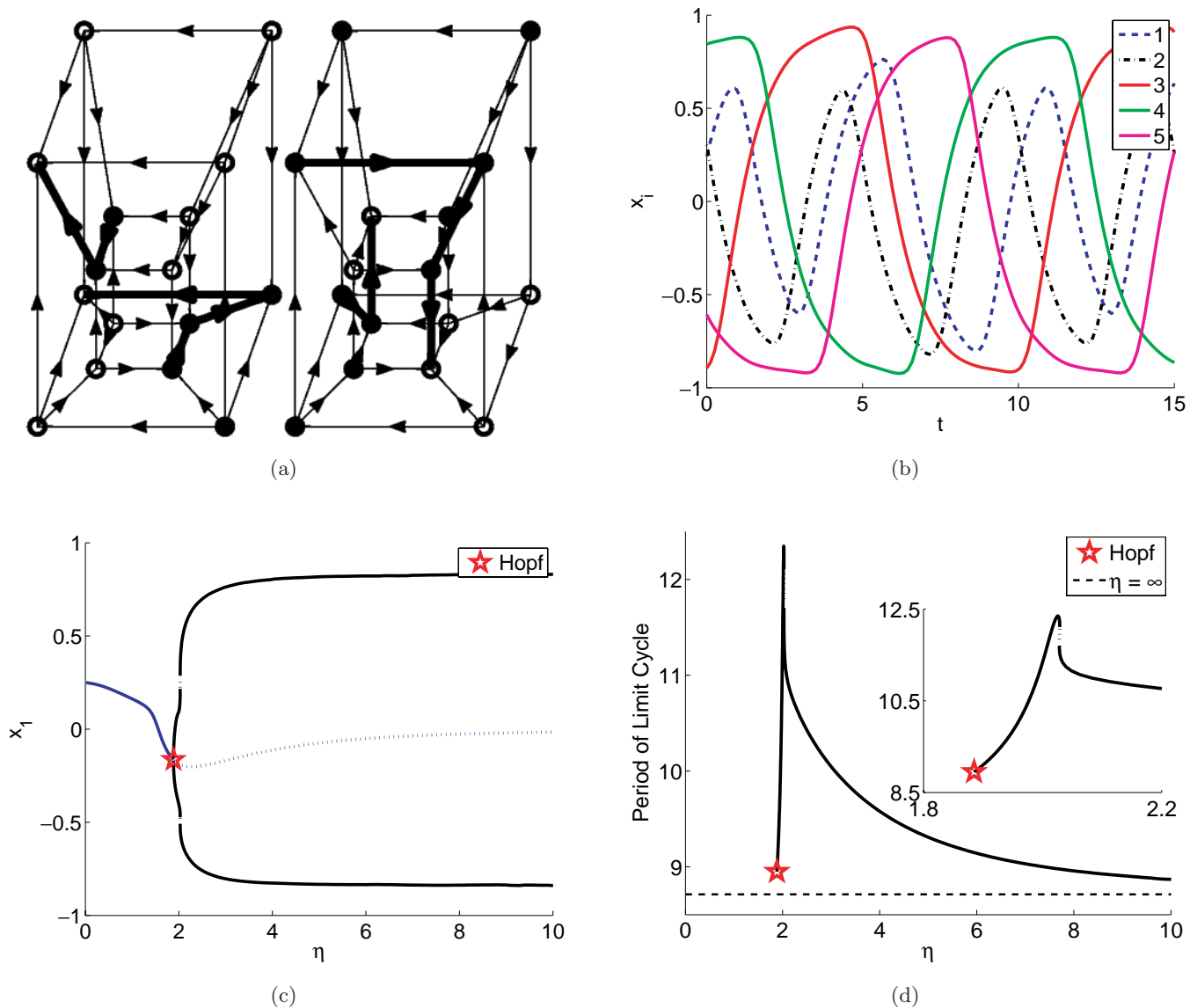
(a)

(b)

(c)

(d)

Fig. 26.   Solution structure of the 18th cyclic attractor in five dimensions [Eq. (A.51)]. Trajectory in (b) has $\eta = 3$. Refer to the Appendix for an explanation of panels. The inset in (d) is a magnification near the Hopf bifurcation.